OMEGA: FACTS, HOPES, AND DREAMS

HARVARD UNIVERSITY

PREPARED FOR
OFFICE OF NAVAL RESEARCH

JUNE 1974

Unclassified

SECURITY CLASSIFICATION OF THIS PAGE *(When Data Entered)*

AD 782 396

REPORT DOCUMENTATION PAGE		READ INSTRUCTIONS BEFORE COMPLETING FORM
1. REPORT NUMBER Technical Report No. 652 Final Report	2. GOVT ACCESSION NO.	3. RECIPIENT'S CATALOG NUMBER
4. TITLE *(and Subtitle)* OMEGA Facts, Hopes, and Dreams		5. TYPE OF REPORT & PERIOD COVERED Final Report 6. PERFORMING ORG. REPORT NUMBER
7. AUTHOR(s) J. A. Pierce		8. CONTRACT OR GRANT NUMBER(s) N00014-67-A-0298-0008
9. PERFORMING ORGANIZATION NAME AND ADDRESS Division of Engineering and Applied Physics Harvard University Cambridge, Massachusetts		10. PROGRAM ELEMENT, PROJECT, TASK AREA & WORK UNIT NUMBERS
11. CONTROLLING OFFICE NAME AND ADDRESS		12. REPORT DATE June 1974 13. NUMBER OF PAGES 156
14. MONITORING AGENCY NAME & ADDRESS*(if different from Controlling Office)*		15. SECURITY CLASS. *(of this report)* Unclassified 15a. DECLASSIFICATION/DOWNGRADING SCHEDULE

16. DISTRIBUTION STATEMENT *(of this Report)*

Approved for public release; distribution unlimited.

17. DISTRIBUTION STATEMENT *(of the abstract entered in Block 20, if different from Report)*

18. SUPPLEMENTARY NOTES

19. KEY WORDS *(Continue on reverse side if necessary and identify by block number)*

Composite Signals
Ambiguity
Errors of Prediction
Correlation
Propagational Predictions
Lane Identification
Difference-Frequency Navigation
Computation of Position

20. ABSTRACT *(Continue on reverse side if necessary and identify by block number)*

This paper summarizes a number of ideas that may help to improve the accuracy and reliability of the Omega radio aid to navigation. The study begins with an introduction to the use of coherent signals at various frequencies, and proceeds, using this nomenclature, to show ways in which errors of prediction and propagation can be reduced. It continues with suggestions of how a greater amount of coherent information can be added to the Omega signal format to permit world-wide lane identification, which is needed for improving the efficiency of search and rescue operations, and for other purposes. The

DD FORM 1 JAN 73 1473 EDITION OF 1 NOV 65 IS OBSOLETE
S/N 0102-014-6601

conclusion is a study of practical computations for determining latitude and longitude when several time differences are known but when there is no prior knowledge about position.

The intent is to provide suggestions for modest improvements in accuracy and a major increase in the reliability and utility of this position-finding system.

Office of Naval Research

Contract N00014-67-A-0298-0008

NR-371-013

OMEGA

Facts, Hopes, and Dreams

By

J. A. Pierce

Technical Report No. 652

Final Report

June 1974

The research reported in this document was made possible through support extended the Division of Engineering and Applied Physics, Harvard University by the U. S. Army Research Office, the U. S. Air Force Office of Scientific Research and the U. S. Office of Naval Research under the Joint Services Electronics Program by Contracts N00014-67-A-0298-0006, 0005, and 0008.

Division of Engineering and Applied Physics

Harvard University Cambridge, Massachusetts

ib

ERRATA TR 652

Page	Line	
19	7	insert "propagation" before "time"
25	4	read "zero" instead of "scale"
34	7	insert "the" before "3.4 kHz"
53	Fig. 16	The two solid curves should be marked "σ_0", not "$\sigma_{3.4}$" and "σ_2"
55	5	insert "in Eq. (28)" after "first term"
113	5	Read "an" instead of "a" before "inertial"
129	2	insert "root" before "sum"

TABLE OF CONTENTS

LIST OF FIGURES

LIST OF TABLES

1. INTRODUCTION

Omega[1, 2, 3, 4] is a radio aid to navigation having very long range that operates in the Very Low Frequency (VLF) part of the radio spectrum. Signal strength and the repeatability of times of arrival are such that eight closely-synchronized transmitters can provide adequate signals to the entire surface of the earth with a satisfactory amount of overlapping. Measurements are made of the phases of received signals, usually taken in pairs to establish hyperbolic lines of position. These lines are stable and predictable enough to yield positions with errors of only a mile or two.

It is the intent of this paper to discuss forward-looking propagational aspects of Omega, not the system as a whole. Except when required for arguments herein, introductory material and matters such as design of equipment or operational experience must be sought in some of the references cited, or elsewhere.

It is an unfortunate fact that, even after fifteen years of Omega experimentation and operation, the consistency of measurements made at a given point still exceeds the precision with which values at that point can be predicted from propagational theory. It seems, therefore, that efforts to understand the facts of radio wave propagation in the very-low frequencies ought to be continued. This paper summarizes certain of these facts that have become clear in the last few years of the writer's research on wave propagation in support of the Omega system.

These facts and ideas constitute a set of suggestions that may, in several ways, improve the accuracy, reliability or convenience of Omega. Since the writer will no longer be in a position to teach these and similar

concepts, this paper is an effort to leave these matters in an ordered way that may help others in carrying this kind of study into the future.

2. COMPOSITE SIGNALS

Many of the ideas and observations to be reported can most easily be expressed in the nomenclature of composite signals.[5,6] This concept will therefore be explained first.

Omega transmitting-station synchronization is achieved, within very close limits, by insuring that (although they are actually radiated sequentially) all antenna currents at all stations at all frequencies pass through zero in the positive sense at the same selected instants of atomic time. Thus the time zero of all radiated signals, including all beats between different frequencies, is absolute.

Under this condition the phase of a difference-frequency between two Omega carrier frequencies from a single station, received at a distant point, may be defined as

$$\phi_{2-1} = \phi_2 - \phi_1 \qquad (1)$$

where

ϕ_{2-1} = total phase change along the transmission path at the difference frequency

ϕ_2 = the same at the higher carrier frequency

and

ϕ_1 = the same at the lower carrier frequency.

For each phase shift

$$\phi = 2\pi fd/v = 2\pi fT \qquad (2)$$

where

f = frequency

d = distance

v = velocity of propagation

and

T = time of propagation along the path from transmitter to receiver.

Substitution converts Eq. (1) into time units*, which the writer finds it most convenient to discuss, giving

$$T_{2-1} = \frac{f_2 T_2 - f_1 T_1}{f_2 - f_1} \tag{3}$$

where the subscripts are as in Eq. (1).

The most widely-separated Omega frequencies are 10.2 and 13.6 kHz. For this pair of frequencies, Eq. (3) becomes

$$T_{2-1} = 4T_2 - 3T_1 \tag{4}$$

or, in terms of actual frequencies in kiloherts,

$$T_{3.4} = 4T_{13.6} - 3T_{10.2} \tag{5}$$

It should be noted that the propagation times for the two carrier frequencies correspond to phase velocities in the "wave guide" formed by the space between the surface of the earth and the base of the ionosphere, while the difference frequency travels at the group velocity in the waveguide.

*The most convenient time unit for Omega purposes, is the period of 10.2 kHz, which is sometimes divided by 100 to give centicycles (or Cecs) of 10.2 kHz. The latter unit is therefore about 0.98 microsecond.

At the Omega frequencies, the daytime phase velocities are slightly greater than the velocity of light. The phase velocities are a little less than the velocity of light at night. The group velocities are nearly 1% slower than the phase velocities.

Various relations between the phase and group velocities can be explored, and fruitfully used, by writing a general expression for composite signals of which Eq. (5) is a special case. The simplest equation of this kind is, in terms of a mixing parameter m,

$$T_c = m T_2 - (m - 1) T_1 \tag{6}$$

or, alternatively and often more usefully,

$$T_c = T_1 + m(T_2 - T_1) \tag{7}$$

where T_c is the propagation time of a composite signal and T_1 and T_2 have been defined above.

When m has the value $f_2/(f_2 - f_1)$, the composite time T_c becomes the propagation time for the difference frequency $(f_2 - f_1)$. In the case of primary interest, where f_1 and f_2 are 10.2 and 13.6 kHz, $f_2/(f_2 - f_1) = 4$, as in Eq. (5).

There are only three values of m for which the composite propagation time has simple values, as shown in Table 1.

Theoretically, analytically, or instrumentally, m can assume any value. Except for the cases in Table I, all propagation times are a compound, or composite, of the phase and group times. There seem, however, to be only two regions of m where the composite signals are of especial interest. These can be located experimentally or, to a fair approximation, analytically.

TABLE I

Singular Values of the Composite Propagation Time T_c

Generalized Values		Values for the Omega Frequencies Cited	
m	T_c	m	T_c
0	T_1	0	$T_{10.2}$
1	T_2	1	$T_{13.6}$
$f_2/(f_2-f_1)$	T_{2-1}	4	$T_{3.4}$

3. COMPOSITE SIGNALS TO MINIMIZE STANDARD DEVIATION

The first of these regions can be found by assuming that a single mode of propagation exists in the earth-ionosphere waveguide. In this waveguide the mean proportional between the phase and group velocities or, to a sufficient approximation, the mean of the two velocities should be a constant equal, presumably, to the velocity of light. This assumption can be inverted, by Eq. (2), to give

$$T_c = \frac{T_p + T_g}{2} \tag{8}$$

where T_p and T_g are generalized phase and group times of propagation, respectively.

Because there is a significant amount of dispersion in the waveguide, we may adopt the mean of the phase times at f_1 and f_2 as the generalized phase time T_p, by saying

$$T_p = \frac{T_1 + T_2}{2} \quad . \tag{9}$$

The group time is, of course, the time for the difference frequency, which has been defined in Eq. (3) as

$$T_g = \frac{f_2 T_2 - f_1 T_1}{f_2 - f_1} \quad . \tag{10}$$

Substitution of the values from Eqs. (9) and (10) into Eq. (8) yields

$$T_c = \frac{(3f_2 - f_1) T_2 - (3f_1 - f_2) T_1}{4(f_2 - f_1)} \quad . \tag{11}$$

If we define

$$m_o = \frac{3f_2 - f_1}{4(f_2 - f_1)} \tag{12}$$

it turns out that

$$\frac{3f_1 - f_2}{4(f_2 - f_1)} = m_o - 1 \tag{13}$$

and Eq. (11) reduces to

$$T_c = m_o T_2 - (m_o - 1) T_1 \tag{14}$$

which is a special case of Eq. (6).

Using the value of m_o defined in Eq. (12), which is equal to 9/4 when f_1 and f_2 are taken as 10.2 and 13.6 kHz, we may expect to observe a composite propagation time that is nearly invariant despite changes of height or conductivity of the surfaces in the earth-ionosphere

waveguide. Experimentally we find that there is much truth in the second part of this statement, but there is a residual change in the time of propagation between day and night as the height of the reflecting layer changes.

An explanation for this diurnal change in the propagation time is as follows. The optimum composite signal, with $m = m_o$, presumably travels at the velocity of light along the "axis" of the waveguide. In a plane parallel waveguide the axis would be at half the height and the length of the axis would equal the length of the waveguide. Between the curved earth and curved ionosphere, however, the "axis" is at about 3/8 of the height* of the layer while we can only measure our propagation distances along the surface of the earth as the layer height is not accurately known. It follows that when the layer height increases at night the composite signal (although still traveling at the same velocity) must traverse a greater distance so that the time of propagation is somewhat greater.

The first four figures illustrate this especially interesting composite signal, with m equal to the m_o of Eq. (12). Figure 1 shows the behavior of the propagation time during a large Sudden Ionospheric Disturbance (SID), associated with a solar flare, that began at about 1708 GMT on 8 July 1968. The time taken by the signals to travel from Hawaii to Cambridge is expressed in periods of the lowest Omega frequency, 10.2 kHz. This unit is equal to 1/10200 second or 98+ microseconds. At about

*The factor 3/8 is related to the average height at which rays travel by reflection between the earth and the reflecting layer. In mode theory, it is the height at which the mode resonance angles cross in the waveguide. This factor is by no means an exact constant, but it should lie between 1/3 and 1/2 of the layer height.

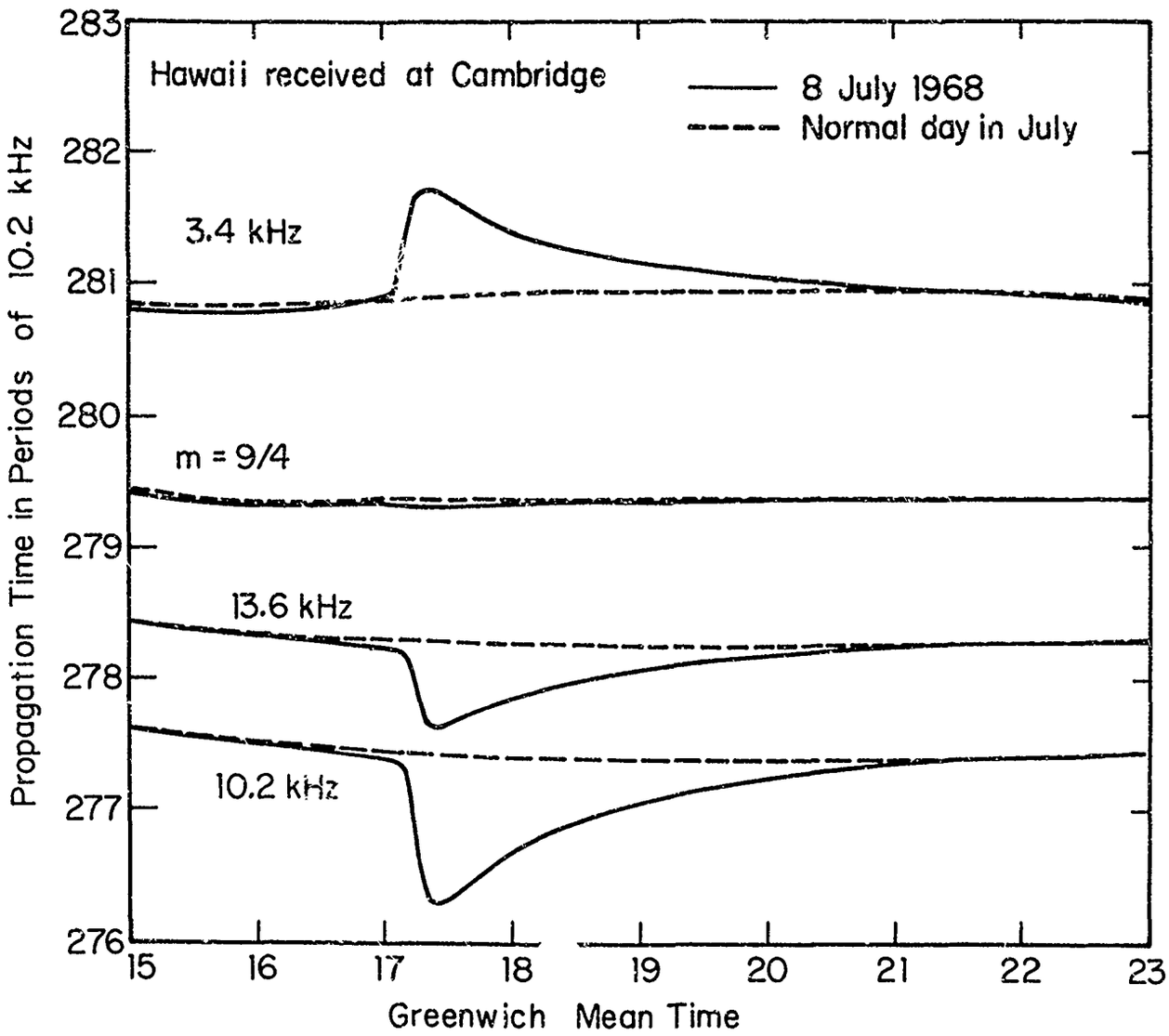

Figure 1: A Large Sudden Ionospheric Disturbance at Various Values of m.

1725 GMT the 10.2 kHz signal had a time of propagation 100 microseconds less than it had had at, say, 1705. The abnormal ionizing energy of the solar flare, which depressed the ionized layer, gradually declined, but its effect was noticeable for almost four hours. At 13.6 kHz the effect was similar but considerably smaller, while at 3.4 kHz--the difference frequency--the effect was similar but inverted in sense. The approximate cancellation of the effect of the SID when $m = 9/4$ is of primary importance.*

An example of another propagational anomaly, from a different primary cause, is shown in Fig. 2. This diagram shows the first two days of an average "Polar Cap Anomaly" (PCA) caused by corpuscular bombardment of the ionosphere by protons, and perhaps other charged particles, shot out in a solar eruption. These heavy ions penetrate to the base of the ionosphere chiefly near the polar regions where the horizontal component of the earth's magnetic field is small. Events of this kind often last for a week or more. This one began near 10^h GMT on 9 June 1968 and declined in magnitude after about 40 hours. As in Fig. 1, the effect is seen to be greatest at 10.2 kHz, to reverse at 3.4 kHz, and to approximately vanish when $m = 9/4$.

Figures 1 and 2 illustrate the effects of the two primary kinds of propagational anomalies in the VLF region of the radio spectrum. Almost all recognizable anomalies of either kind have behaved in the same general

---

*It should be admitted that although a continuous 10.2 kHz record was available at this time, the 13.6 kHz record, upon which the other curves depend, was available only in hourly samples. Figure 1 therefore draws upon art as well as observation.

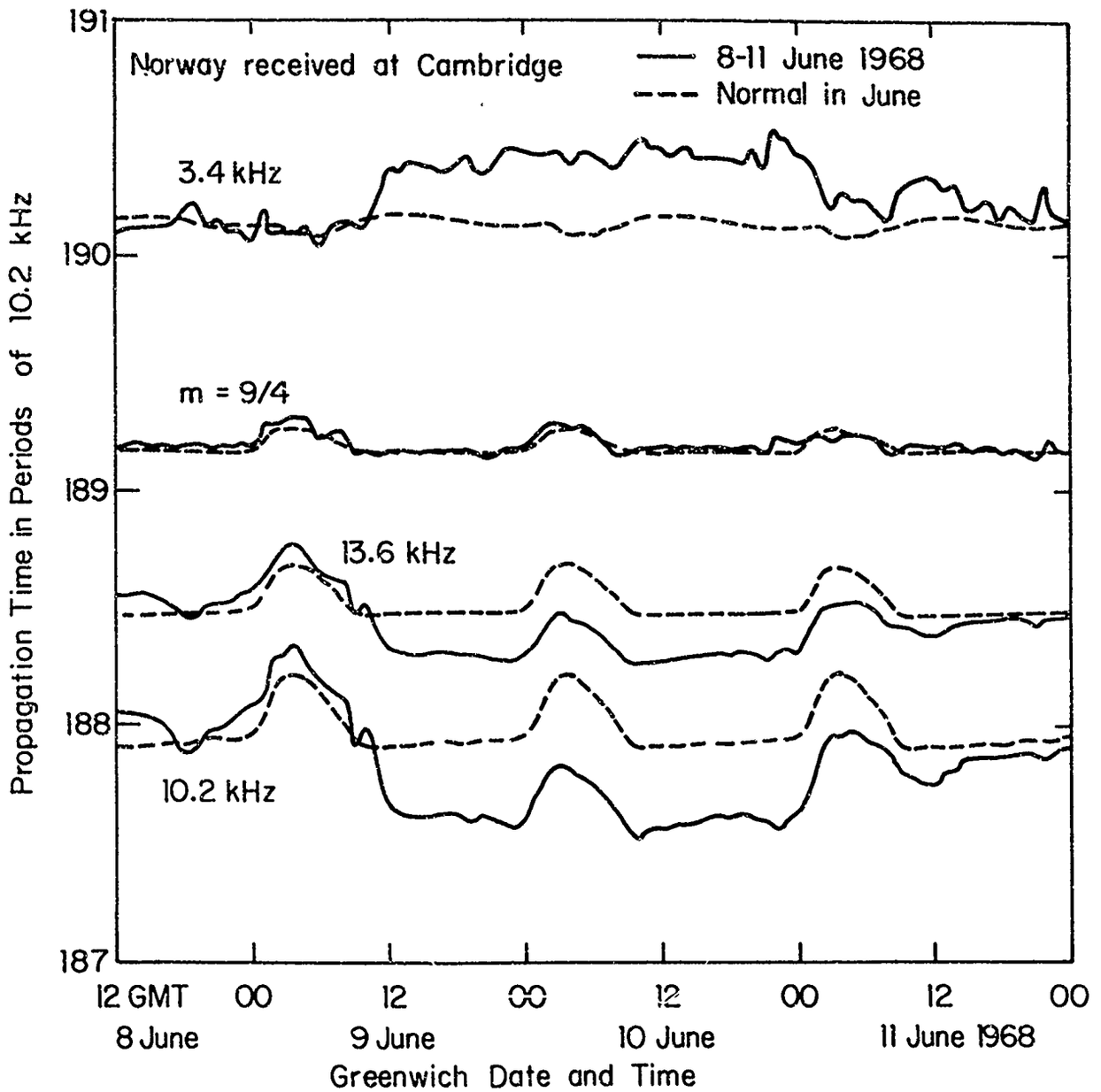

Figure 2: A Polar Cap Anomaly at Various Values of m

way. The degree of cancellation when $m = 9/4$ varies somewhat, and at times a very rapid commencement of an SID may affect the two frequencies at different rates so that there is a short transient effect before the composite signals settle into a steady state. Sometimes such a transient effect can be attributed to instrumental causes, such as a difference in dynamic characteristics or in signal-to-noise ratio between the two radio-frequency channels.

It is reasonable to assume that the normal fluctuations in the time of arrival of a VLF signal may consist in part of unrecognized anomalistic propagation. If this be true or if, for any reason, there should be a high degree of correlation between the fluctuations at neighboring frequencies, the theory of composite signals outlined above predicts that the standard deviation should be at a minimum when $m = m_o$. Another way of making this statement is to say that this composite signal should travel at a velocity near that of light and should be less affected by changes in the conductivity of the waveguide surfaces than either the phase or the group velocity.

Figure 3 shows that at least the longer-distance signals in Omega obey this rule. Here the ordinate is m, and it should be remembered that the two carrier frequencies of 10.2 and 13.6 kHz are represented by $m = 0$ and $m = 1$, while $m = 4$ corresponds to the difference frequency. The standard deviations of Fig. 3 are for the month of December, 1970, and are root-mean-square values for all of the 24 hours in the day, taken separately. Similar curves for the summer exhibit a somewhat smaller standard deviation, but are otherwise much like Fig. 3. The reasons for the minimum near $m = 1$ for the Trinidad signal will be discussed later, as will some of the details of diurnal behavior.

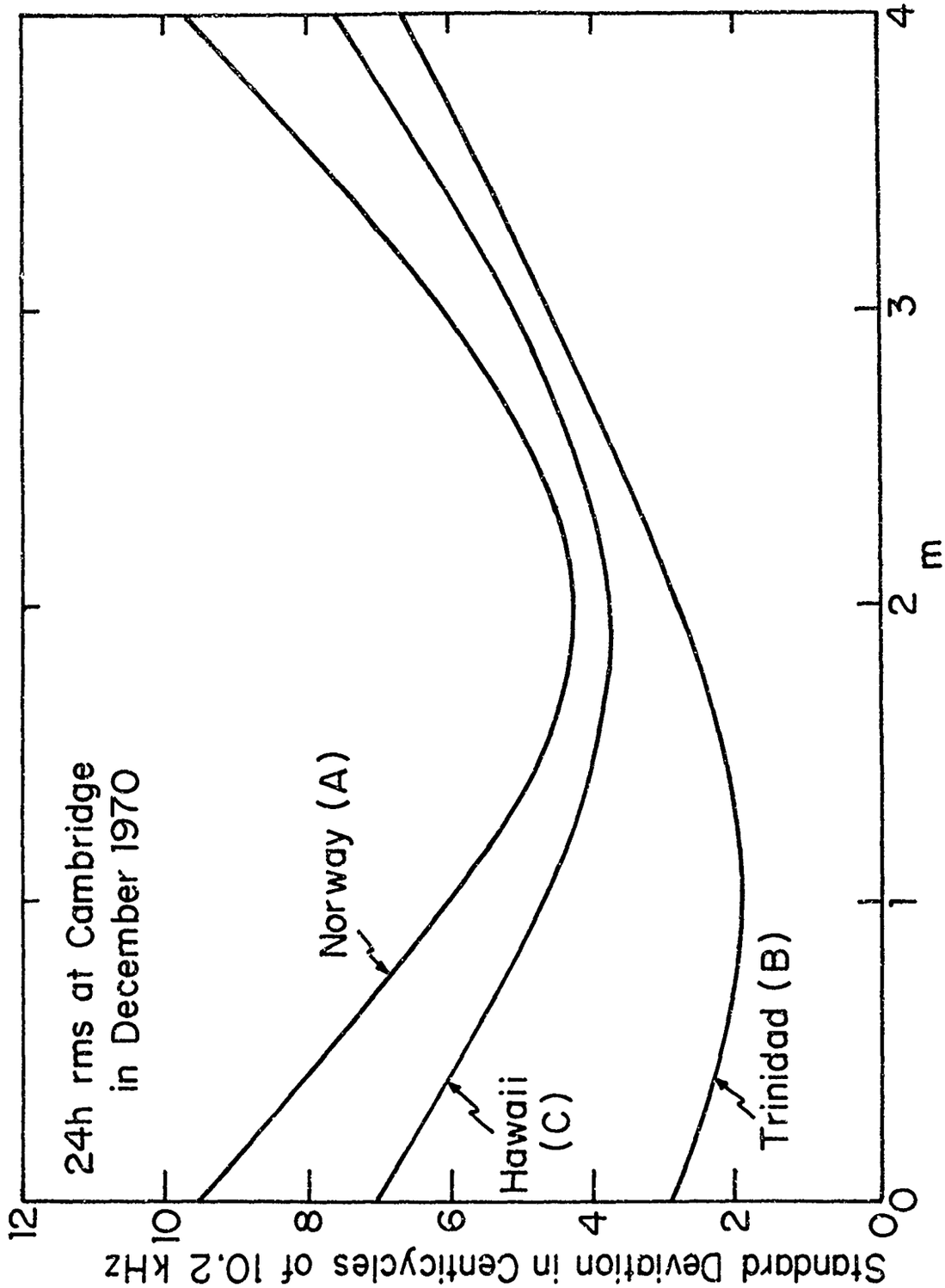

Figure 3: Standard Deviation as a Function of m for Various Stations Observed at Cambridge.

We have seen that very large variations in the time of arrival are better compensated by the composite-signal treatment than are long-term standard deviations. This seems to be because there is higher correlation between fluctuations when they are large. This may be equivalent to saying that there is an uncorrelated phase noise (principally due to instrumental uncertainties and to actual atmospheric noise) to which there are added highly-correlated propagational fluctuations. This effect is shown in Fig. 4, where standard deviations at $m = 9/4$ are plotted against the corresponding standard deviations at 10.2 kHz. These data were taken by pairs of stations, and the deviations are somewhat larger than those for the "worst" station of the pair. Each point in Fig. 4 shows the standard deviations observed at a given hour of the day during a calendar month in the period between late 1967 and the end of 1972. The graphs for 03 and 06 hours GMT are chosen as near midnight in the area including the transmitters and the receiver, while the 15 and 18 hour graphs represent conditions near noon. Two points are worthy of notice: (1) the composite deviations at night are about twice those by day, and (2) the composite deviations show no great sign of increasing under those conditions that produce carrier-frequency deviations much larger than normal.

These matters will be more fully discussed when we come to the study of correlation between signals. Before that, however, it will be well to derive the second important value of the parameter m.

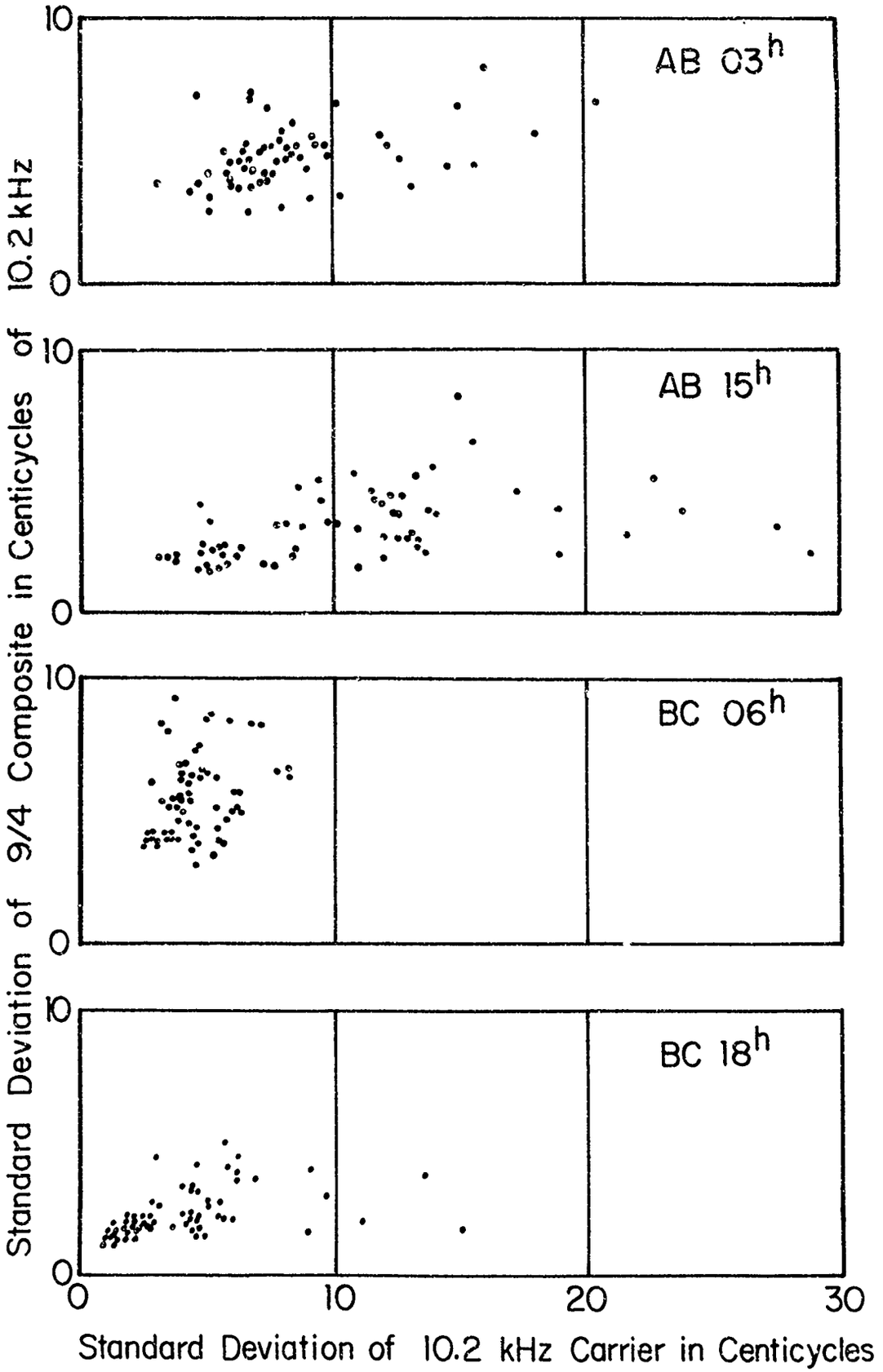

Figure 4: Comparison of Standard Deviation for m = 0 and m = 9/4 over a Long Period.

4. COMPOSITE SIGNALS TO MINIMIZE DIURNAL VARIATION

To find a composite propagation time that is, as nearly as possible, diurnally invariant, we may begin by observing that there is in fact an inversion as m increases, because the phase time is smaller in the daytime than at night while the group time is less at night than by day. The value of m that equates day and night propagation times can be derived, following Watt and Croghan,[7] as follows. The velocity of the composite signal is defined as intermediate between phase and group velocities by saying

$$v_c = v_p(1 - P) + Pv_g \tag{15}$$

where P is a proportioning parameter.

From Watt[8] this velocity can also be defined, in an approximation to the mode-theory velocity, as

$$\frac{v_c}{v_o} = 1 - \frac{h'}{a} - \left(P - \frac{1}{2}\right)\left[(2\pi n + \phi_g + \phi_i)\ \frac{v_o}{4fh}\ \right]^2 \tag{16}$$

where

v_o = velocity of light

h' = height of ray crossings in the waveguide

a = radius of the earth

n = mode number (1 in this case)

ϕ_g = phase shift at reflection at the surface of the earth

ϕ_i = phase shift at reflection at the ionosphere

f = frequency

and h = height of the reflecting layer.

Watt and Croghan then take

$$h' = 0.30\,h$$ (a different estimation of the value 3/8 suggested in an earlier footnote)

$$\phi_g = 0$$

$$\phi_i = -\pi$$

although all of these values are approximate and are not independent of h.

With these values Eq. (16) reduces to

$$\frac{v_c}{v_o} = 1 - \frac{0.30h}{a} - \left(P - \frac{1}{2}\right) \frac{v_o^{2_h - 2}}{16f^2} \qquad (17)$$

Differentiating with respect to h and setting the result equal to zero produces

$$P = 0.5 + 4.2 \cdot 10^{-24} f^2 h^3 \qquad (18)$$

Taking the day and night heights as 70 and 90 kilometers and the frequencies as 10.2 and 13.6 kHz leads to a mean value of h as 80 km and of f as 11.9 kHz. P is then found to be 0.8. Since

$$m = \frac{f_2 P}{f_2 - f_1} \qquad (19)$$

Watt and Croghan's solution suggests that a moderately uniform velocity should be found for this pair of frequencies when m = 3.2.

Bjøntegaard[9] has performed much the same analysis by graphical methods working from Wait's curves.[14] He finds the value of m that leads to minimum day-to-night variation to be 3.35.

At this point in our discussion it must be said that a true assessment of the value of m yielding minimum diurnal variation must take account of

all hours of the day, because (on a transmission path spanning many hours of longitude) there may be more hours of sunrise and sunset conditions than there are of full night or full day. It is, nevertheless, advantageous to continue the discussion of day versus night conditions a little longer.

A rough determination of what we may now call m_1, the value of m at which diurnal variation is a minimum, can be made in terms of the height of the "trapezoid" representing the change in time of arrival of a signal between day and night. If this height be measured at the two frequencies f_1 and f_2 and if, for convenience, it be called ΔT, we see that

$$m_1 = \frac{\Delta T_1}{\Delta T_1 - \Delta T_2} \tag{20}$$

where each ΔT is proportional to $(c/v_{night} - c/v_{day})$ with c the velocity of light. This derivation requires some averaging of daytime levels, which usually vary inversely with the altitude of the sun, and takes no account of sunrise and sunset periods. It does, however, give an easy experimental determination that is approximately correct. Three examples of reciporcal-velocity values permitting this kind of solution are shown in Table II.

The quantities tabulated are values of c/v (which require only to be multiplied by a distance, expressed as the time for a theoretical signal to traverse the geodesic at the velocity of light, to become propagation times). Values and certain differences between them are given in the table for the three sets described as follows:

(A) Transcribed from Naval Research Laboratory Report No. 6663.[10] This report suggests that the values are theoretical ones derived from Wait. Internal evidence indicates that there is perhaps some admixture of experimental evidence in the values cited.

TABLE II

Various Estimates of Reciprocal Velocity

	c/v_2 13.6 kHz	c/v_1 10.2 kHz	$c/v_2 - c/v_1$	m_1	c/v at m_1
(A) from NRL Report 6663:					
Night	1.00240	1.00040	0.00200		
Day	0.99967	0.99661	0.00306		
Night-Day	0.00273	0.00379		3.57	1.0075
(B) from FAA experimental data:					
Night	1.00223	1.00018	0.00205		
Day	0.99978	0.99667	0.00311		
Night-Day	0.00245	0.00351		3.31	1.0070
(C) Nominal:					
Night	1.00250	1.00040	0.00210		
Day	1.00035	0.99730	0.00305		
Night-Day	0.00215	0.00310		3.26	1.00724

Note: $c/v = c/v_1 + m(c/v_2 - c/v_1)$

(B) Experimental data from a survey conducted by Pickard and Burns, Inc., for the Federal Aviation Administration and privately communicated to the writer. The data cover observations of diurnal variations of either two or three Omega pairs over one or two days at each of seventeen locations, ranging from Argentina to Alaska and from Newfoundland to Alberta. The data are somewhat doubtful, as the equipment used did not resist noise impulses as well as it should have. Values of m_1

for the individual pairs lay between 1.5 and 5.0, and were weighted in a complex way to derive the numbers cited in Table II (B).

(C) Nominal values adopted by the writer after consideration of (A) and (B) above and many other blocks of data. These nominal values will be used from time to time below.

Figures 5 and 6 illustrate a way of examining m_1. In each diagram an "m-line" is drawn through the mean values of time at 10.2 (m = 0) and 13.6 kHz (m = 1) for each of the 24 hours of the day for a chosen group of dates. Such groups of dates are often taken as half-months, because it is well to average many days without including too much seasonal change in the times of sunrise and sunset. Figure 5 shows the propagation time for the signals travelling from Hawaii to Cambridge in May, 1971. The grouping of the lines when m is somewhat greater than 3 is clearly marked. It is also interesting to note that a tendency to group in the neighborhood of $m = 9/4$ can be seen, principally in the daytime hours (those lines that are lower at the left side of the diagram) but also to some extent at night.

Figure 6 is entirely similar to Fig. 5, except that it shows time differences for the pair Norway-Hawaii as seen at Cambridge in February, 1969. Because the two transmitters are separated by nearly 12 hours in longitude, the positive diurnal variations from Norway tend to coincide with the negative diurnal variations from Hawaii. The relative amplitude of the variations in Fig. 6 is therefore magnified in comparison with Fig. 5, although the time difference itself (and consequently the mean slope of the lines in Fig. 6) is smaller. The grouping near $m = 3.3$ is, however, still conspicuous.

A simpler but perhaps less instructive way of exhibiting these effects is to plot standard deviation against m. Figure 7 shows such a diagram for

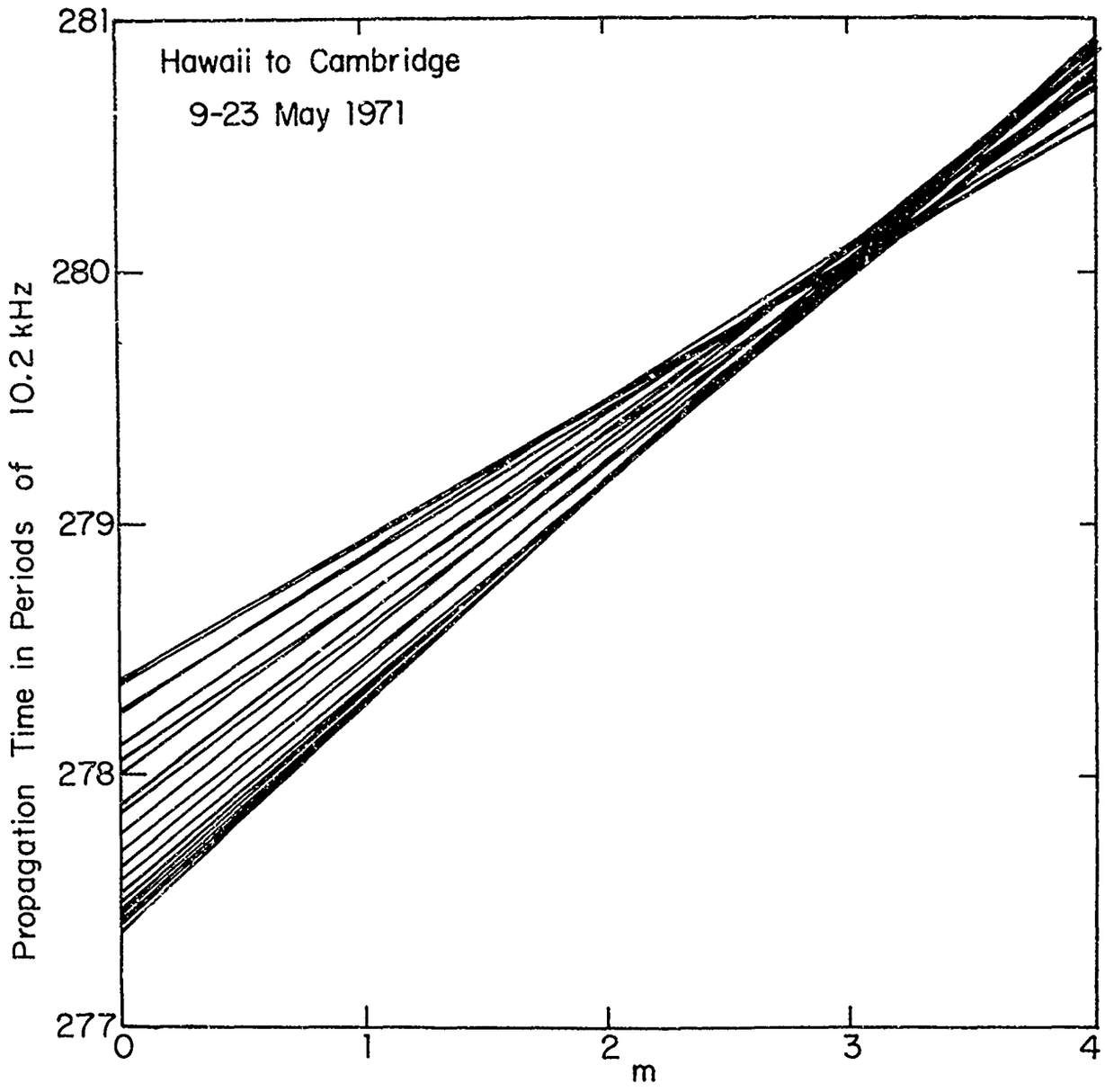

Figure 5: "m-lines" for Hawaii at Cambridge in May.

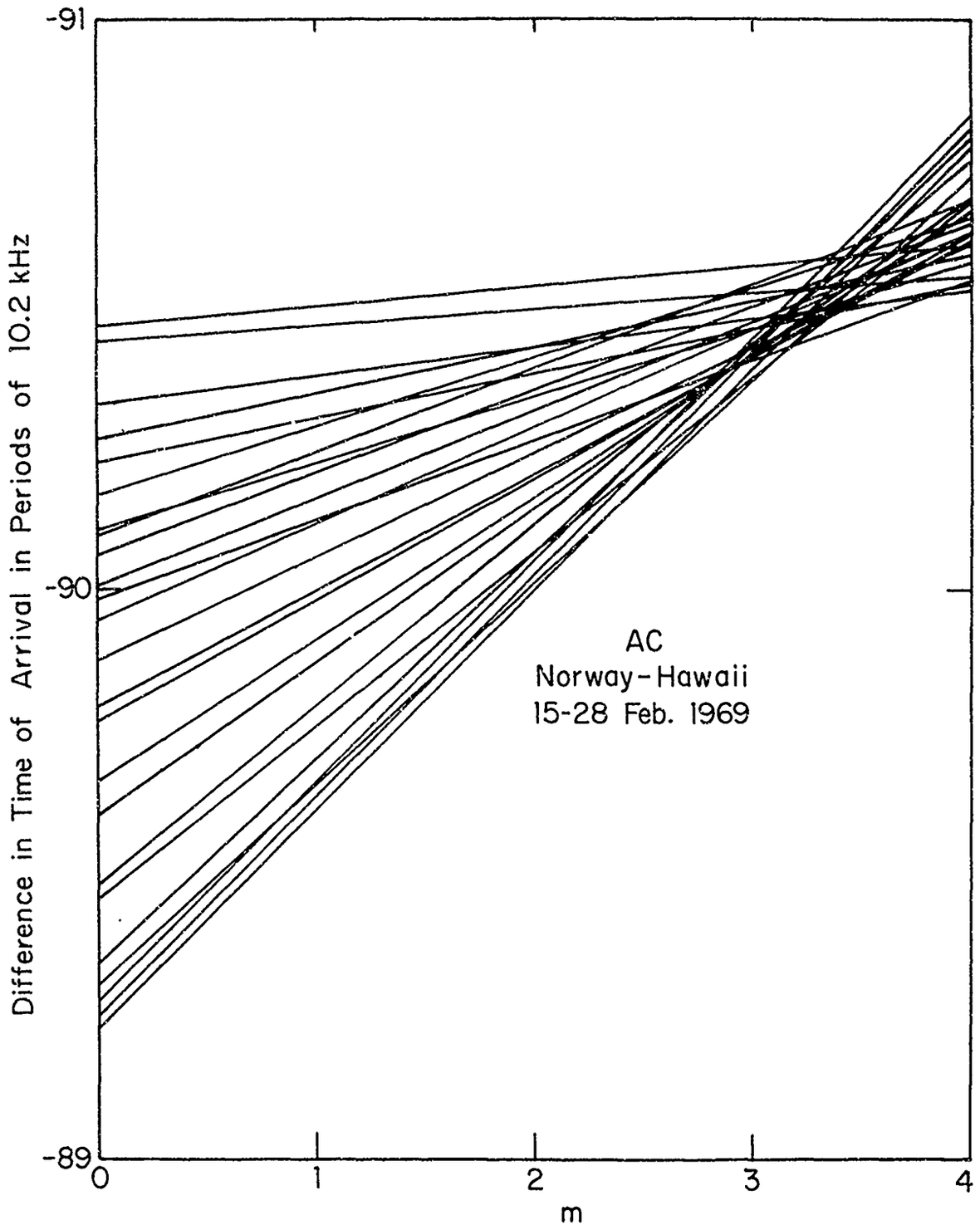

Figure 6: "m-lines" for Norway-Hawaii at Cambridge in February

the rms of the three long-distance pairs observable at Cambridge in June 1968 and December 1970. Minima in the neighborhood of $m = 9/4$ and $m = 3$ are clearly shown. Two important conclusions may be drawn from Fig. 7:

(1) When using diurnal predictions for navigational purposes, as indicated by the lower pair of curves, the standard deviation near $m = 9/4$ is about half of that at $m = 0$ (10.2 kHz).

(2) Without diurnal compensation (the upper pair of curves) the standard deviation near $m = 3$ is about the same as that for $m = 0$ with compensation.

Neither of these statements takes any account of the errors of prediction that are an important, or even dominant, factor in determining navigational accuracy. While these will be discussed below, it is perhaps fair to say here that prediction errors seem to behave in much the same way as propagational fluctuations, so that the statements above remain reasonably accurate.

Figure 8 is an effort to show why an m near 3.0 is, for some purposes, to be preferred to one near 3.3. The ordinate here is the velocity of light divided by the velocity of the signal, or relative time. This diagram shows lines at the nominal values from Table II, each surrounded by a hatched area purporting to indicate the typical standard deviation. Since the standard deviation increases markedly above $m = 9/4$, the total spread is least when m is near 3.0, even though the nominal lines actually cross near $m = 3.3$. This means that, if one wishes to operate without the need for applying diurnal corrections to the observed data (except as necessary for purposes of lane identification, as is discussed below) a value of m at or near 3.0 is probably best.

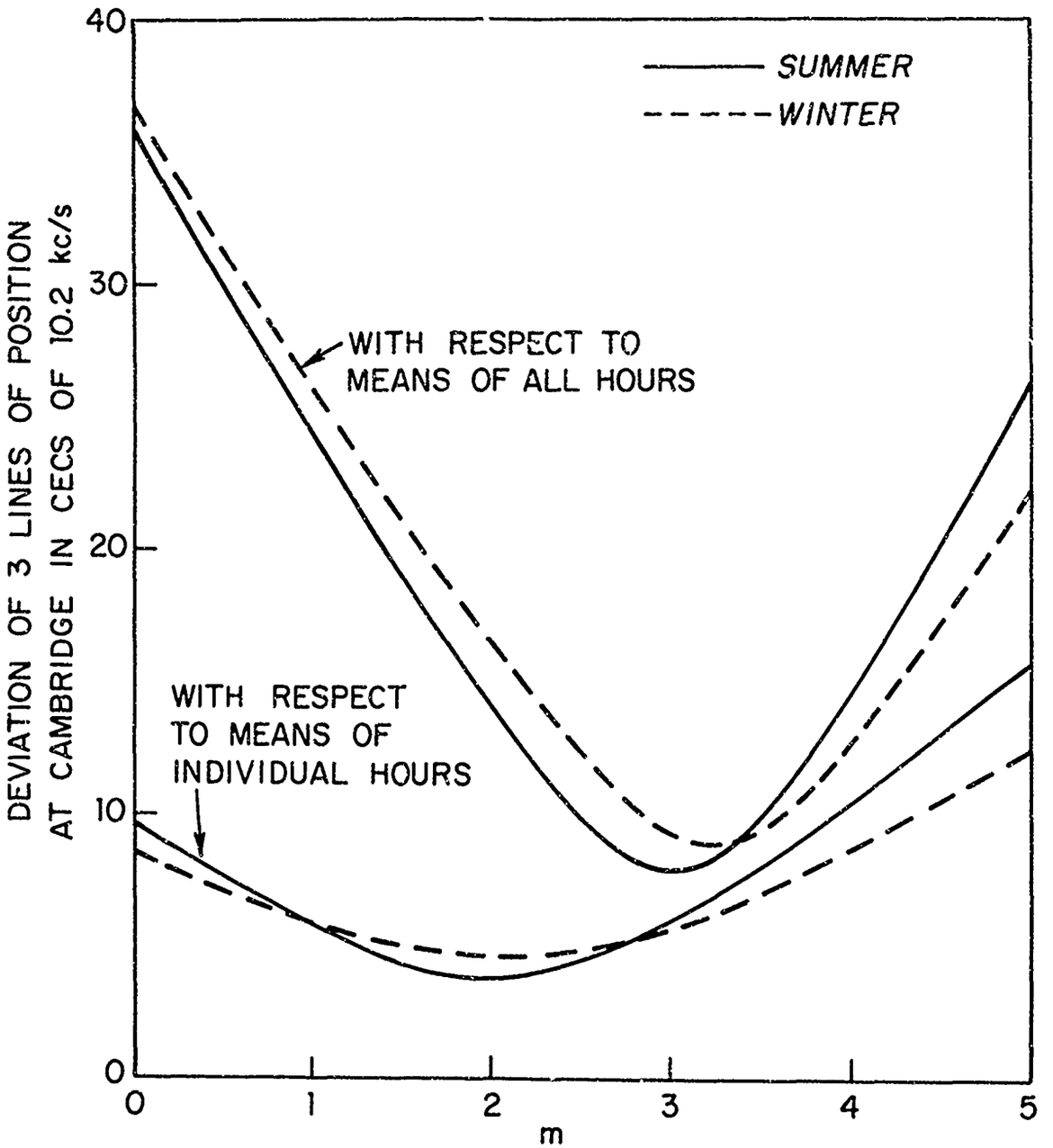

Figure 7: Summer and Winter Variation of Standard Deviation as a Function of m, with and without Diurnal Correction.

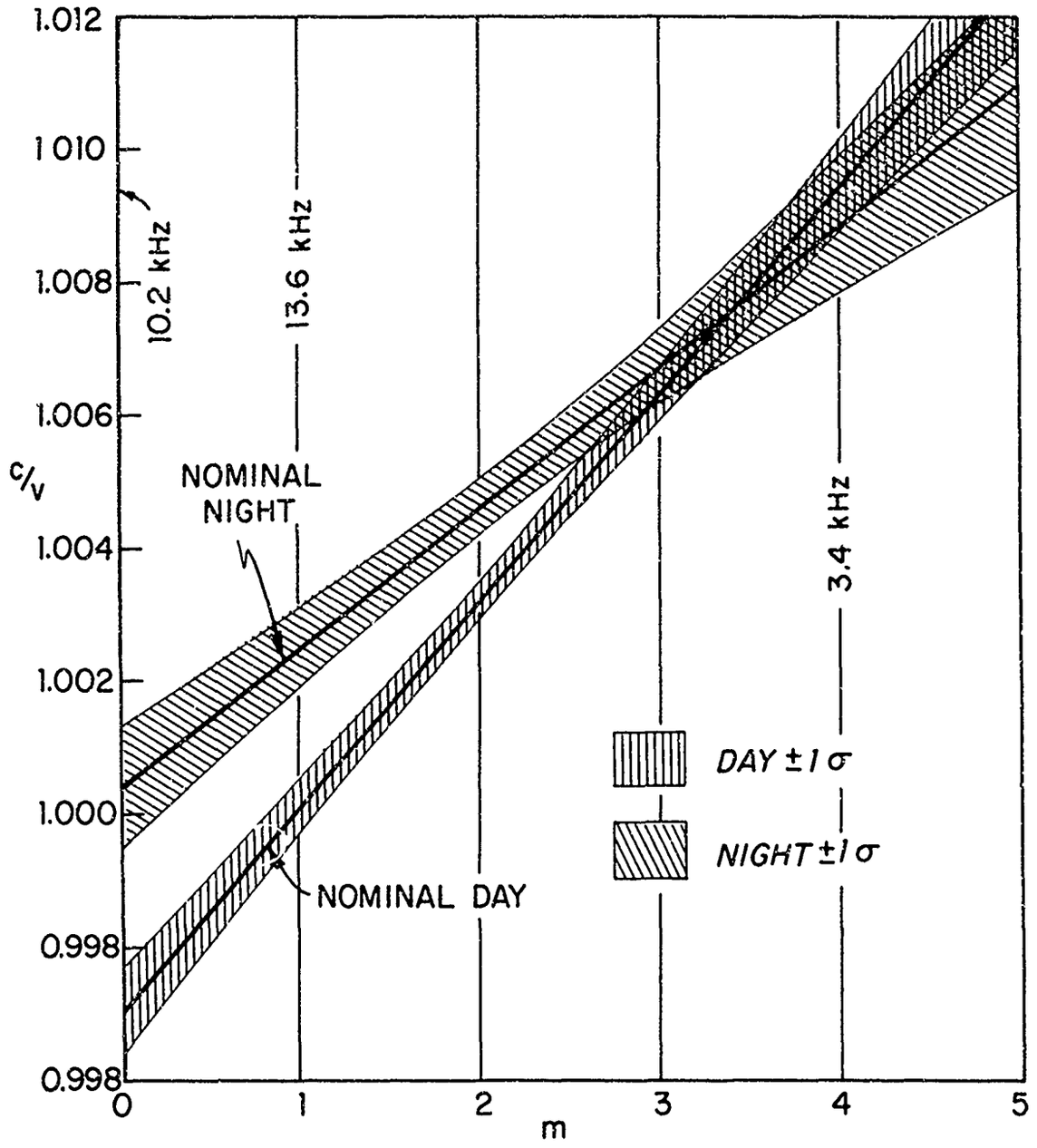

Figure 8: Day and Night Nominal Reciprocal Velocities as Functions of m.

5. A NOTE ON DETERMINATION OF THE ZERO OF OMEGA TIME

To validate occasional examples of the time of arrival of the signals from a single Omega station (which has already occurred in the cases of Fig. 1 and Fig. 5) it is necessary to establish the difference between the time scale of the Omega stations and that of the local clock at the receiving point. This is done by comparing the 24-hour means of various times of arrival with the corresponding means predicted by the U. S. Navy.[11] A determination of clock error can be made each day, for example, in terms of the 10.2 kHz signal from Trinidad. The precision of this determination can be estimated by intercomparison with similar measurements for other stations and at other frequencies. An example of such data for a period of ten days in October, 1972, is shown in Table III. This period was chosen as one in which there were fairly large discrepancies between stations while the local clock showed good consistency.

TABLE III

Mean Cambridge Clock Errors and Standard Deviations
for 15-24 October, 1972
in Centicycles of 10.2 kHz

With Respect to	Value of m		
	0 (10.2 kHz)	1 (13.6 kHz)	9/4
Norway	32.4 ± 3.9	28.3 ± 2.3	22.8 ± 0.9
Trinidad	19.0 ± 1.0	19.1 ± 1.2	18.9 ± 2.0
Hawaii	26.3 ± 1.3	25.4 ± 1.1	24.7 ± 1.2

The large differences for the various measurements on Norway are caused primarily by vagaries (and difficulties in prediction) in propagation in the arctic region. An example of this was shown above in Fig. 2. The standard deviations for the carrier frequencies are correspondingly large. Trinidad, on the other hand, shows excellent agreement between the mean values, and the carrier-frequency standard deviations are smaller than that for the composite signal. Hawaii exhibits both good agreement and uniform standard deviations.

It is the writer's custom to determine the mean clock error each day for the carrier frequencies using all stations except Norway, and also to measure the means for all stations for the 9/4 composite signal. These two mean determinations for the block of data cited in Table III are:

Carrier frequencies (excluding Norway)	Mean 22.5 Cecs	Standard deviation 2.1 Cecs
Composite signals (including Norway)	Mean 22.1 Cecs	Standard deviation 1.4 Cecs

The size of these last standard deviations indicates that the close agreement between the two determinations of the mean is fortuitous. Experience over several years, however, shows that these two daily determinations usually agree to two or three centicycles (of 10.2 kHz) and that the mean of the two determinations is probably accurate to at least the same order.

6. NOISE

Before further discussion of the uses of composite signals, it is necessary to examine the effects of noise. In a phase-measuring system, noise may be regarded as any temporary disturbance of an observed phase.

Such disturbances may be produced by actual atmospheric noise interfering with the desired signal, by fluctuations in propagation time that have no known correlation in time or frequency, or by instrumental uncertainties that vary from time to time.

Atmospheric noise is the first and most serious problem. In the Omega spectrum one may be so unfortunate as to "hear" all of the hundred lightning flashes that occur each second, on the average, somewhere on earth. These noise impulses are very large, as thousands of amperes flow in a miles-long column of ionized air and radiate energy much more powerfully and efficiently than do any man-made transmitting antennas. The current transients are very short, building up in a few microseconds and dying in a somewhat underdamped way in a few hundred microseconds. They therefore radiate relatively simple pulses of short duration in comparison to the spaces between them. The radiation covers a wide band of frequencies, but is most intense near five kilohertz. Because this frequency is poorly propagated in the earth-ionosphere waveguide, the impulse at a considerable distance settles into an oscillating pulse of non-uniform frequency and a few cycles duration, having a quasi-period controlled by the interval of 50-100 microseconds typical of the time delay between successive multiple reflections in the propagation medium.

This lightning impulse, as received, has its maximum energy near 10-12 kHz, or exactly in the Omega frequency band. Field strengths produced at the receiving antenna may be of any size up to many volts per meter, depending upon the distance from the lightning source. Because desired Omega signals often have a field strength no greater than 10-100 μv/m, no linear receiver having enough gain to utilize the Omega signals could avoid being overloaded by the noise impulses. This overloading may

saturate an iron-cored inductor in a tuned circuit, changing its inductance and therefore its phase shift, or it may cause unwanted rectification in amplifiers, creating spurious transient biases that react upon the observed phase of a signal. These saturation effects must last longer than the reciprocal of the bandwidth of the circuit being saturated, and may last many times longer, depending upon the time constants of the circuits and the degree of overloading.

The cures for this kind of behavior are either to limit the amplitude that can be produced in a circuit, or to close a gate when a noise impulse is observed so that the impulse cannot reach a sensitive part of the receiver or measuring circuitry. By one of these techniques, the measurement of the phase of a signal can be restricted to those times when the signal exceeds the instantaneous noise level. With hard limiting there is always an output of full amplitude whether it be due to signal or noise or a combination of the two. The noise components, however, have no stable phase and, in a phase detector, approach zero output with increasing integration time. Gating, on the other hand, should remove all output from a phase detector during the noisy intervals and therefore ought to be preferred. This improvement can be achieved in a perfect digital system, no doubt, but the writer has never managed to produce an analog gating system that was preferable to a good hard-limiting system, partly because it is difficult to establish a gate threshold that is not considerably above the signal level.

The requirements for a good receiver channel are easy to state, but are not often realized without great care and effort. The most important statement is that between limiters the receiver should be absolutely linear. Selective circuits must not have phase characteristics that change with the

amplitude of a signal or with signal-to-noise ratio. Limiters themselves must have essentially infinite bandwidth and be accurately symmetrical. "Excess" selectivity must be provided so that the effective bandwidth is not greatly different for very weak signals or heavily-limited ones.

In practice, these criteria require that not more than 20-25 db of gain be achieved between limiters, and less should be used in the later stages of the receiver. The writer usually has four such distributed limiters in a fixed-station receiver designed to operate with a large antenna and relatively low overall gain. Mactaggart[12] has described a very carefully-designed aircraft receiver which uses seven limiters in each radio-frequency channel.

One of the reasons for this lecture on relatively obvious matters is that the writer has generally found that they are not understood. Only one out of many receivers brought to him for examination has been satisfactory in these various respects. A more immediate reason for introducing this discussion at this point is that the behavior of a difference frequency or one of the recommended composite signals will not be satisfactory unless the noise rejection in the receiver is excellent.

The reason for the requirement for greater rejection of noise for composite signals than for carrier-frequency signals can be found from Eq. (22) (to be derived later), by setting the correlation coefficient between frequencies to zero. The results of this solution are shown in Fig. 9, for three values of $\sigma_{13.6}/\sigma_{10.2}$. The minima between $m = 0.5$ and $m = 0.7$ indicate the obvious fact that the smallest error from the uncorrelated signals will be attained by using their average, properly weighted. For values of m greater than unity, the curves of Fig. 9 become quite linear, and the values of $\sigma_c/\sigma_{10.2}$ are seen to be approximately equal to

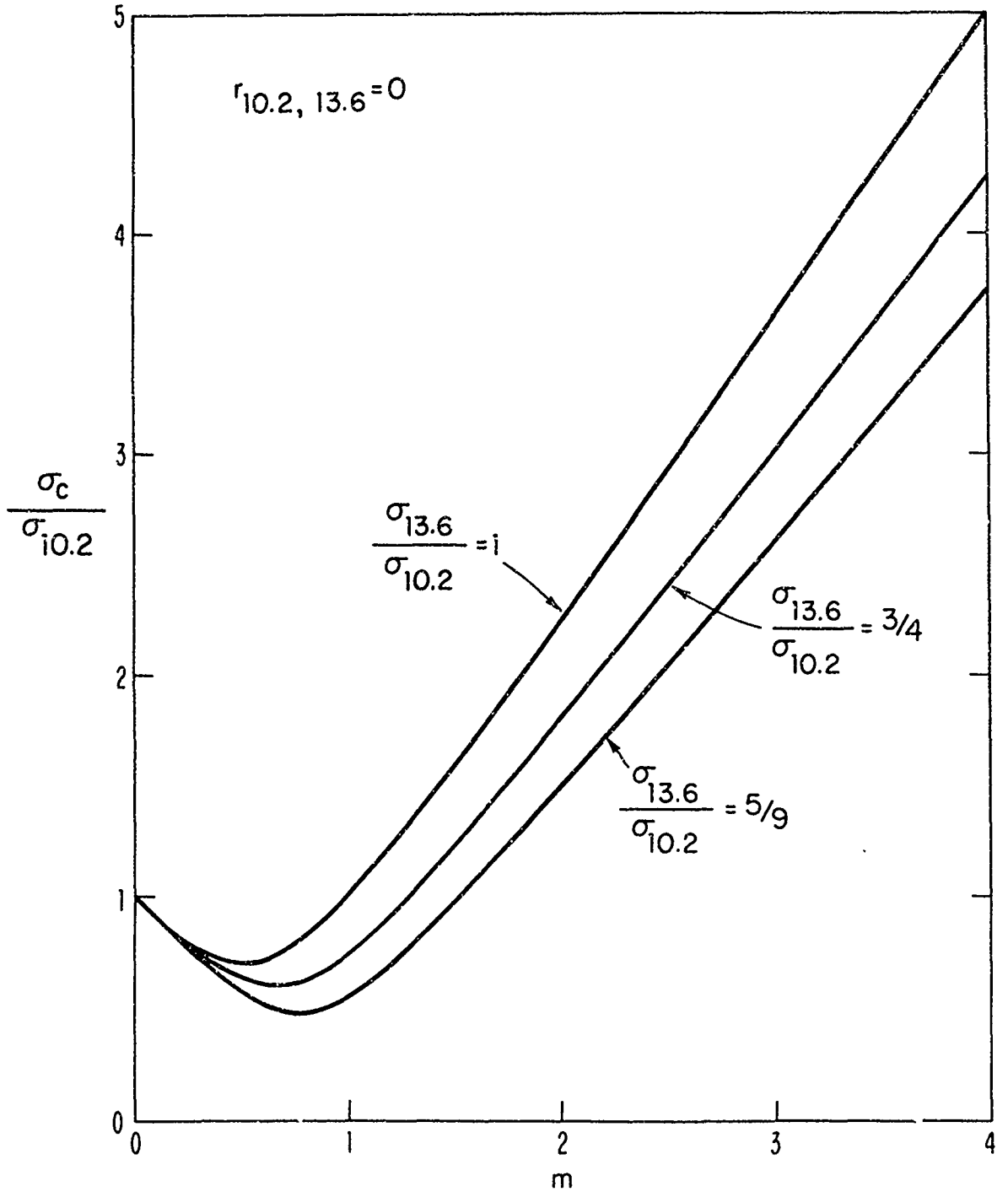

Figure 9: Standard Deviation of Composite Signals referred to 10.2 Kilohertz, under Conditions of Zero Correlation.

m. This means that the effects of noise upon phase errors will be about four times as great at the difference frequency 3.4 kHz, where $m = 4$, as at the carrier frequencies at $m = 0$ and $m = 1$.

Figure 9 also helps to explain the location of the minimum of standard deviation for the Trinidad signal at Cambridge, which was near $m = 1$ for the example shown in Fig. 3. In the case of this signal, the propagational fluctuations are usually small and the noise contributions add a relatively large quantity of uncorrelated error components. Another way of describing this effect is to say that if noise be added to perfectly-correlated signals that show a minimum of standard deviation at, say, $m = 9/4$, the vertex of the parabola relating standard deviation to m must move toward higher standard deviation and toward lower m, until the condition of Fig. 9 is approached as a limit.

Fortunately, as will be shown later, the uncorrelated component of propagational phase fluctuations appears to be very small. It follows that good measurements of the composite signals may be made if the effects of atmospheric noise (and of instrumental uncertainties) have been reduced to a minimum. Part of this reduction can be achieved through integration, but the first and most important steps must be taken through careful design of receiver channels.

7. AMBIGUITY

It is not too early in this discussion to issue a serious warning: it is an inconvenient fact that thoughtless use of composite signals can make lane identification (the choice of a whole number of periods) impossible. This subject requires careful explanation.

The utility of Omega, or any other VLF aid to navigation, has its

cornerstone in the observed fact that the time of transit of a low-frequency signal has good day-to-day repeatability, although there is a characteristic day-to-night variation that is larger than we might like. It is conceivable that, by perfectly continuous signal tracking, a navigation aid might be made useful if the long-term standard deviation (at a given hour of the day) were as large as a carrier period. The prospect, however, would be discouraging, especially if the quasi-period of variations in time were short.

Fortunately, at the lowest frequency used in Omega, the observed standard deviation of the time difference between the two signals of a pair is typically about 1/10 period. This ratio offers a good probability that if a "cycle count" should be lost it can be recovered in one way or another. The possible ways are determined primarily by the wavelength, which is about 16 nautical miles, or 30 kilometers, at the frequency cited. Since a navigator can move directly toward one station of a pair while moving away from the other, the phase difference between the signals of the pair can change by 360 degrees for a distance of 1/2 wavelength. Thus the minimum ambiguity at 10.2 kHz is about 15 km or 8 nautical miles. This distance is large enough for a celestial fix, for example, to provide an external way of resolving the Omega ambiguity.

The reason for the multiple ambiguities in Omega is that only the relative phase of a signal is measured while it is necessary, or at least advisable, to transmit a burst of signal lasting some 10,000 carrier periods. In Loran A, by contrast, a single relatively-short pulse is radiated at a very low repetition frequency, so that the sequence of signals from a pair of stations is interlaced, with master and slave pulses always arriving alternately at the receiver. There is thus no ambiguity, except for the trivial question of which side of the baseline the navigator is on.

Loran C is a system intermediate between Loran A and Omega. Here accuracy is increased by measuring the relative phases of carrier-frequency cycles. This is done, however, with a large relative bandwidth so that the envelope of each pulse rises to maximum amplitude in about eight or 10 carrier periods. It is thus possible to examine the shape of the pulse envelope and identify a particular carrier cycle as the one occurring at the point of inflection of the envelope, or by some other similar definition. This process is facilitated by using very high-powered transmitters so that the pulse shapes are not too seriously affected by atmospheric noise.

Omega operates at a frequency about ten times lower than that of Loran C, but unfortunately is constrained by technical limitations (chiefly the very low radiation resistance attainable in antennas at the Omega frequencies) to use bandwidths many times narrower than those found useful for Loran C. This means that each Omega "pulse" rises to maximum in 100 to 200 carrier periods or at least 10 to 15 milliseconds. This length of rise time is common to all VLF transmissions. Its meaning for navigational purposes is illustrated by recalling the writer's fascination with the idea that the seconds pulses radiated some years ago from the Naval radio Station in the Panama Canal Zone had a rise time greater than the transit time from Panama, so that each beginning could be detected at Cambridge before the transmitting antenna current had reached full amplitude in Panama.

Because the Omega transmitter power level is a hundred times less than that of Loran C, while the atmospheric noise is greater and signals are used at much greater distances, it is hopeless to think of lane identification through use of the "pulse" envelope, although this method may be of some use in coarse determination of approximate position.

The internal method for lane (or cycle) identification in Omega[1] is the

use of several frequencies so spaced that the beats between them are at sub-multiples of the carrier frequencies. Unfortunately the precision of phase measurement is so poor, because of propagational uncertainties and poor signal-to-noise ratios at typical distances, that this process must be carried out in a number of stages. The first step, and the most difficult one, is the selection of one out of each successive three periods of 10.2 kHz, by measuring the phase of 3.4 kHz signal obtained by beating the 10.2 kHz carrier with a second carrier at 13.6 kHz.* The difficulty in this process stems primarily from the variations in dispersion. If one assumes, as shown in Fig. 7, that the typical standard deviation at 10.2 kHz (m=0) is 10 centicycles while the standard deviation at 3.4 kHz (m=4) is 15 centicycles of 10.2 kHz, he might deduce that the standard deviation of the difference between 10.2 and 3.4 kHz would be about 18 centicycles of 10.2 kHz. As this value is reasonably small in comparison with the critical limit of 50 centicycles or 1/2 period of 10.2 kHz, a fair reliability would be falsely deduced. The error in this estimate lies in the neglect of a negative correlation between the times (or phases) measured at these two frequencies. The effects of anomalous propagation show a distinct tendency to be -7/9 as large at 3.4 kHz as at 10.2 kHz, and diurnal effects also show a negative correlation of different ratio. The positive identification of a 10.2 kHz period in terms of 3.4 kHz can therefore not always be guaranteed when propagational conditions are difficult.

Frequency differences at and below 3400 Hz (of which only 1133 1/3 Hz is transmitted at present) all travel at the group velocity of the medium rather than the phase velocity appropriate to the carriers. Although there are minor differences between frequencies due to non-linearity of the

*This discussion frequently takes the form of speaking of a single signal. In practice, however, measurements are usually made of the differences between signals of a pair. This makes no difference at the core of the analysis.

dispersion, these differences are so small as to be relatively unimportant. In summary, it now appears that lane identification from lower frequencies up to 3400 Hz will show considerably greater reliability than will identification of 10.2 kHz or the other carrier frequencies. This difference may be of operational significance for some purposes, and it will be further examined in another section of this paper.

The reason for the warning with which this section begins is as follows. The use of a composite signal, as shown in Eq. (6) among others, involves taking the difference between quantities each of which is a time multiplied by a factor ordinarily greater than unity. The potentially-unfortunate results are best shown by an example. Suppose the frequencies to be 10.2 and 13.6 kHz. For minimum standard deviation Eq. (12) shows that m_o should be 9/4, and the multiplying factors for Eq. (6) are 2.25 for $T_{13.6}$ and 1.25 for $T_{10.2}$.

The 10.2 kHz signal is ambiguous in quanta of 100 Cecs, so its contribution to the composite time is ambiguous in units of 125 Cecs. At 13.6 kHz, the cyclic ambiguity is 75 Cecs (of 10.2 kHz) which is multiplied by 2.25 to give 168.75 Cecs as the unit of ambiguity. To leap immediately to a worst case, suppose there to be a miscount of 3 cycles of 13.6 kHz and a simultaneous mis-estimate of 4 cycles at 10.2 kHz, in the same algebraic sense. The resultant error of the composite time would be 4(125) - 3(168.75) = -6.25 Cecs of 10.2 kHz. Because the propagational standard deviations tend to be larger than this quantity, and because simple patterns of cyclic errors can be constructed to yield a net error that is any multiple of 6.25 Cecs of 10.2 kHz, the possibility of direct lane identification for this specific composite signal is essentially zero.

For other values of m in Eq. (6), the details of such a calculation vary widely, but in every case we find that a new kind of ambiguity has been added to the problem of lane identification. This observation leads to an important rule: if lane identification is required, it must be established through direct use of the carrier- and difference-frequency times. After this has been done, the times determined through the lane-identification process can be used to gain the advantages of composite signals without introducing further ambiguities.

This entire subject will be carried further when we are ready to examine the possibilities of ambiguity resolution on a world-wide basis, which would permit a number of useful services that cannot now be performed by Omega.

8. DISTRIBUTION OF DEVIATIONS

"Ordinary" deviations from a long-term mean or, hopefully, from a predicted transmission time may be attributed to minor fluctuations in the height of the lower ionosphere. There are, however, two kinds of unusual disturbances that have been mentioned above: the sudden ionospheric disturbance (SID) and the polar cap anomaly (PCA). Both of these are abnormal depressions of the height of a given contour of ionization caused by an increase in energy received from the sun. The SID is associated with a solar flare that emits an unusual amount of ultra-violet and X-ray energy. Because this burst of energy travels at the velocity of light, the ionospheric effects are coincident with the visible flare on the surface of the sun and are detected only on the sunlit hemisphere of the earth. The SID, like the flare, typically builds up to a maximum in 5 or 10 minutes and

frequently subsides within an hour. The PCA is caused by the emission from the sun of an unusual number of charged particles of which the most important are probably protons. Because of their charge, these corpuscles generally penetrate to the lower levels of the ionosphere more or less along the lines of the earth's magnetic field and arrive in maximum numbers in the circumpolar zones recognized by their maximum auroral activity. The PCA is therefore primariiy a phenomenon observed on trans-arctic propagation, such as on the path from Norway to Cambridge. Some of the charged particles producing the PCA occasionally travel at half the speed of light, but the majority (even from the same solar event) take several hours, or even days, to reach the earth. Because of this distribution of velocities in a corpuscular outburst, a PCA is a relatively long-lasting phenomenon that may take ten days or more before its influence becomes negligible. The effects are usually somewhat greater in the daytime than at night.

Since both kinds of anomalies reduce the height of the layer, we find that the distribution of deviations from the normal or the mean value are considerably skewed. It is seldom that the propagation time of a carrier-frequency signal exceeds the normal by more than one or two standard deviations, but there may be very large reductions from time to time. In the case of a difference frequency these statements are, of course, reversed, because of the reciprocal behavior of variations in phase and group velocities that we have discussed above.

This reversal, with the intermediate case of the 9/4 composite, is shown in the form of histograms in Fig. 10. The data for this figure represent noon-time conditions for the Norway-Trinidad pair in a two-year period near the last maximum of solar activity. The deviations are

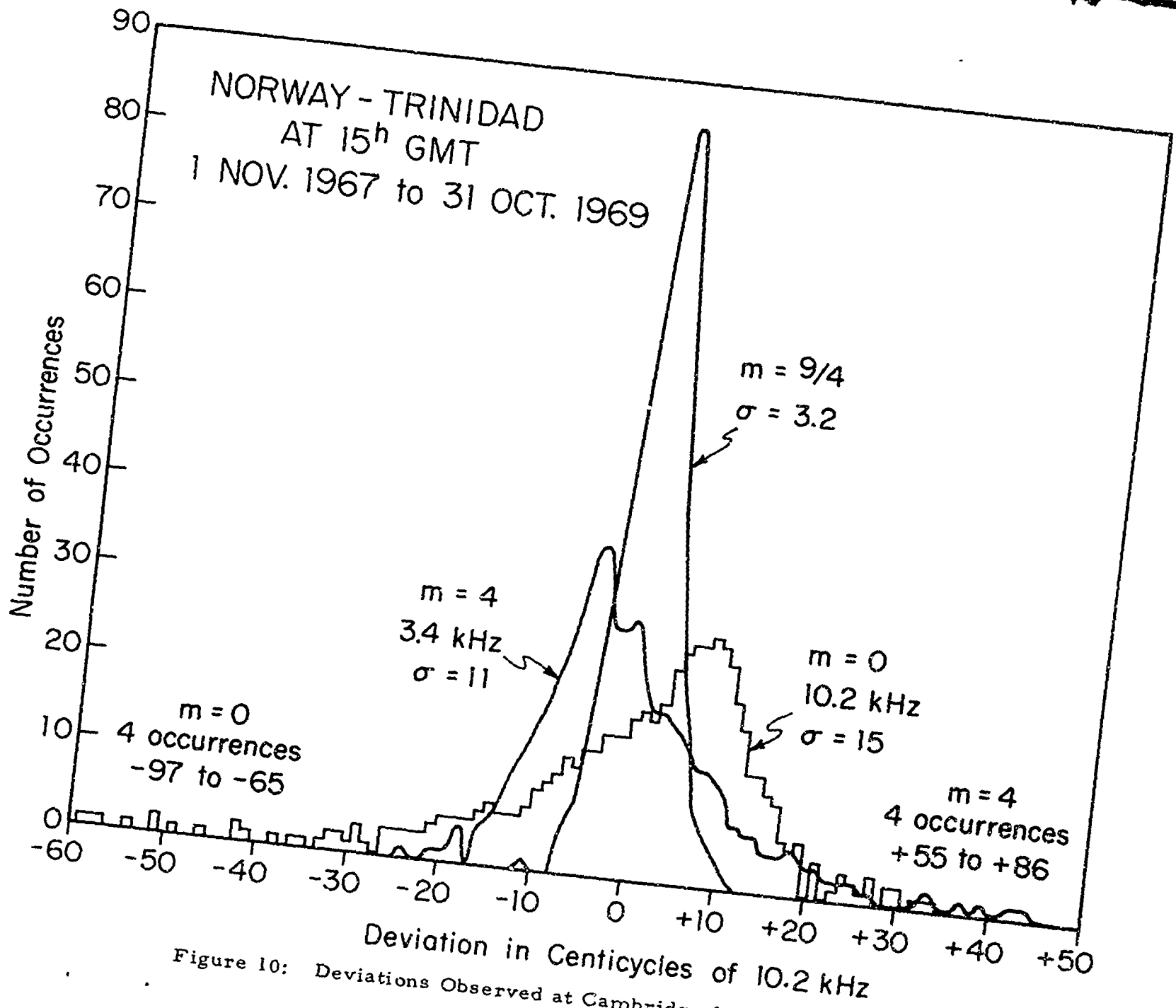

Figure 10: Deviations Observed at Cambridge for Three Values of m.

therefore larger, and anomalies more frequent, than for average conditions, and especially more than at the time of writing, near a minimum of activity. Three different styles have been used in connecting the plotted points of Fig. 10, in the hope of making the distinctions between the three curves as clear as possible. The deviations were, as need hardly be said, taken with respect to the means of the entire two-year period. The long negative tail at 10.2 kHz and the positive one at 3.4 kHz are obvious. The distribution for $m = 9/4$ is reasonably near the gaussian.

Similar data for the same dates are shown in different form in Fig. 11. Here the observations include a single daytime and a single night-time point for each day, for each of two pairs. The data therefore represent both day and night and both high- and low-latitude characteristics. They are plotted as the probability of a deviation being exceeded, without regard for algebraic sign. The curve for 10.2 kHz exhibits the ordinary characteristics of this function. There is a relatively gaussian variation down to 0.1 probability or less, with an essentially negative-exponential variation at the lower probabilities. A straight line fitting the exponential tail would intercept the probability axis near 0.1. This presumably indicates that, at this active part of the solar cycle, about ten percent of the measurements could be identified as abnormal. Averaged over the entire solar cycle, the corresponding figure would probably be near three percent.

Except for the reversal of sign (not shown in Fig. 11) the overall characteristics of the 3.4 kHz distribution do not differ greatly from those at 10.2 kHz. There is little difference near the top of the curves, and something like the 7/9 ratio mentioned in Section 6 can be seen in the low probabilities. For $m = 9/4$ the deviations are about half as large as for

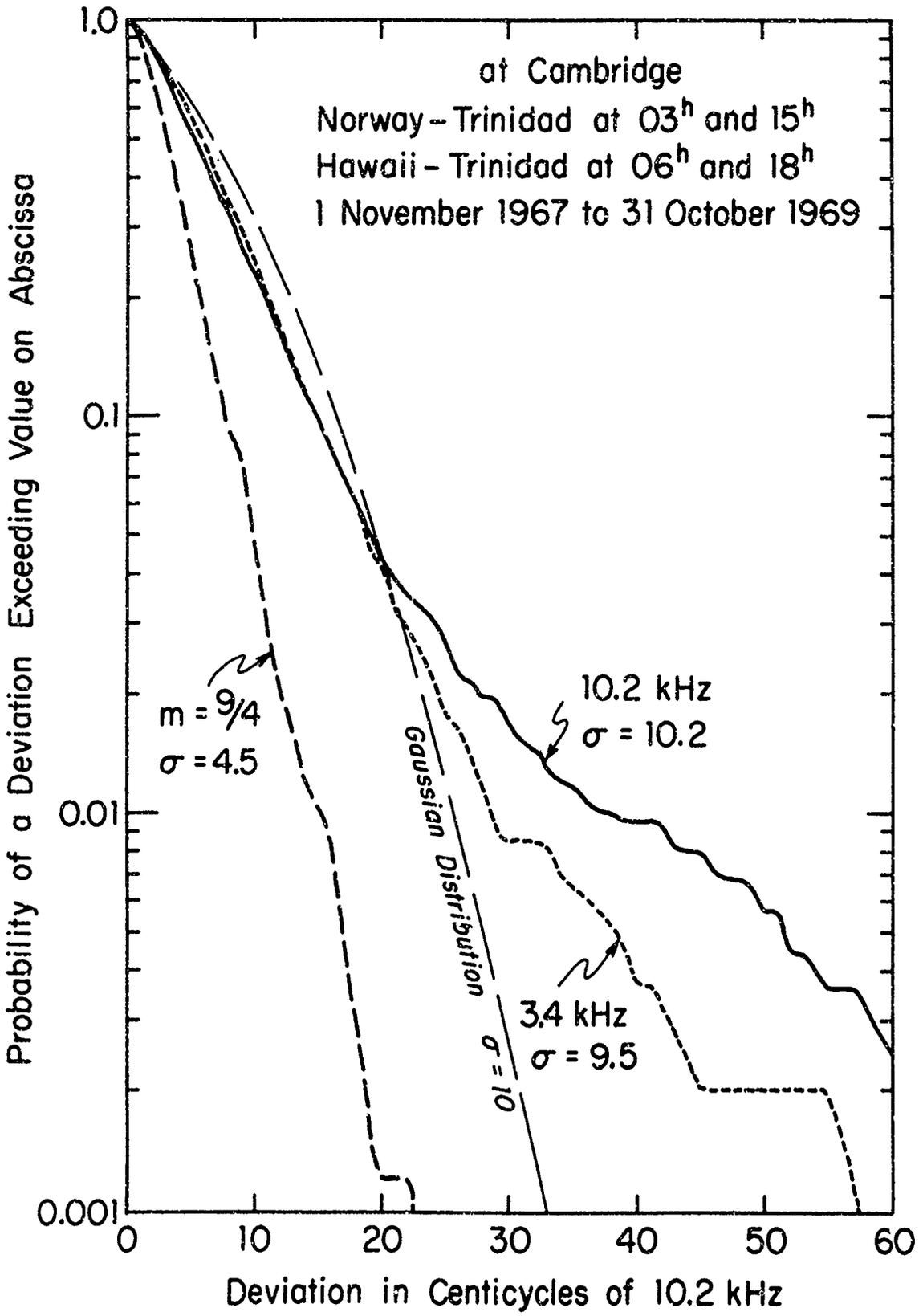

Figure 11: Probability of Exceeding Deviations for Three Values of m.

10.2 and 3.4 kHz, and the exponential tail is much less evident.

The fact that the 3.4 and $m = 9/4$ deviations are as small or smaller than those at 10.2 kHz does not indicate that those composite signals are to be preferred for all purposes. It has been shown in Section 6 that the effects of atmospheric noise are worse for the composite signals (because of the multiplication discussed above). As a result, the minute-to-minute variations are considerably larger for the composites. The composite deviations, however, seem to vary about a more long-term-stable mean, probably because the group velocity is inherently more uniform than is the phase velocity in the dispersive medium. The carrier-frequency signals, in comparison, are relatively constant in phase for minutes, or even hours, but show greater changes from day to day than do the composites. The long-term rms values, as shown in Fig. 11 are very similar. It remains true, however, that tracking speed and sensitivity to motion through small distances are much superior for the carrier frequencies.

9. ERRORS OF PREDICTION

The navigational error, in a system like Omega, is equal to the difference between an observed phase and one predicted for the position of the navigator. When ground-wave propagation can be used, as in Loran, predictions can be made with excellent accuracy. In Omega, on the other hand, predictions[13] can, at present, only be made in terms of the dominant waveguide mode. Dimensional instability in the waveguide and lossy surfaces that cause variations in the phase shifts at reflection combine to make the prediction uncertain. Phase shifts due to received

noise and undesired higher-order modes in the waveguide also induce fluctuations that must be accepted as errors.*

It is an unwelcome fact that the errors of prediction in Omega are at present generally larger than the standard deviation of the observed signals. It is to be expected that this dominance of prediction errors may eventually be overcome under the influence of further observation and study, but this fraction of the total error will always be important.

Omega could not be successful were it not for the fortunate fact that all useful signal components travel at nearly the velocity of light. Conditions that cause relatively large variations in phase velocity (transmission across the polar ice-caps, for example, with their abnormally low ground conductivity) are also conditions that induce large losses. There is therefore a filtering action, so that at long distances those signal components traveling at about the speed of light are dominant. This is a wordy way of saying that the various conditions affecting the velocity of a signal must have relatively small coefficients, usually of the order of a part in a thousand or less.

Most important among the factors included in the Navy computer program for phase velocities are:

1. Radio frequency
2. Time of day, } which define the altitude of the sun
3. Time of year, }
4. Excitation phase of the signal in the waveguide
5. Path shortening (A recognition of the fact that the layer height

*The writer tends to believe that the second mode will presently be found to be sufficiently stable to permit rough prediction. This would provide some increase in accuracy and a very considerable improvement in the reliability of lane identification.

directly over a transmitter or receiver is unimportant because the rays or modes propagate at low angles above the horizontal)

6. Conductivity of the surface of the earth along or near the transmission path

7. Direction of propagation with respect to the magnetic field of the earth.

8. Geomagnetic latitude

9. Geographic latitude

10. Solar activity index, and

11. Special terms under time of day representing sudden photo-detachment of electrons from negative ions at sunrise and re-attachment at sunset.

It is obvious that not all of these factors are independent. For example, the changes of velocity with direction of propagation also depend upon latitude. Clearly, determination of the coefficients and even the laws relating velocity to these factors can only be done approximately until many more studies have been carried out. The Navy's "Sky Wave Compensation" tables[11] are revised from time to time as additional knowledge is acquired, so that operational accuracy is improving with the passage of time. It is unfortunate that the information stored in the Navy tables is cumbersome and difficult to use. More and more interest is being evinced in the use of computer type receivers that calculate the required velocities as they go. This creates a desire for simpler computation programs, provided that they do not too seriously degrade accuracy. Some progress has been made in programs that "truncate" the Navy program to reduce the computation time and memory capacity required.

The writer has for some time been interested in the use of "nominal" velocity calculations of almost absurd simplicity. These are based upon a single phase velocity for each frequency in the daytime and another at night. These two are combined by simple interpolation, dependent only upon the fraction of each transmission path illuminated at the chosen time. All of the factors in the tabulation above are neglected, except the first three.

When examined carefully, this approach is found to have lost or blurred much useful detail. It is surprising, however, to find that the root-mean-square errors, averaged over long periods and for many transmission paths, are very satisfactory. The nominal values used for the frequencies 10.2 and 13.6 kHz have been given above in Table II in Section 4. Corresponding values for other frequencies will be defined later.

To exhibit the navigational errors for various circumstances, it is convenient to plot the rms error against m. Such a diagram shows at once the effects for the carrier frequencies 10.2 and 13.6 kHz (at $m = 0$ and $m = 1$), for the difference frequency ($m = 4$) and for other values of m. In each case the standard deviation (σ) is plotted as the limit that would be approached if the errors of prediction were reduced. It might be mentioned that at Cambridge an error of about 11 Cecs of 10.2 kHz is equivalent to one nautical mile in position, for each of the pairs. In the following figures the rms values plotted are for all 24 hours of the day, taken separately.

Figure 12 shows the variation of errors for each of the long-distance pairs observed in Cambridge in February, 1969. The Navy calculations upon which the "Navy" errors were based are those for 1972, as it is demonstrable that the improvement in prediction techniques greatly outweighs any change with date. The "nominal" predictions were made as

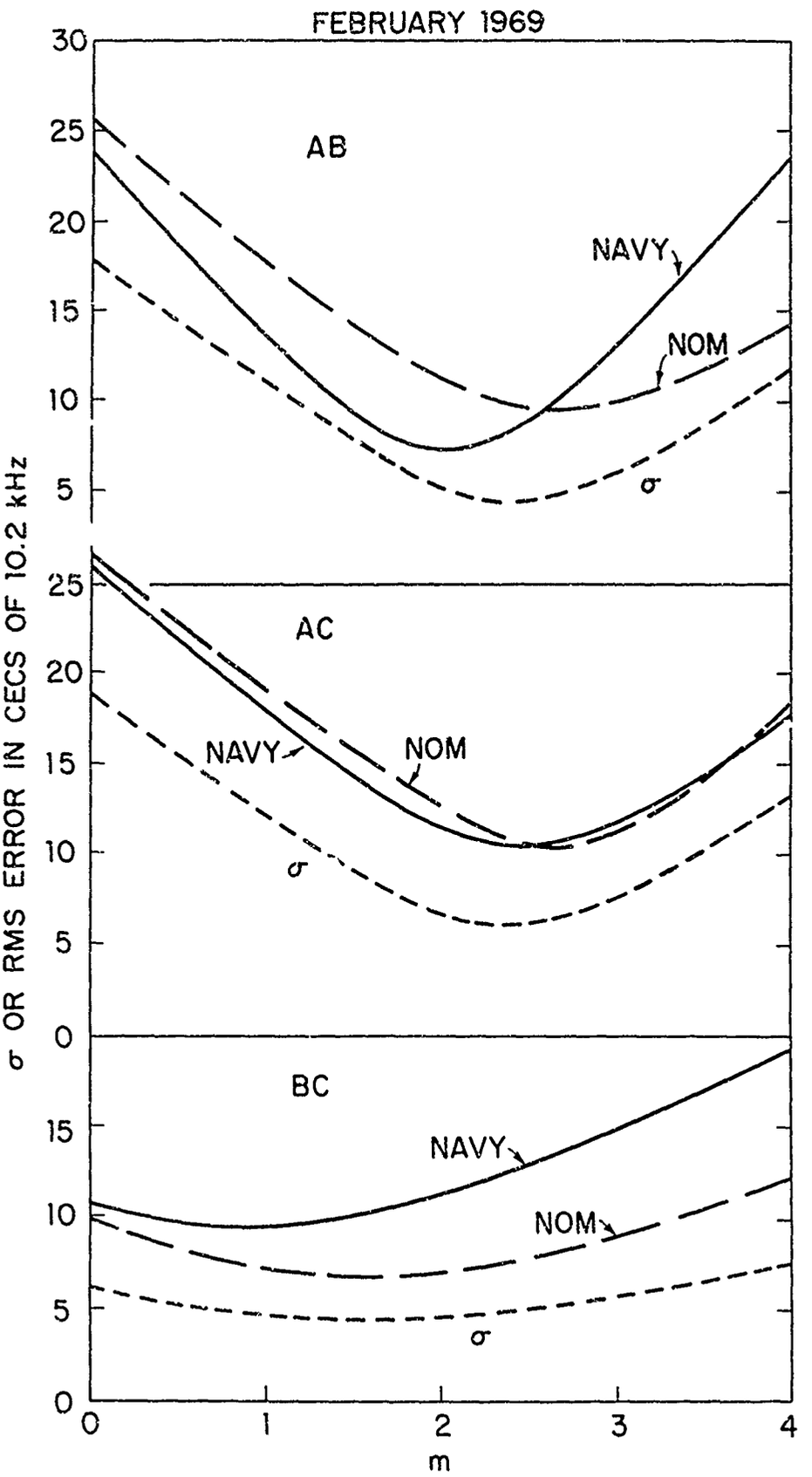

Figure 12: Root-Mean-Square Errors versus m, for Three Pairs at Cambridge.

described above with time and frequency the only variables. For the AB pair, the Navy predictions are seen to be distinctly better at the carrier frequencies and actually to approach the optimum near $m = 1.5$. For the difference frequency (3.4 kHz or $m = 4$), however, the Navy prediction errors are much larger than the nominal ones. There is little to choose between the prediction methods for the AC pair, where the 3.4 kHz errors are seen to be distinctly smaller than those at 10.2 kHz. For some curious reason, probably accidental, the nominal values are better than the Navy ones for all values of m for the BC pair.

In Fig. 13 we have plotted the root-mean-square values for all three pairs combined, in the hope that this is relatively typical of navigational experience. This figure is given primarily to show that a diagram of this kind can vary considerably from one sample to another. The errors for the nominal calculations are, as they should be, greater than those with respect to the Navy tables, except in the region of large m in December.

Figure 14 shows, it is hoped, a fair average of Omega behavior. It is for a period intermediate between high and low solar activity. The term "annual" means that it is made up of six samples uniformly distributed through the year. It shows, interestingly enough, that the Navy predictions are better for the carrier frequencies, but that the nominal calculations average a little better for the difference frequency. In either case the rms navigational errors are substantially twice the propagational standard deviations, indicating that much improvement in prediction techniques is still possible.

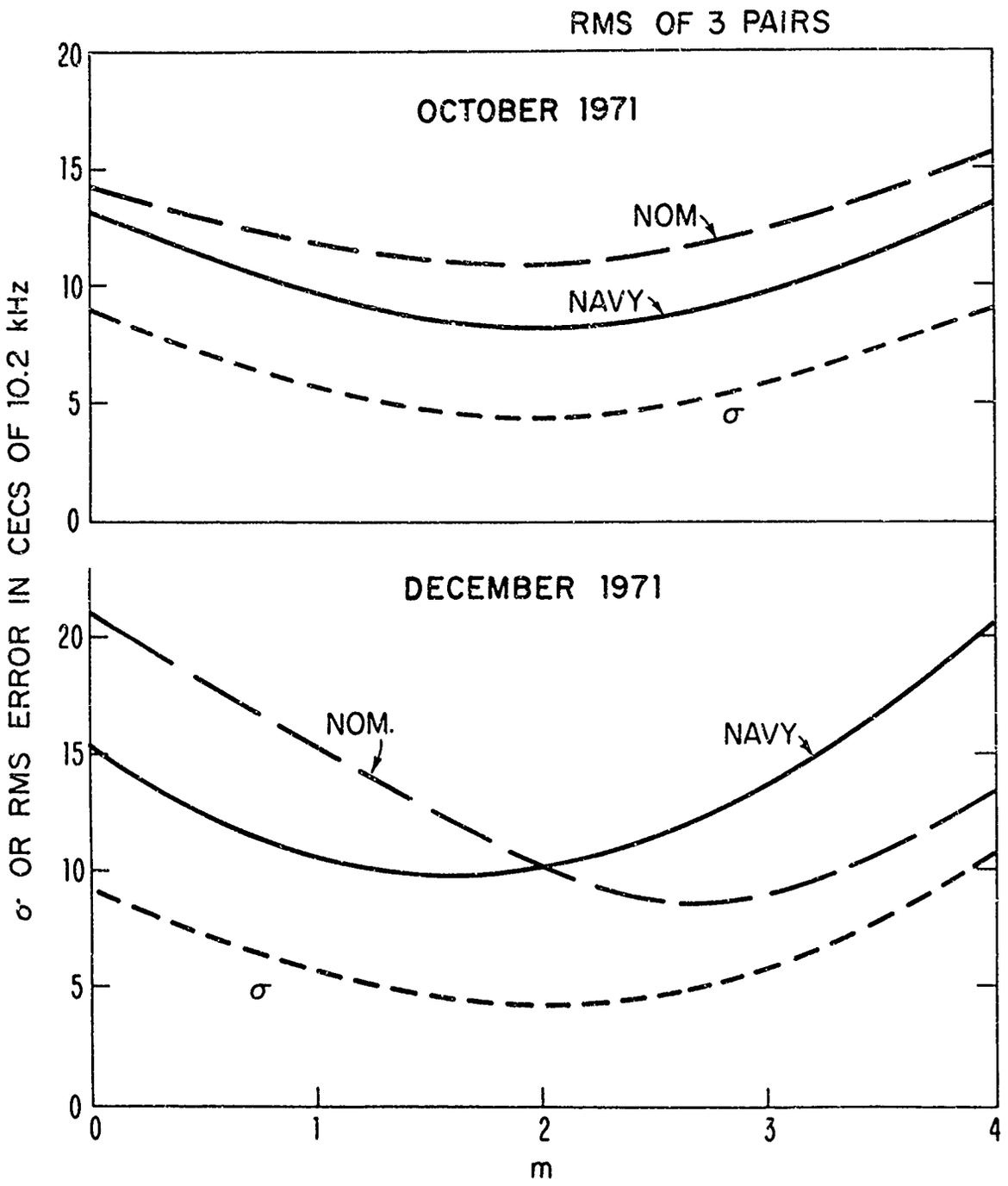

Figure 13: Root-Mean-Square Errors at Cambridge, for Two Dates in 1971.

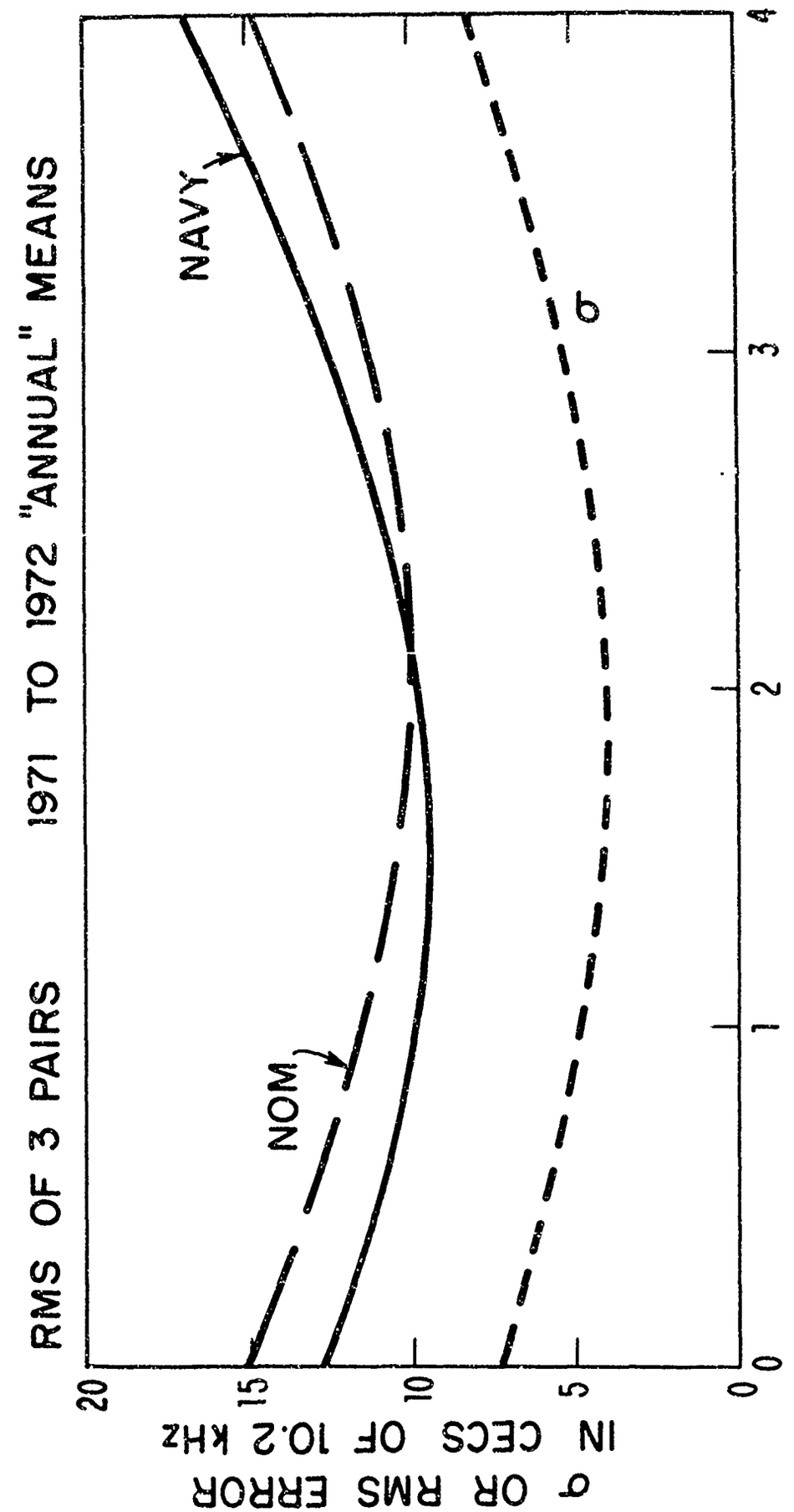

Figure 14: "Annual Mean" RMS Errors at Cambridge as a Function of m.

10. CORRELATION

It is found that at Omega frequencies, the 20-km day-to-night variation in height of reflection (with accompanying changes in conductivity) leads to relative changes of two or three parts in a thousand in the time of transmission of a signal. This diurnal variation is an order of magnitude larger than the root-mean-square value of the random variations ordinarily observed. The random fluctuations in a time, or time difference, measurement thus correspond to fluctuations of the order of 2% of the height of the base of the ionosphere. Two conclusions follow upon consideration of this magnitude:

(1) It is not likely that there will be much correlation between the times of arrival of signals from stations thousands of miles apart, as atmospheric influences are likely to vary considerably over such distances and presumably affect the height of the layer.

(2) If propagation can be described in terms of a single waveguide mode, the instantaneous effects of a minor variation in layer height should be very similar at such closely-spaced frequencies as those in the Omega spectrum, and the correlation between variations at various frequencies from a single station, or pair of stations, should be high. Even if there is a noticeable amount of higher-mode propagation on a transmission path, the higher-mode components may be quite phase-stable at a given distance, so that the high correlation between frequencies <u>at a fixed receiving point</u> is observed, although the mean transmission time is more difficult to predict than it would be in the case of a single mode. If the propagational correlation is indeed high, we shall need to consider the effects of "noise", whether this be actual atmospheric noise or

uncorrelated error components due to different instrumental errors at different frequencies, or other causes.

The station-to-station correlation is simply explored. We may write the variance equation

$$\sigma_{AB}^2 = \sigma_A^2 + \sigma_B^2 - 2r_{A,B}\,\sigma_A\,\sigma_B \qquad (21)$$

where

σ_{AB}^2 = variance of the time difference between stations A and B

σ_A^2 = variance of the time of arrival of the signal from A

σ_B^2 = variance of the time of arrival of the signal from B

and

$r_{A,B}$ = coefficient of correlation between signals A and B.

If measurements of signal times are made in terms of a local time standard of high accuracy, it is possible to determine σ_A, σ_B, and σ_{AB} independently. From these measurements the coefficient of correlation can be determined, as that is the only remaining variable in Eq. (21). Observations of this kind have been made from time to time in Cambridge, where three long-distance signals have usually been available: A in Norway, B in Trinidad, and C in Hawaii. All three pairs have been examined and the results averaged to give the two examples shown in Fig. 15. As is to be expected when studying the variations of variations, the scatter is large. Hourly examples are shown for two different dates to illustrate the general fact that little true diurnal variation can be detected in diagrams of this kind. The

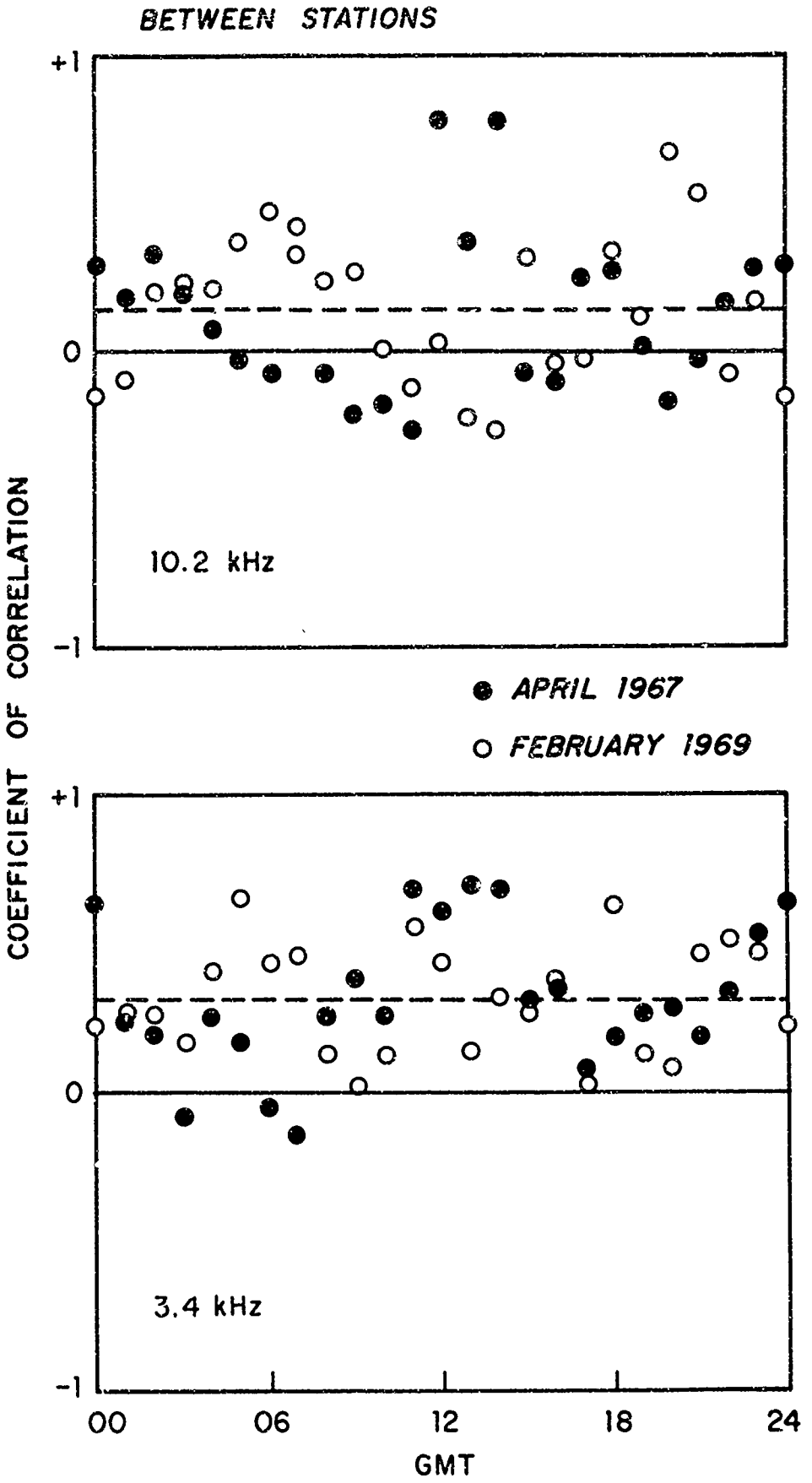

Figure 15: Observed Correlation between Signals from Pairs of Stations, at 10.2 and 3.4 Kilohertz.

only conclusion to be drawn is that there appears to be a positive coefficient of correlation of about 0.1 or 0.2 at the 10.2 kHz carrier frequency, and one about twice as large at the difference frequency of 3.4 kHz. These values may have been increased by time fluctuations of the clock in Cambridge, which have been assumed to be zero in the analysis. These magnitudes assure us that while a low correlation is indeed detectable, it is by no means large enough to be an important factor in navigational accuracy.

The correlation between frequencies is a far different matter, as suggested above. Its analysis is a little more complex and is conveniently combined with examination of the value of m that leads to minimum standard deviation. From Eq. (6) we write the variance equation

$$\sigma_c^2 = m^2 \sigma_2^2 + (m-1)^2 \sigma_1^2 - 2r_{1,2}\, m(m-1)\, \sigma_1\, \sigma_2 \qquad (22)$$

where σ_c^2 is the variance of a composite signal, the subscripts 1 and 2 refer to the lower and higher of a pair of frequencies, respectively, and $r_{1,2}$ is the coefficient of correlation between variations at the two carrier frequencies.

Restricting Eq. (22) to the frequencies 10.2 and 13.6 kHz and to the difference frequency 3.4 kHz for which $m = 4$, we have

$$\sigma_{3.4}^2 = 9\sigma_{10.2}^2 + 16\sigma_{13.6}^2 - 24\, r_{10.2,13.6}\, \sigma_{10.2}\, \sigma_{13.6} \qquad (23)$$

from which $r_{10.2,13.6}$ may be determined.

An example of data, solved for r in terms of σ at these three frequencies and plotted as a function of $\sigma_{13.6}/\sigma_{10.2}$ and the correlation coefficient, is shown in Fig. 16. While the scatter from

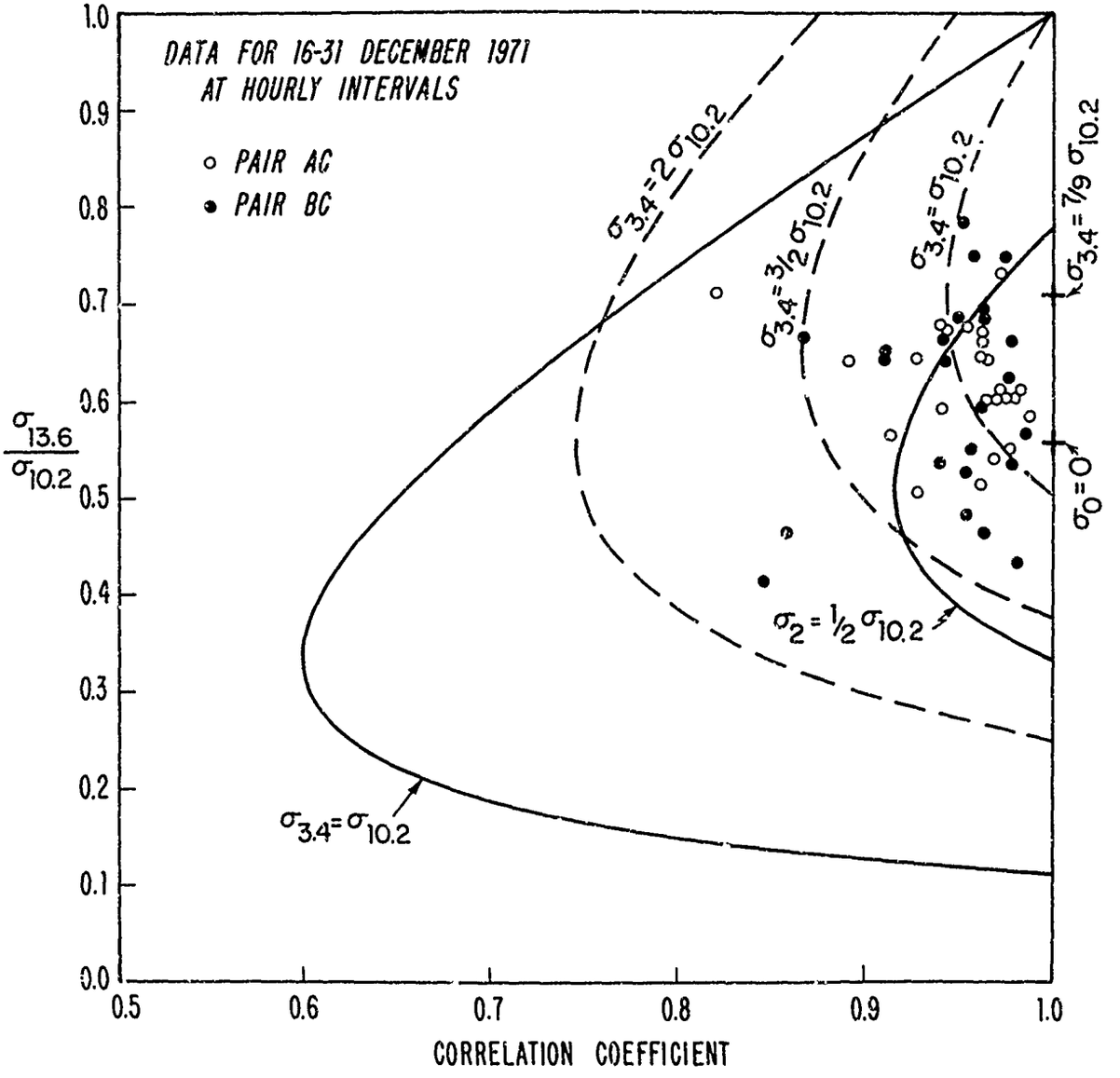

Figure 16: Observed Values of $\sigma_{13,6}/\sigma_{10.2}$ and Calculated Contours versus Coefficient of Correlation.

hour to hour is quite evident, the points in this example have average coordinates of $\sigma_{13.6}/\sigma_{10.2} = 0.61+$ and $r = 0.94+$. Contours of constant σ_o (at $m = 9/4$) and $\sigma_{3.4}$ (at $m = 4$), as referred to $\sigma_{10.2}$, have been derived from Eq. (22), and are also shown on Fig. 16. These contours show that about half of the hourly values of σ_o are less than one-half of the concurrent values of $\sigma_{10.2}$; and about half of the hourly values of $\sigma_{3.4}$ are smaller than $\sigma_{10.2}$ for the same hours.

To find the vertex of the parabola relating σ_c to m, we expand Eq. (22) for the chosen frequencies:

$$\sigma_c^2 = m^2 \sigma_{13.6}^2 + m^2 \sigma_{10.2}^2 - 2m\sigma_{10.2}^2 + \sigma_{10.2}^2 - 2r_{10.2,13.6} m^2 \sigma_{10.2} \sigma_{13.6} + 2r_{10.2,13.6} m\sigma_{10.2} \sigma_{13.6} \tag{24}$$

Setting $d\sigma_c^2/dm = 0$, we have

$$0 = 2m\sigma_{13.6}^2 + 2m\sigma_{10.2}^2 - 2\sigma_{10.2}^2 - 4r_{10.2,13,6} m\sigma_{10.2} \sigma_{13.6} + 2r_{10.2,13.6} \sigma_{10.2} \sigma_{13.6} \tag{25}$$

from which

$$m_o = \frac{\sigma_{10.2}^2 - r_{10.2,13.6} \sigma_{10.2} \sigma_{13.6}}{\sigma_{10.2}^2 + \sigma_{13.6}^2 - 2r_{10.2,13.6} \sigma_{10.2} \sigma_{13.6}} \tag{26}$$

Using this value of m_o in Eq. (22) we find the minimum variance

$$\sigma^2_{min} = m_o^2 \sigma^2_{13.6} + (m_o - 1)^2 \sigma^2_{10.2}$$

$$- 2r_{10.2,13.6} m_o (m_o - 1) \sigma_{10.2} \sigma_{13.6} \quad (27)$$

$$= m_o^2 (\sigma^2_{10.2} + \sigma^2_{13.6} - 2r_{10.2,13.6} \sigma_{10.2} \sigma_{13.6})$$

$$- 2m_o (\sigma^2_{10.2} - r_{10.2,13.6} \sigma_{10.2} \sigma_{13.6}) + \sigma^2_{10.2} \quad (28)$$

Since it can be shown that the magnitude of the first term is one-half that of the second

$$\sigma^2_{min} = \sigma^2_{10.2} - m_o(\sigma^2_{10.2} - r_{10.2,13.6} \sigma_{10.2} \sigma_{13.6}) \quad (29)$$

This may be simplified for computation by writing

$$R = r_{10.2,13.6} \sigma_{10.2} \sigma_{13.6} = \frac{9\sigma^2_{10.2} + 16\sigma^2_{13.6} - \sigma^2_{3.4}}{24} \quad (30)$$

Then

$$A = \sigma^2_{10.2} - R \quad (31)$$

and

$$B = \sigma^2_{10.2} + \sigma^2_{13.6} - 2R \quad . \quad (32)$$

From (26)

$$m_o = A/B \quad (33)$$

and from (29)

$$\sigma^2_{min} = \sigma^2_{10.2} - A m_o \quad (34)$$

Examples of the diurnal variation of m_o for the AC pair are shown in Fig. 17. It will be recalled that the first-approximation expectation is $m_o = 9/4$. For this pair the mean observed value is a little greater than the theoretical one, but for pairs involving the relatively short-distance station B, the mean value of m_o is usually lower than 9/4, probably as a result of a smaller ratio of propagational to instrumental uncertainties.

This effect is also seen in its reaction upon the coefficient of correlation as shown in Fig. 18. Here the correlation is higher for those pairs involving station A (Norway) because the propagation through the arctic zone of geomagnetic activity introduces large variations in the time of transit. The pair AB combines large errors from A and small ones from B, resulting in a correlation coefficient of about 0.98 at night and nearly unity in the daytime. The pair with the smallest standard deviation, BC, shows the lowest coefficient of correlation.

This behavior suggests that there may be a more or less fixed "noise" (defined here as uncorrelated variations, whether due to actual received noise or produced by instrumental errors in the receiving equipment) that combines with highly-correlated propoagational deviations to produce the observed variances.

This concept can be examined by assuming that there are perfectly-correlated variations (primarily propagational) whose mean variance is equal to $r_{10.2,13.6}\,\sigma_{10.2}\,\sigma_{13.6}$, and completely-uncorrelated variations (noise) whose mean variance is $(1 - r_{10.2,13.6})\sigma_{10.2}\,\sigma_{13.6}$. This separation has been carried out for the data used in Fig. 18 to yield the uncorrelated component of the standard deviation that is shown

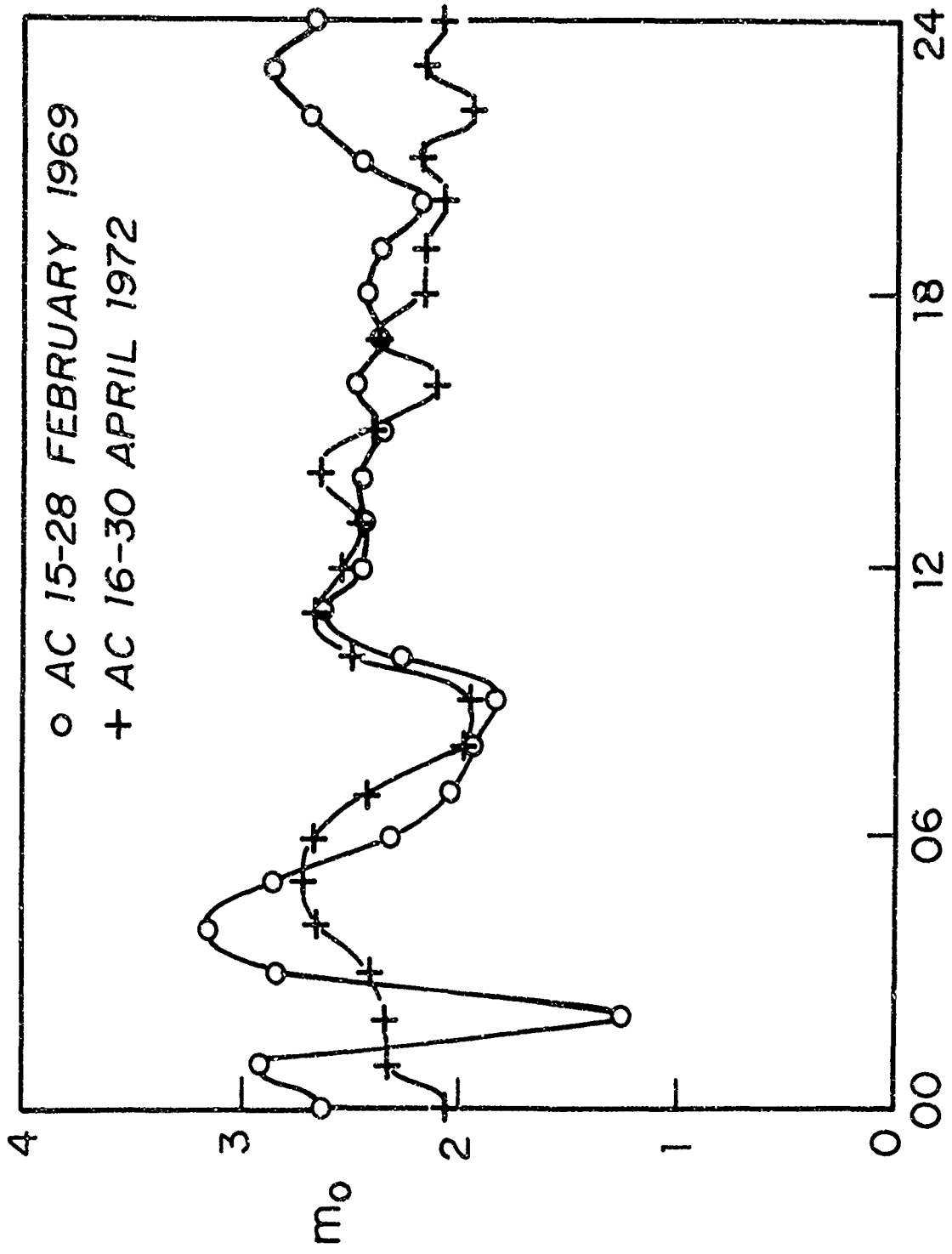

Figure 17: Observed m_o as a Function of Time.

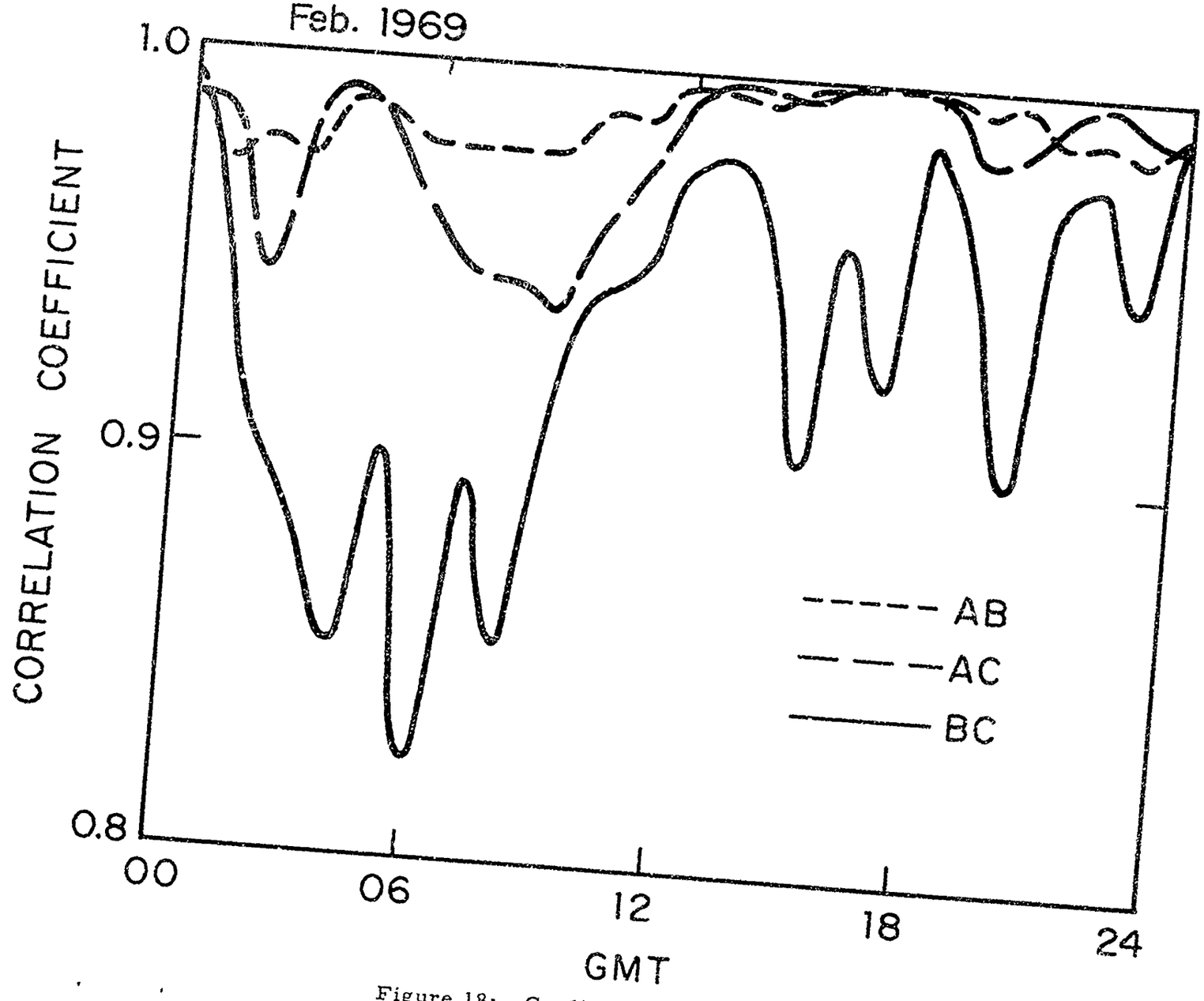

Figure 18: Coefficient of Correlation versus Time.

in Fig. 19. Here it is seen that, although in Fig. 18 the correlation varies widely between the different pairs, there is no great distinction between pairs in the magnitude of the uncorrelated component of Fig. 19. All that can be determined from Fig. 19 is that the uncorrelated errors are not much larger than the nominal errors of measurement and are somewhat larger at night than in the daytime.

It is of interest to plot the uncorrelated deviations against the correlated ones. As shown in the upper part of Fig. 20, or as could be deduced from Figs. 18 and 19, there is no great change in the uncorrelated errors as the correlated ones increase. A noticeable maximum in the region of 10-12 centicycles on the abscissa can be seen. Examination of this effect shows that for the BC pair (where propagational deviations are small) the correlated errors are larger by night than by day, while for the pairs involving A the propagational deviations are larger in the daytime. The 24 points shown in the upper part of Fig. 20 for each pair, do not distinguish between night and day. We have, therefore, in the lower part of the figure, deleted those points corresponding to the sunrise and sunset intervals. The result is that, as in Fig. 19, the night-time uncorrelated errors are about twice the daytime ones, with no distinguishable change as the correlated errors increase.

This hypothesis of perfectly-correlated propagational errors combining with pure noise that is larger by night than by day must not be carried too far, although it is a useful concept. A few short measurements of the standard deviation of small difference frequencies have been made from time to time, particularly in the 1964-1966 era. Although only fragmentary data exist, they are enough to indicate that the standard deviation (in time units) of a low beat frequency is

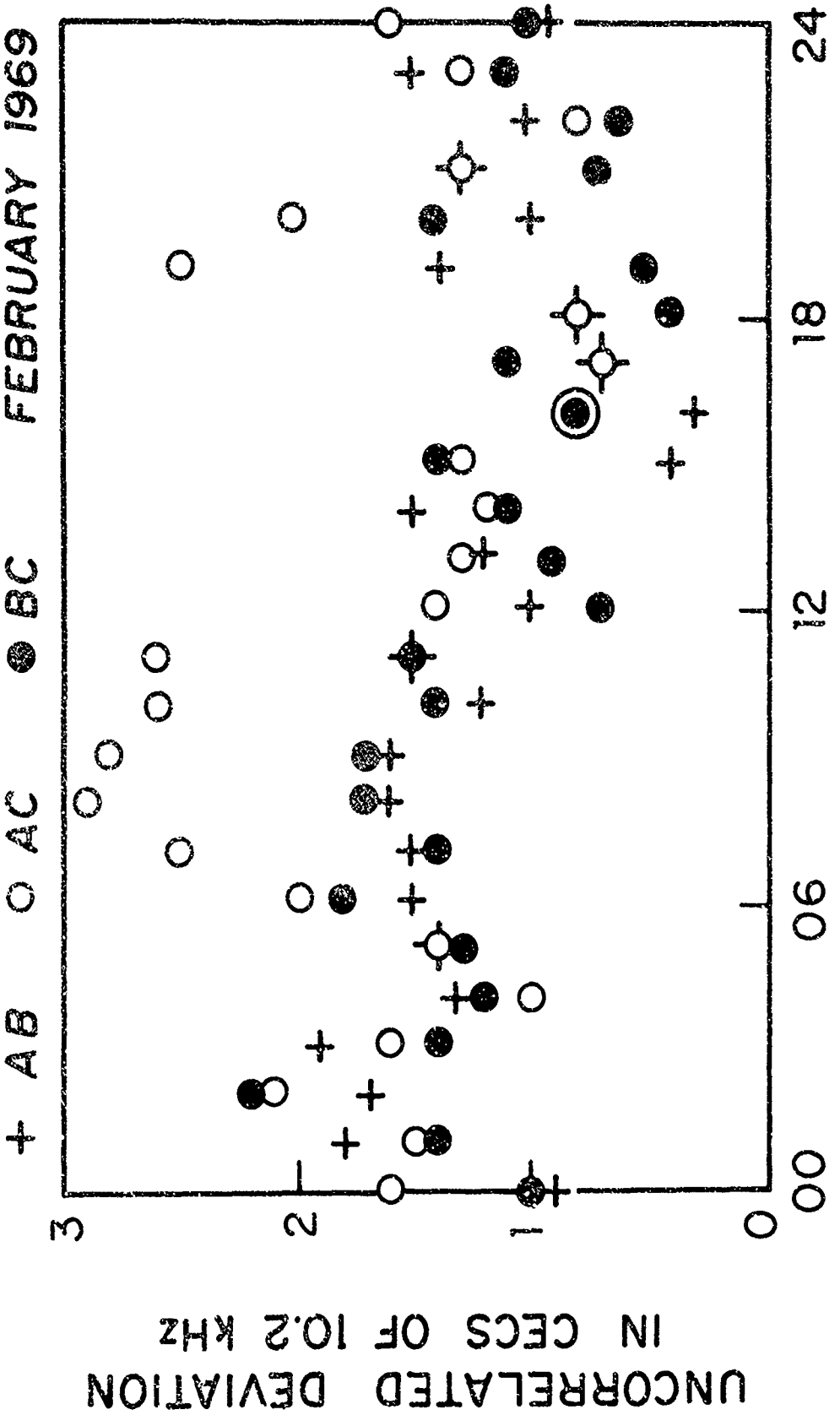

Figure 19: Uncorrelated Deviations versus Time.

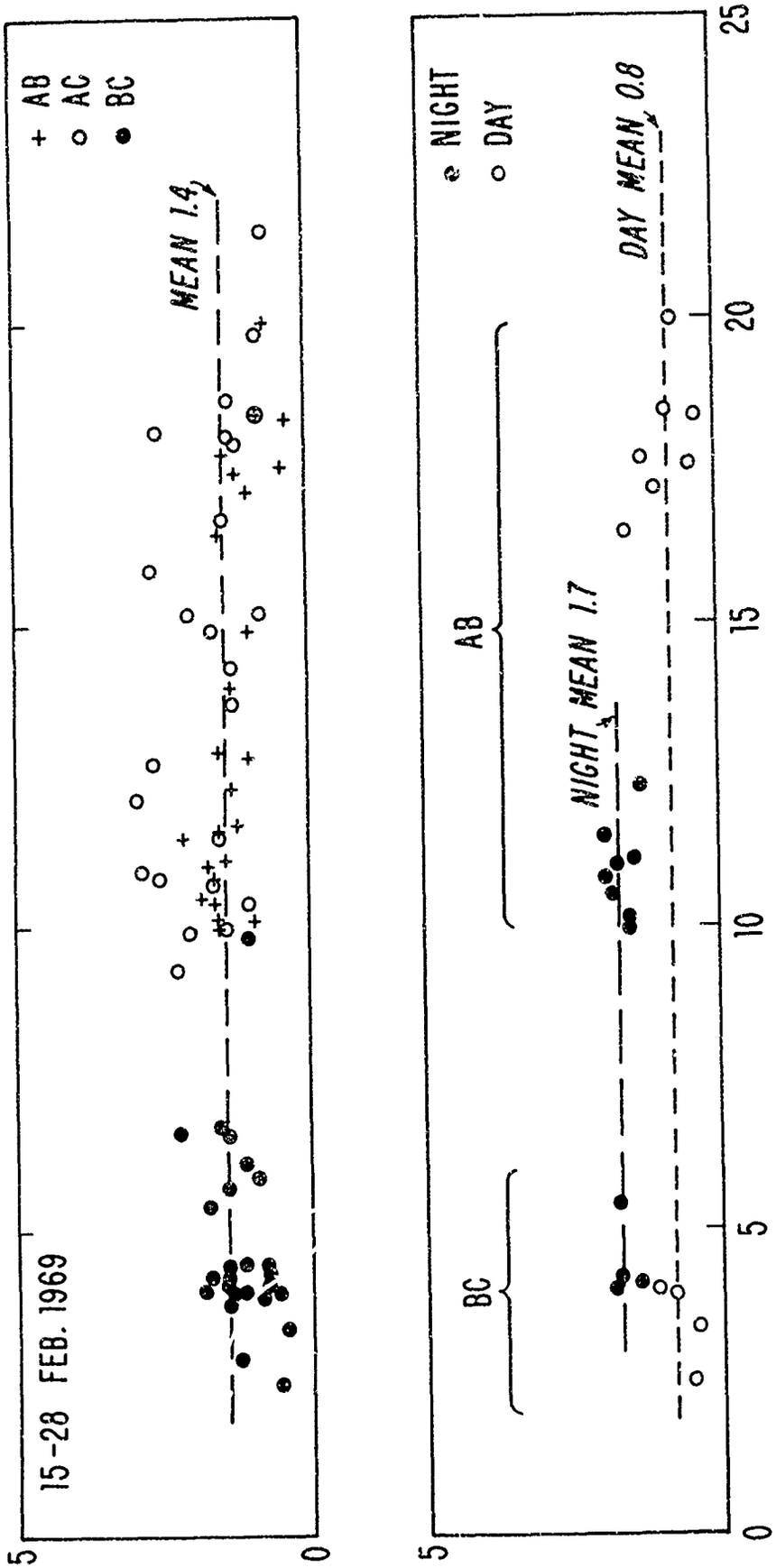

Figure 20: Uncorrelated versus Correlated Deviations at Cambridge.

approximately inversely proportional to the square root of that frequency. This is most reasonably accounted for in theory by assuming that the coefficient of correlation differs from unity by an amount that is proportional to the frequency difference. This is a physically-satisfying idea that is very probably correct, but for which there is no room in the over-simplified analysis outlined above.

11. ESTIMATION OF PROPAGATION TIME FOR FREQUENCIES OTHER THAN 10.2 AND 13.6 kHz

Because there are several untried frequencies that may be used for Omega, it is necessary to examine the details of the relationship between velocity and frequency. This variation is usually expressed in graphical form because there is no completely satisfactory closed expression for the velocity in the "waveguide". The waveguide cut-off is at some small fraction of the Omega frequency band, and near this cut-off frequency the phase vlocity approaches infinity, or at least becomes relatively large in comparison with the velocity of light. As frequency increases, the phase velocity for a particular mode falls more and more slowly. Several curves of this nature[14] are frequently shown with layer height as a parameter. An example of one of these is shown in Fig. 21, where the 10-14 kHz navigation band is shaded.

To the extent that one of these curves of phase velocity as a function of frequency approaches an equilateral hyperbola, its reciprocal approaches a straight line. It is therefore convenient, for purposes of intercomparison and others, to consider the graph of c/v_p against wavelength. The values of Fig. 21 have been transformed in this way

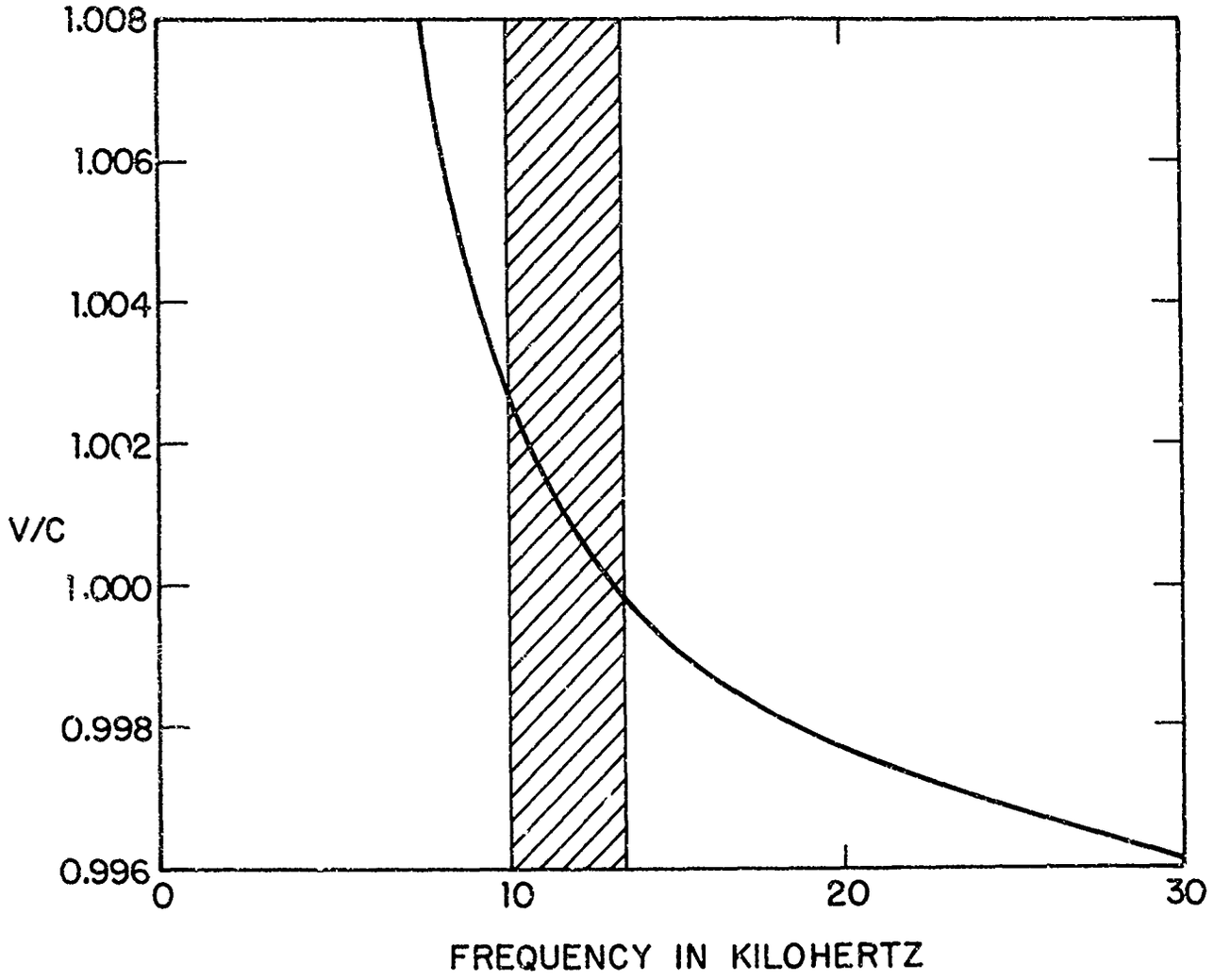

Figure 21: Theoretical Relative Phase Velocity as a Function of Radio Frequency.

in Fig. 22 where the navigation band is again shaded. One of the advantages of this representation is that the chord connecting points at two chosen wavelengths can be produced to zero wavelength, where it intercepts the axis of ordinates at the value of c/v_g for the selected pair of wavelengths.

Now the scale of m is an inverted and displaced wavelength scale. Zero wavelength corresponds to the difference frequency, where $m = f_2/(f_2 - f_1)$, while the wavelength corresponding to the lower frequency f_1 has a value of m equal to zero. This can be visualized in Fig. 22, if the edges of the shaded band are taken to correspond to the frequencies 13.6 and 10.2 kHz. The origin and the left and right sides of the shaded band then have the m values 4, 1, and 0, respectively.

The relatively-smaller curvature of this relative time/wavelength diagram is seen in Fig. 22 and again in Fig. 23. In the latter case, the sense of the wavelength has been reversed and the scale of relative wavelength has been taken, for convenience, as the factors by which the frequency 816 kHz is divided to produce the various Omega frequencies.

Determination of the curvatures in Figs. 21-23 is, so far, largely theoretical. Experience has given us fairly accurate velocity values for 10.2 and 13.6 kHz. Corresponding values for other neighboring frequencies have been derived in the following way.

As an approximation to mode-theory phase velocity, Watt[8] has given the formula

$$\frac{v_p}{c} = 1 - \frac{kh}{a} + \left[(2\pi n - \phi_g - \phi_i) \frac{c}{4\pi\sqrt{2}\, fh} \right]^2 \qquad (35)$$

where k is a factor defining the relative height of the axis of the waveguide, cited by Watt as 0.36

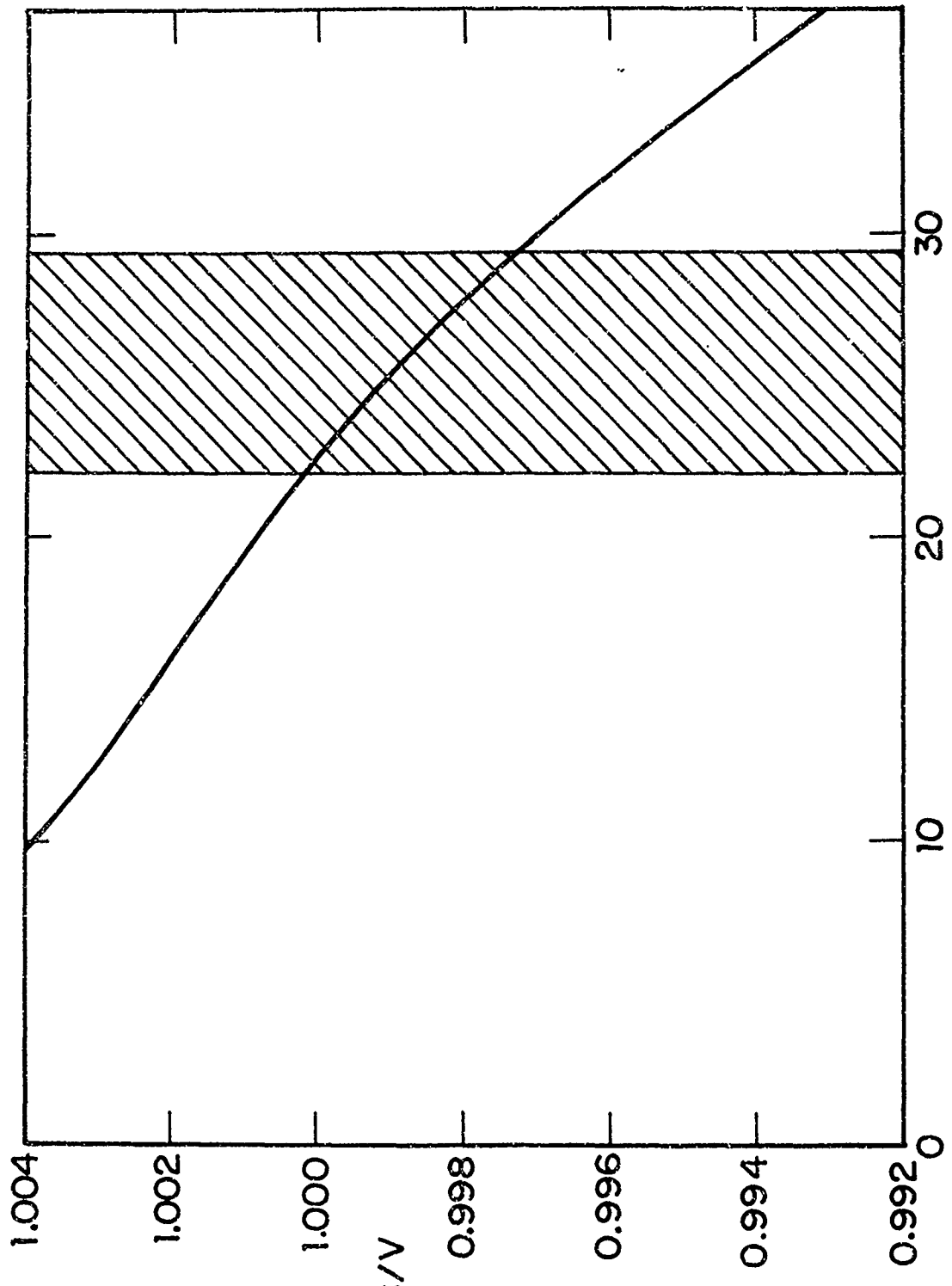

Figure 22: Reciprocal Velocity versus Wavelength

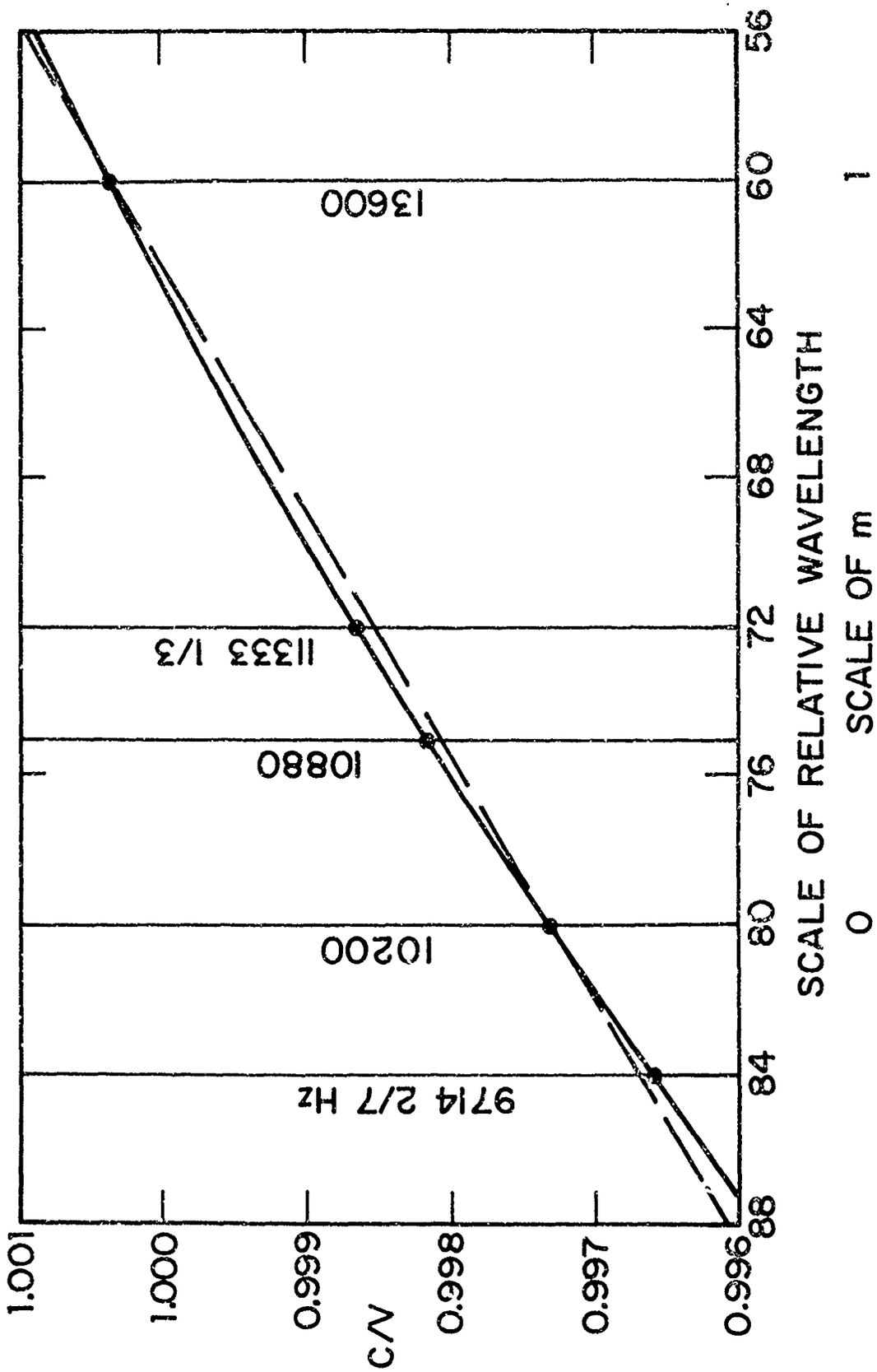

Figure 23: Reciprocal Velocity as a Function of Relative Wavelength, or m.

h = height of the reflecting layer

a = radius of the earth

n = mode number (1 in this case)

ϕ_g = phase shift at reflection at the surface of the earth

ϕ_i = phase shift at reflection at the ionized layer

and

f = frequency.

Having known values of v_p at only two frequencies, it is convenient to assume the nominal heights of 70 and 90 km for day and night conditions, respectively, and to solve for values of k and $(\phi_g + \phi_i)$. Determination of these quantities as functions of height is helped a little by deducing reasonable values at zero height and fitting a power law through three values in each case. The results of these calculations are given in Table IV.

TABLE IV

Values for Use in Equation (35)

Time of Day	Layer Height in kilometers	k	$\phi_g + \phi_i$ in radians	$\phi_g + \phi_i$ in degrees
--------	0	0.5	π	180
Day	70	0.390	2.745	157
Night	90	0.367	2.518	144

We may use these values in Eq. (35) to derive phase velocities that have a reasonable variation with frequency and that accurately fit our

experimental (nominal) values at 10.2 and 13.6 kHz.

Returning to Fig. 23, we see that the computed values for the various frequencies fall on a parabola (because Eq. (35) is second order) that does not differ greatly from the chord between $m = 0$ and $m = 1$. For some purposes it is convenient to slightly distort the scale of m and reduce the variation in velocity to a straight line. This is done by defining the m' that would apply if dispersion were linear and referred to the pair of frequencies 10.2 and 13.6 kHz, as

$$m' = 4 - \frac{40.8 \text{ kHz}}{f_{\text{kHz}}} \tag{36}$$

and then modifying it to

$$m_{\text{eff}} = m' + 0.140\, m'(1 - m') . \tag{37}$$

The constant 0.140 is determined from the values calculated from Eq. (35). It varies only a few parts in a thousand between day and night. It is worthwhile to tabulate values from Eqs. (36) and (37) for a few interesting frequencies in Table V. The chosen frequencies are those, in the Omega part of the spectrum, that are obtained by dividing 816 kHz by an integral divisor that has no prime factor larger than seven. The reasons for interest in some of these frequencies will be explained below.

This table indicates that, <u>if dispersion were linear</u>, the propagation time for a signal at 11 1/3 kHz (for example) would be found at 40% of the way from the time at 10.2 kHz to that at 13.6 kHz. In the actual medium with nonlinear dispersion, the time for 11 1/3 kHz is more nearly 43% of the way between the times for those same frequencies.

TABLE V

Effective values of m referred to the frequencies 10.2 and 13.6 kHz that serve to define expected phase velocities at various other carrier frequencies.

Frequency in Hertz	m'	m_{eff}	Factors of divisor from 816,000 Hz
9714.28+	-0.2	-0.234	2·2·3·7
10074.07+	-0.05	-0.057	3·3·3·3
10200	0.0	0.000	2·2·2·2·5
10880	0.25	0.276	3·5·5
11333.33+	0.4	0.434	2·2·2·3·3
11657.14+	0.5	0.535	2·5·7
12750	0.8	0.822	2·2·2·2·2·2
12952.38-	0.85	0.868	3·3·7
13600	1.0	1.000	2·2·3·5

The primary reason for this transformation is to estimate a family of coherent predictions of propagation times for various interesting frequencies. A secondary reason is that through this mechanism simple arithmetic will yield an estimate of the propagation time for 3.4 kHz based upon observations at any pair of frequencies in the Omega spectrum.

It is, of course, clear that an estimation of the 3.4 kHz propagation time made from any pair of frequencies other than 10.2 and 13.6 kHz becomes less accurate as the difference between the two values of m_{eff} becomes smaller. This is particularly true in the presence of interference

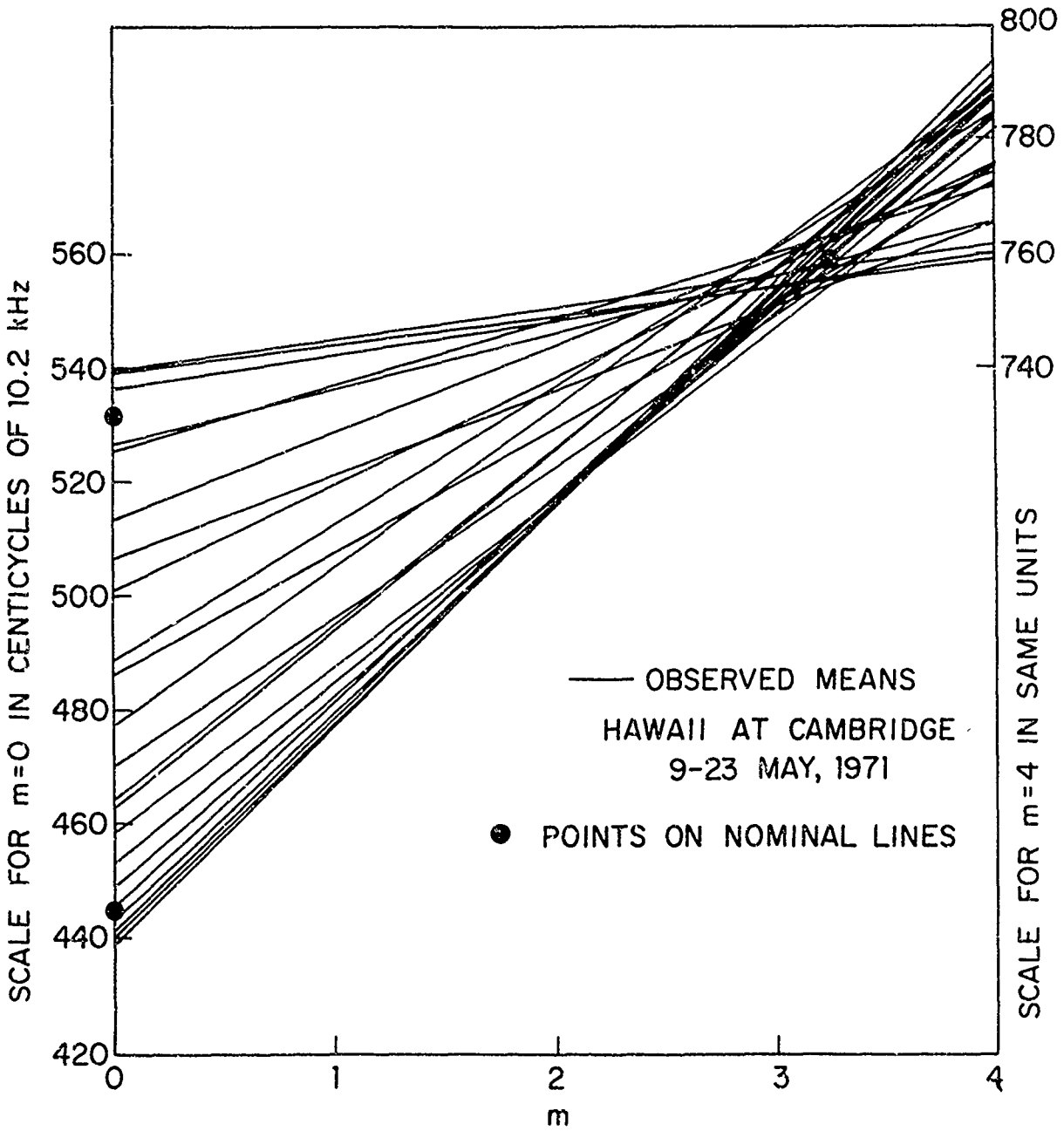

Figure 24: Observed "m-lines" for Hawaii at Cambridge

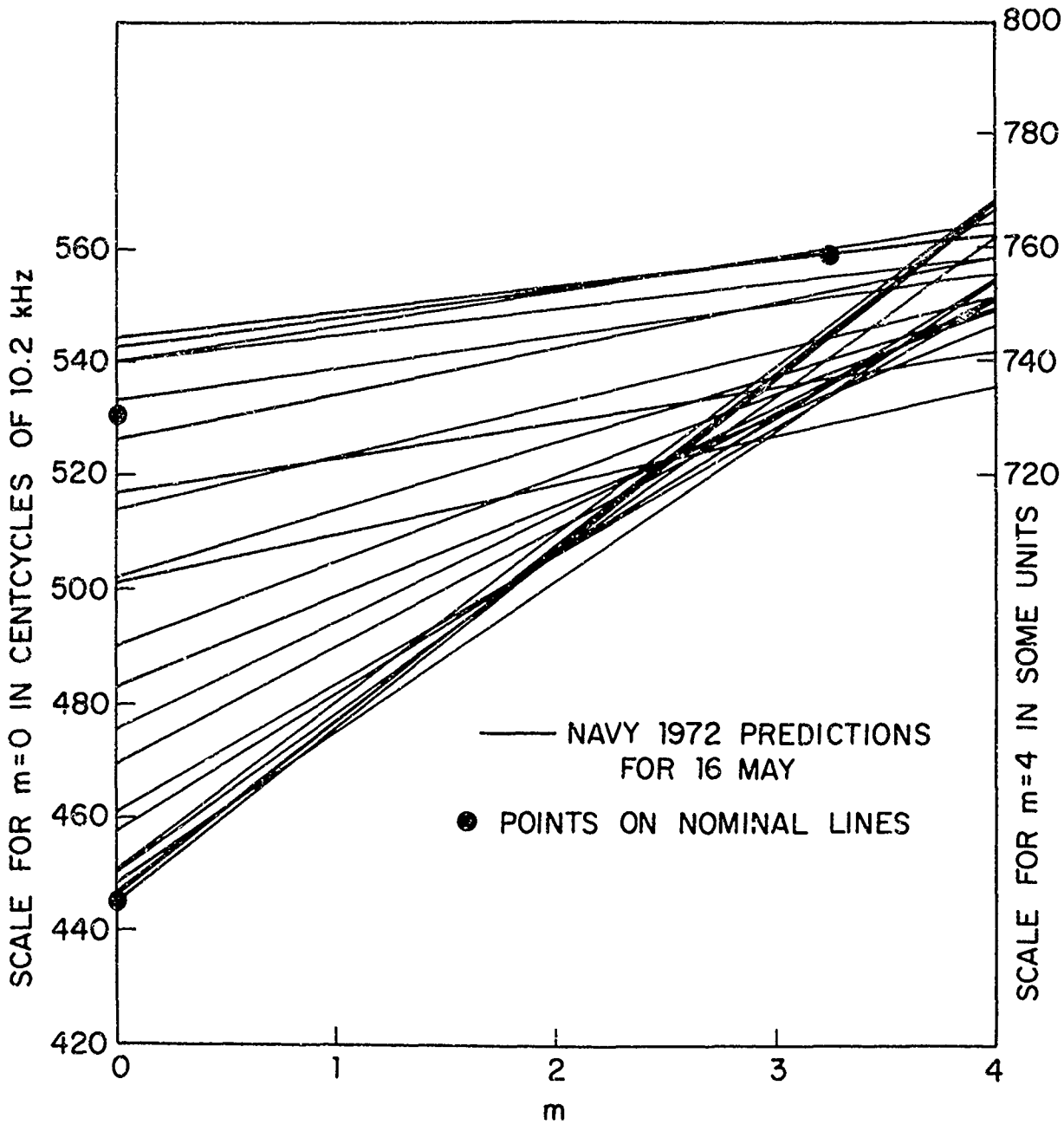

Figure 25: Predicted "m-lines" for Hawaii at Cambridge

from higher-order modes in the waveguide. Under the influence of such modes, the resultant phase may be advanced at one frequency and retarded at another. The effect upon the time of arrival of an observed difference frequency will be large if the frequency difference is small.

12. MODIFICATION OF PREDICTIONS

It has been observed, as in Figs. 12 to 14, that nominal predictions are at least as accurate as the Navy predictions at the higher values of m and especially at the difference frequency, where m=4. It is also seen, in the same figures, that either of kind of prediction tends to be most accurate in the region of $m = 9/4$, as could be anticipated from the elementary theory in Section 3.

It follows from these observations that errors of prediction that are magnified by the multiplications of Eqs. (6) and (7) can be somewhat constrained by independent examination of the group velocity, or the velocity at some other large value of m.

An example of the need for some improvement in prediction is shown by intercomparison of Figs. 24 and 25. Figure 24 shows an observed "m-line" for each of the 24 hours of the day for a block of data in May, 1971. The data are the same as those of Fig. 5 above but are shown here distorted by reducing the ordinates at $m = 4$ by 200 centicycles with respect to the ordinates at $m = 0$. This adjustment reduces the slopes of Fig. 5, and permits the use of a more open scale. The dots mark the day and night nominal values at $m = 0$ and the intersection of the nominal day and night lines at $m = 3.263$. The close grouping of the observed lines near this latter value of m is clear, as it was in Fig. 5.

The Navy predictions are made at 10.2 and 13.6 kHz (m = 0 and 1). Minor errors in these predictions are magnified as m increases. Figure 25 shows the Navy 1972 predictions that apply for the dates of Fig. 24, exhibited in the same way as the observed data of that figure. The deficiencies in the predictions are primarily values that are somewhat too low at large values of m, and a scattering that reduces the tendency to group at an m somewhat greater than 3.

A way of combining easily-made predictions[15] at various values of m is shown in Fig. 26. This diagram shows five dots at time differences (ordinates) appropriate to the time and date given on the figure. Horizontal lines mark the times calculated at the velocity of light and at the velocity used for the Navy charts.

Points at these five values of m can be calculated in the following ways:

at m = 0 — the time is the chart time minus the Sky Wave Compensation given in the Navy "correction" tables[11] for 10.2 kHz.

at m = 1 — the time is the chart time minus 3/4 of the Navy S. W. C. for 13.6 kHz, because that "correction" is tabulated in centicycles of 13.6 kHz.

at m = 9/4 — the time is, as explained above, derived from the nominal daytime reciprocal velocity plus the difference between nominal night and day reciprocal velocities multiplied by the fraction of each transmission path in darkness.

at m = ~ 263 — the time is nominally fixed at 1.00725 times the time calculated for the velocity of light.

at m = 4 — the time shown by the dot is the chart time minus three times the Navy S. W. C. for 3.4 kHz; or, alternatively, four times the time at m = 1 minus three times the time at m = 0.

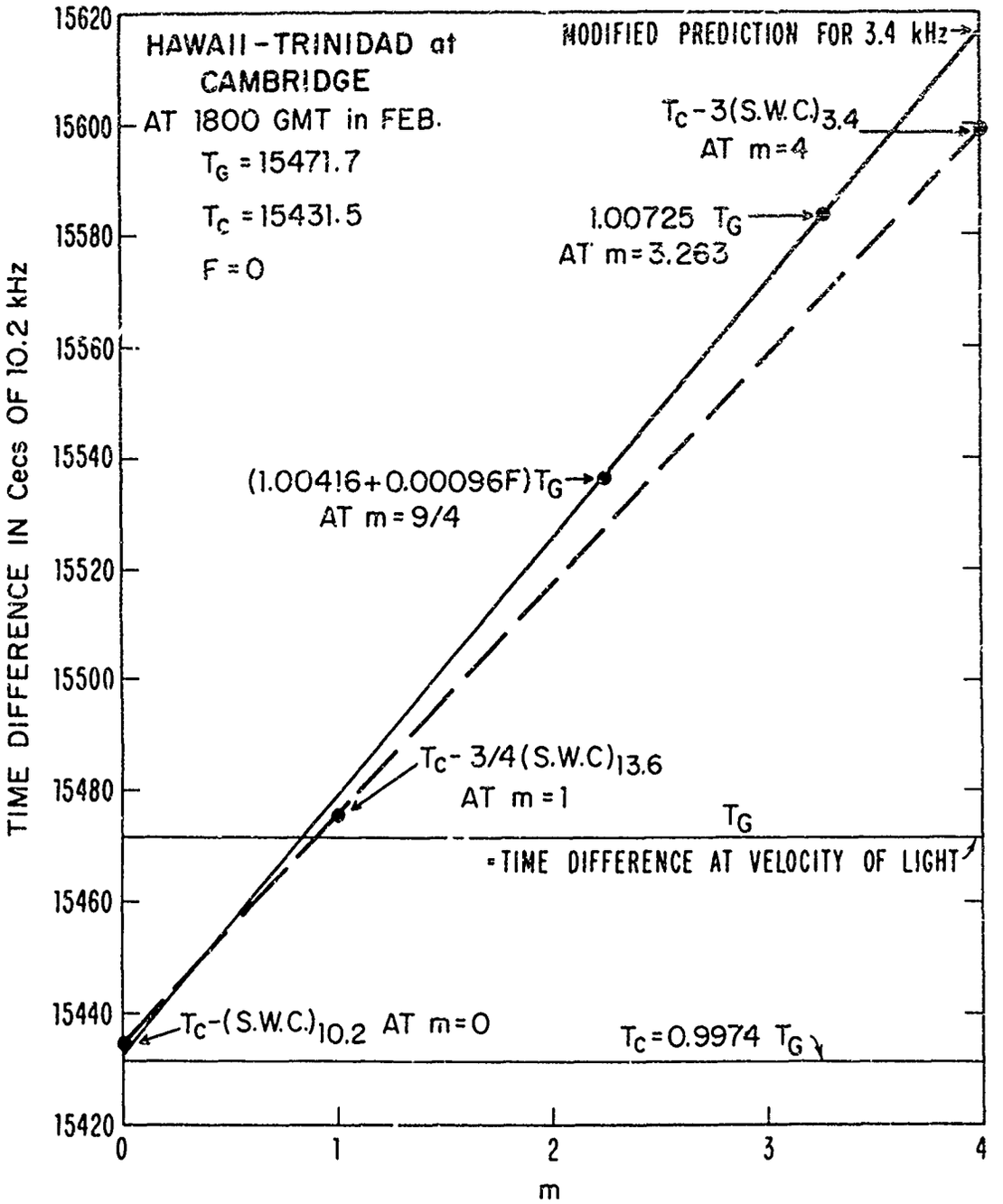

Figure 26: Various Predictions as Functions of m.

Another calculation could be made to give the nominal value at $m = 4$, but it is not needed for our present study. It would be

$$T_{3.4\,nom} = (1.0095 - 0.0007\,F)\,T_G \tag{38}$$

In the case shown in Fig. 26, the nominal prediction for 3.4 kHz would be about 1 Cec below the upper right-hand corner of the figure.

In Fig. 26 a best straight line is drawn through the first four dots described above. A dashed line connects the three points drawn from the Navy predictions, and shows the relatively-large deviation of the 3.4 kHz prediction caused by minor deviations in opposite senses at 10.2 and 13.6 kHz.

For our present purposes, it is not necessary to concern ourselves with all the possible points shown on Fig. 26, or other points that might be calculated. It is obvious that, if (as the writer believes) the "fixed" point at $m = 3.263$ is especially easy to predict accurately, a line drawn from the Navy prediction at $m = 0$ through the fixed point cannot differ greatly from any other line through the points shown in Fig. 26, excepting the point representing the Navy prediction at $m = 4$. It is therefore possible to deduce a modified prediction for 3.4 kHz from the Navy prediction at 10.2 kHz.

The slope of the line connecting the points at $m = 0$ and $m = 3.263$ is

$$S = \frac{1.00725\,T_G - [T_C - (S.W.C.)_{10.2}]}{3.263} \tag{39}$$

where

T_G is the transit time at the velocity of light

T_C is the transit time at the charted velocity

and

S. W. C. is the Navy Sky Wave Compensation

By definition

$$T_G = \frac{T_C}{0.9974} \tag{40}$$

and Eq. (39) reduces to

$$S = 0.003019\ T_C + 0.3065\ (S.W.C.)_{10.2} \tag{41}$$

For any value of m

$$T = T_C - (S.W.C.)_{10.2} + mS \tag{42}$$

or

$$T = (1 + 0.003019\ m)\ T_C - (1 - 0.3065\ m)\ (S.W.C.)_{10.2} \tag{43}$$

Letting $m = 4$,

$$T_{3.4} = 1.01208\ T_C + 0.226\ (S.W.C.)_{10.2} \tag{44}$$

This relationship may be reduced to a "Modified Sky-Wave Compensation" for 3.4 kHz by subtracting T_C and reversing the sign.

$$\text{Modified } (S.W.C.)_{3.4} = -0.01208\ T_C - 0.226\ (S.W.C.)_{10.2} \tag{45}$$

This construction of a presumably-improved prediction for 3.4 kHz is, of course, applicable to the signals from a single station or the time difference between the signals of a pair.

Figure 27 shows an example of the comparison between Cambridge data and the Navy, and also the modified, predictions. The improvement seen resides partly in adjustment of the level of the predictions to the level of the observed points, but it is perhaps more important that the shape of the diurnal curve is much more similar to the observed diurnal variation. It is clearly necessary to produce the best possible predictions at 3.4 kHz, as the prediction error at that frequency is probably the most important single contributor to errors in lane identification.

The methods of this section can be applied by a navigator or a receiver software designer. It is, however, much more important that this, or some similar recognition of the degree of correlation that applies between signals at 10.2 and 13.6 kHz, be used to improve the generally-used predictions. It will be most satisfactory when the Navy prediction methods improve to the extent that this kind of modification can no longer enhance operational accuracy.

13. CORRECTIONS OF OBSERVED READINGS

Methods somewhat analogous to those of Section 12 can be used to "correct" observed data to provide a modest reduction of differences between observed and predicted times of propagation. These methods are, in reality, simply translating the error pattern of a composite signal to an observed frequency, or to some other interesting or convenient value of m.

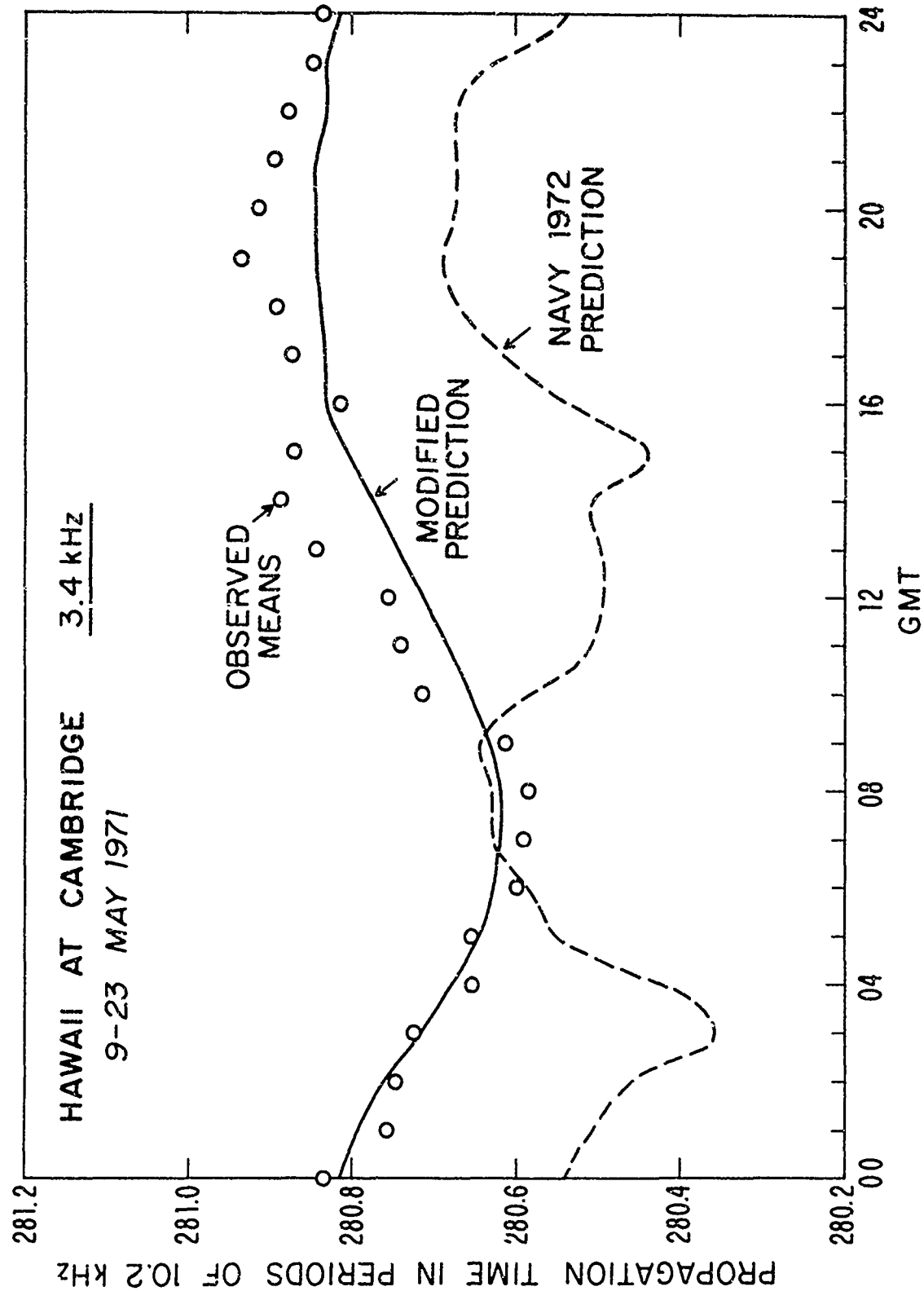

Figure 27: Navy and Modified Predictions and Observed Means for Hawaii at Cambridge.

This disclaimer will be discussed more fully below, because without explanation the treatment may seem to call upon magic rather than science.

Figure 28 is a generalized diagram that will introduce the correction concept, although its use is simpler than the figure suggests. Let us suppose that the line having an intercept at T_N is a true normal (or average) representation of time as a function of m, although its actual position cannot often be known in an observational sense. The dotted line beginning at T_P is a predicted estimate of the same truth. It is shown, as appears to be usual, to be nearer the truth near $m = 9/4$ than nearer $m = 0$.

Now let us suppose that a pair of observations at $m = 0$ and $m = 1$, as shown by the dots on Fig. 28, are made at a time when the phase velocity is anomalously high, such as during an S. I. D. The line through these points, marked T_{obs} at $m = 0$, is shown as intersecting the T_N line (representing long-term average truth) near $m = 9/4$, as the examples shown in Figs. 1 and 2 have shown is usually the case.

A "corrected" value of time at 10.2 kHz, for example, can be calculated by producing the line T_{obs} to $m = 9/4$ and then by constructing a line (dashed in Fig. 28) through the value of T_{obs} at $m = 9/4$ back to $m = 0$ at the slope of the predicted line T_P. The resulting intersection at T_{corr} is the corrected value of the observed time T_{obs}. It is seen that, as drawn, this corrected time is not only closer to the predicted time T_P than is T_{obs}, but is actually closer to T_P than is the normal truth T_N. Since a navigational error is the difference between an observation and the prediction of that observation this approach to T_P represents a reduction in error. To say the same thing in other words, if the approximations used in drawing Fig. 28 are justified, the corrected error under anomalous

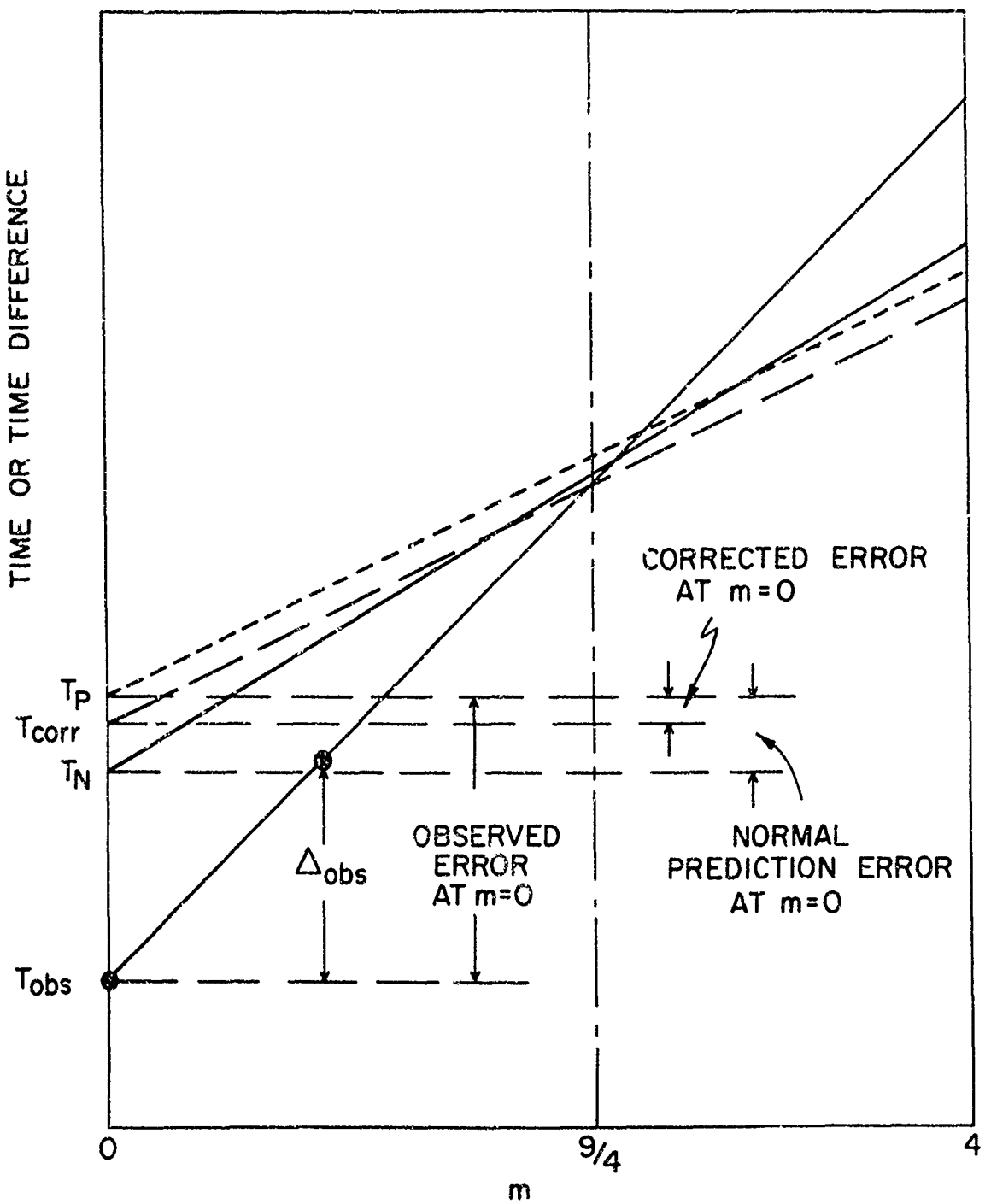

Figure 28: Diagram Explaining the Correction Technique.

conditions may actually be smaller than is the normal prediction error at a time when propagation coincides with the truth line.

At 10.2 kHz, for example,

$$T_{corr} = T_{obs} + 9/4\ (\Delta_{obs} - \Delta_{pred}) \tag{46}$$

where

T_{obs} = observed value at 10.2 kHz (as shown in Fig. 28)

Δ_{obs} = observed time at 13.6 kHz minus observed time at 10.2 kHz (observed slope shown in Fig. 28)

Δ_{pred} = predicted time at 13.6 kHz minus predicted time at 10.2 kHz (predicted slope)

The same method can be used to correct an observation at any value of m. For another example, at 3.4 kHz (m = 4),

$$T_{corr\ 3.4} = T_{obs\ 10.2} + 9/4\ \Delta_{obs} + 7/4\ \Delta_{pred} \tag{47}$$

or

$$T_{corr\ 3.4} = T_{obs\ 3.4} - 7/4\ (\Delta_{obs} - \Delta_{pred}) \tag{48}$$

It is clear that, provided the observed m-line pivots accurately about the value of the truth line at $m = 9/4$, the corrected error is independent of m. In general, therefore, this correction results in transferring the observed errors at $m = 9/4$ to the predicted time value at the chosen m.

There is a tendency for the correction process to compensate for errors of prediction that are caused when the T_P line does not coincide with the truth line T_N. It therefore seems possible that simpler and less accurate predictions can be used without serious degradation of operational

results. The primary utility of the correction, however, is to reduce the scattering of observations to the scattering applicable at $m = 9/4$. The overall effect of this treatment is to reduce the curves of error of Figs. 12-14, for example, to horizontal lines intersecting the observed curves at $m = 9/4$.

Examples of the results of the correction process are shown in Figs. 29-32. Figure 29 shows the individual hourly points observed at 10.2 kHz on the Trinidad-Hawaii pair in February, 1972. The line shown is the Navy 1972 prediction. It is conspicuous that the Navy prediction rises rather sharply after the minimum at 11^h GMT. The observed data rose much more slowly, especially between 11^h and 13^h, and remain lower than the predictions until after 18^h.

When subjected to the correction process, as shown in Fig. 30, there is no particular improvement in the night-time hours 00-10 GMT. After that, however, the corrected observations are constrained to agree much more closely with the predictions, and the scatter is reduced. Over the 24 hours, the rms error is 12 Cec of 10.2 kHz in Fig. 29 and 8 Cec in Fig. 30.

Figure 31 shows observed time differences at 3.4 kHz for the same pair and date as in Fig. 29. The predicted line in this case is the nominal one, which fits the data somewhat better than does the Navy prediction. Corrected to the nominal values, in Fig. 32, the scatter is somewhat reduced throughout and the means of the corrected points approach the predicted values more closely, especially in the later hours of the Greenwich day. The rms error, over all 24 hours, is reduced from 13 Cec to 7 Cec by the correction process.

These methods must not be taken to be cure-alls. They do, however, exhibit some worthwhile reduction in rms errors, and do seem to take some of the requirement for extreme precision out of the prediction problem. Like other uses of the composite-signal idea, these should not be attempted unless the lane-identification problem has been solved, or can be shown to be unimportant.

It is the writer's belief that these methods should be examined carefully by potential users or designers. If they work as well in other parts of the world as they do in Cambridge, they will supply another useful weapon for use in the war against errors.

14. POSSIBLE ADDITIONAL OMEGA FREQUENCIES

About a decade ago, the plan for Omega[1] proposed to resolve lane ambiguities on an essentially world-wide basis. This plan suggested the use of six harmonically-related frequencies, extending down to 11 1/3 Hz. There were to be three carrier frequencies at 13600, 11333 1/3, and 10200 Hz, each modulated by one of the frequencies 226 2/3, 45 1/3, and 11 1/3 Hz. Beats between the carrier frequencies would provide differences at 3400 and 1133 1/3 Hz. One of each three cycles of 10200 Hz would be identified by the phase of the 3400 Hz signal; one of each three cycles of 3400 by the phase at 1133 1/3 Hz; and the modulation frequencies would extend the identification in ratios of 5, 5, and 4. Taking the minimum distance corresponding to a unit cyclic error at 10200 Hz to be 8 nautical miles (actually 14.70 km), the proposed pattern, if successful, would have extended the separation between ambiguities to $\frac{10200}{11\ 1/3} \times 8 =$ 7200 nautical miles.

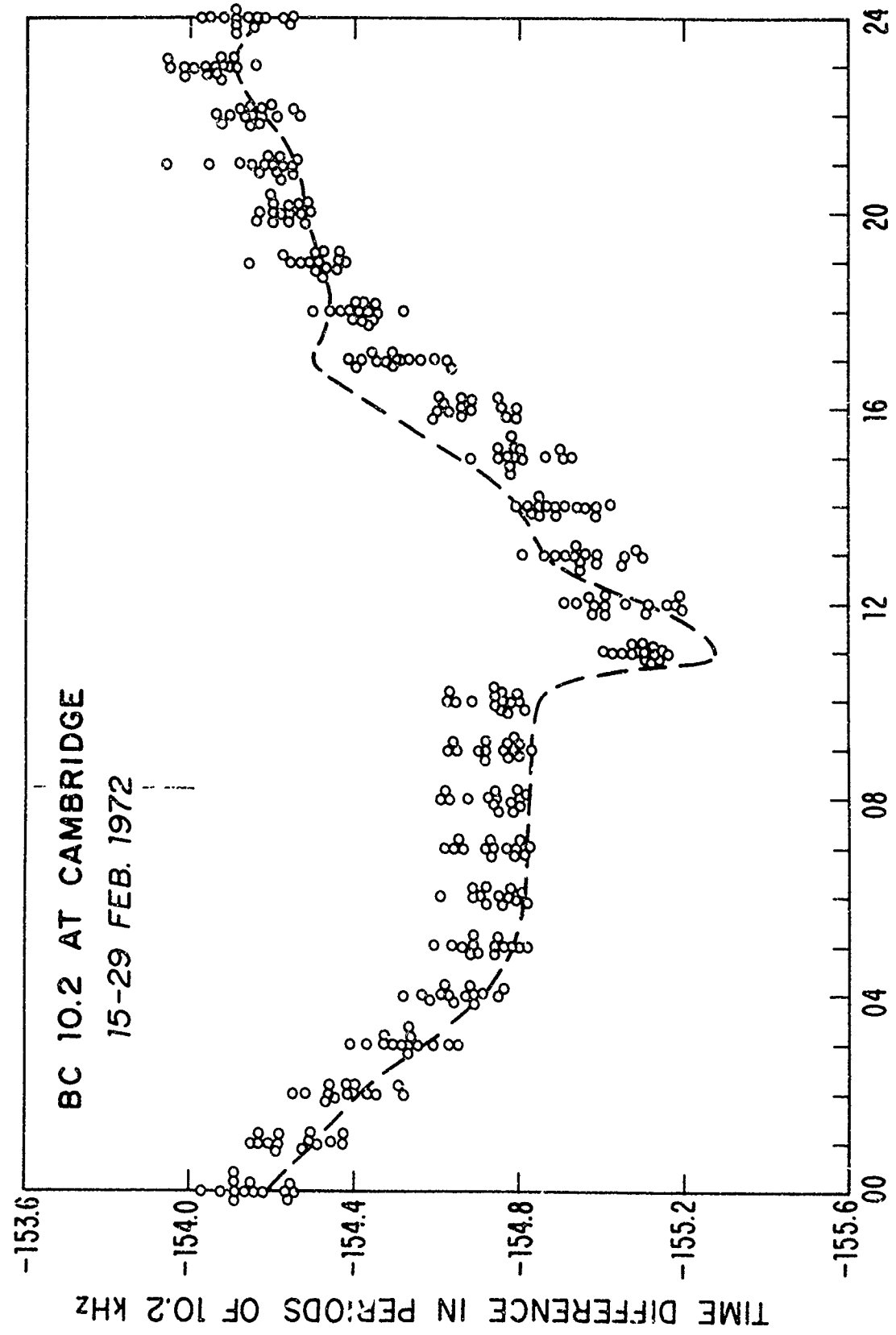

Figure 29: Uncorrected 10.2 Kilohertz Observations and Navy Prediction

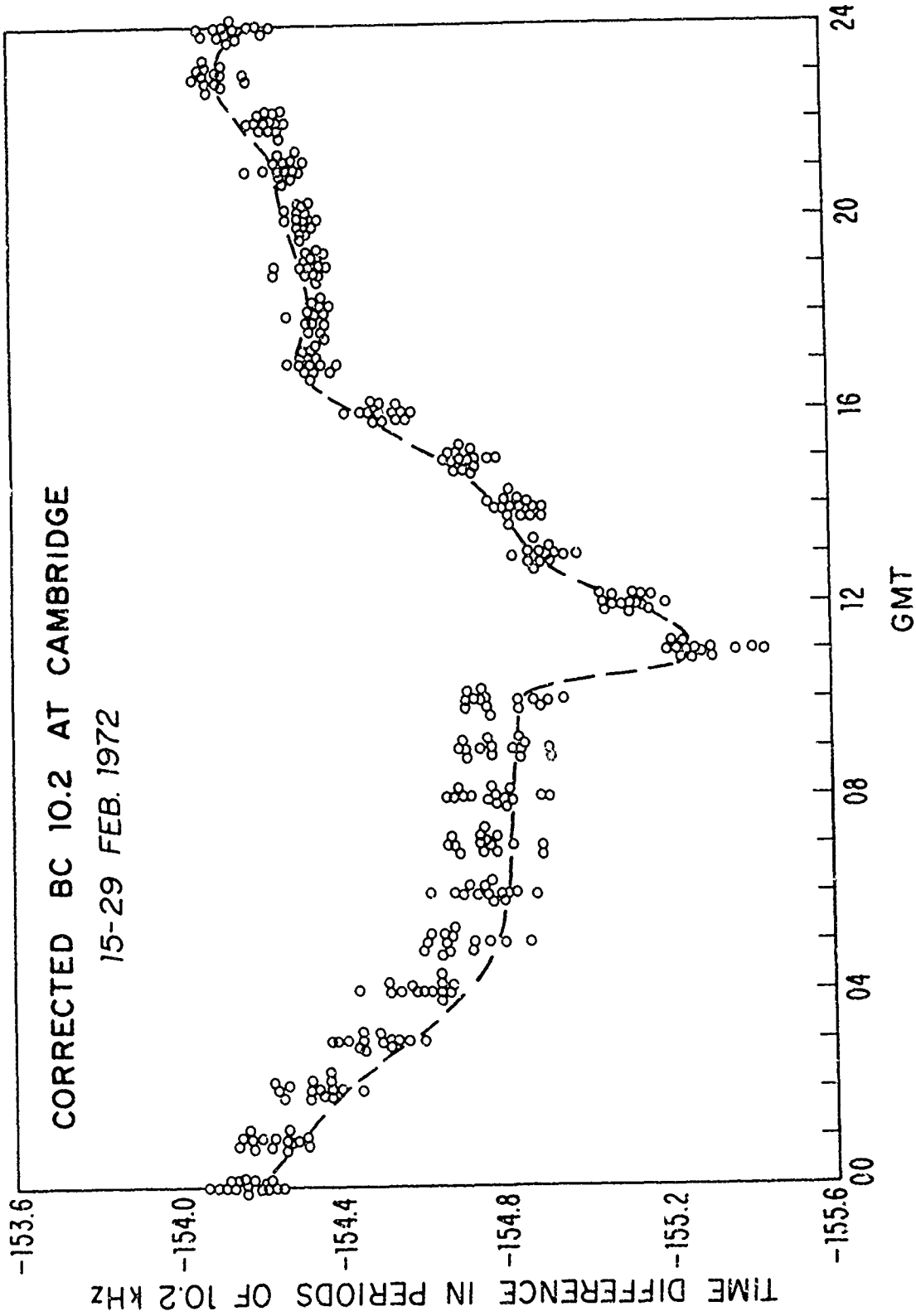

Figure 30: Corrected 10.2 Kilohertz Observations and Navy Prediction

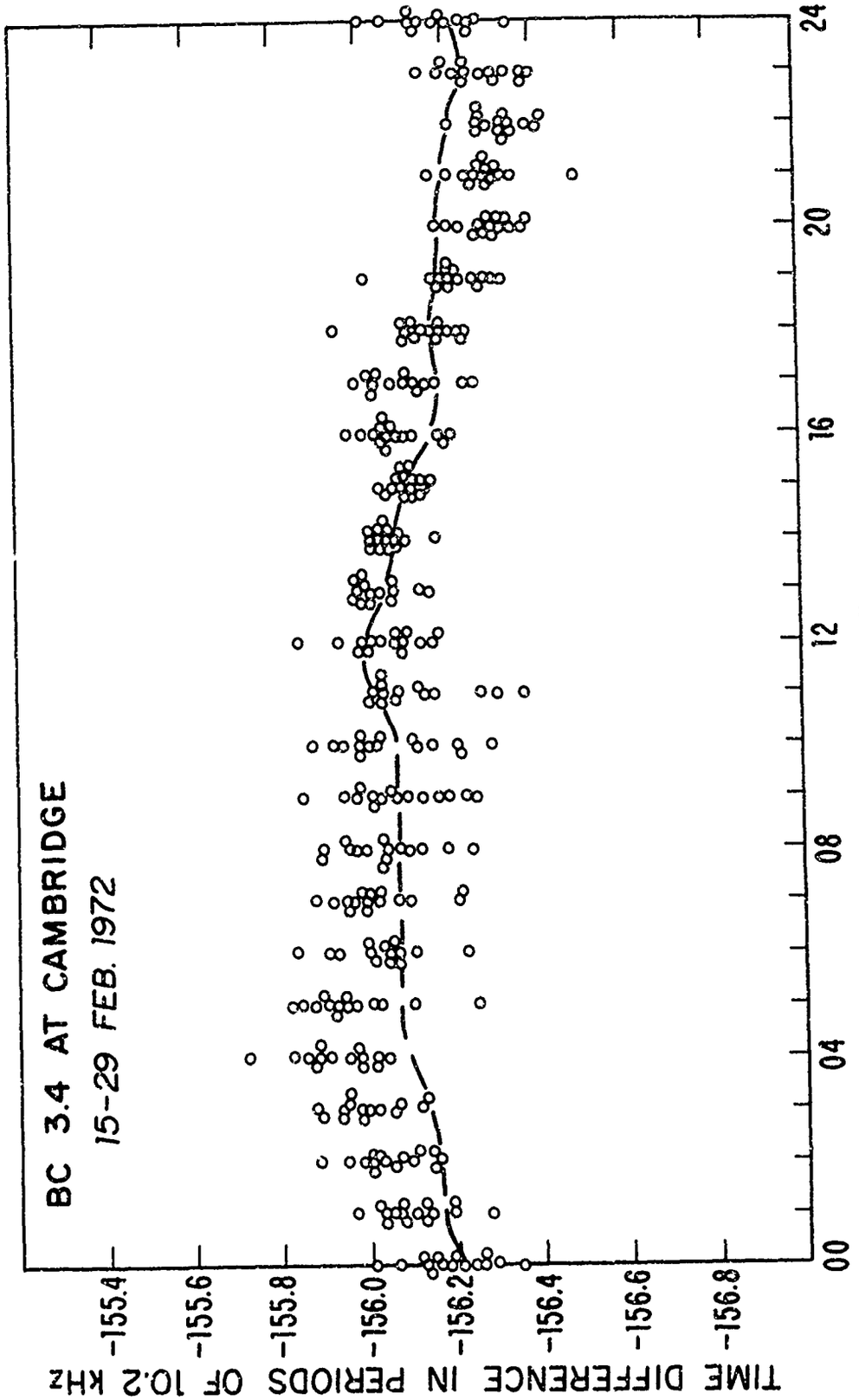

Figure 31: Uncorrected 3.4 Kilohertz Observations and Nominal Prediction

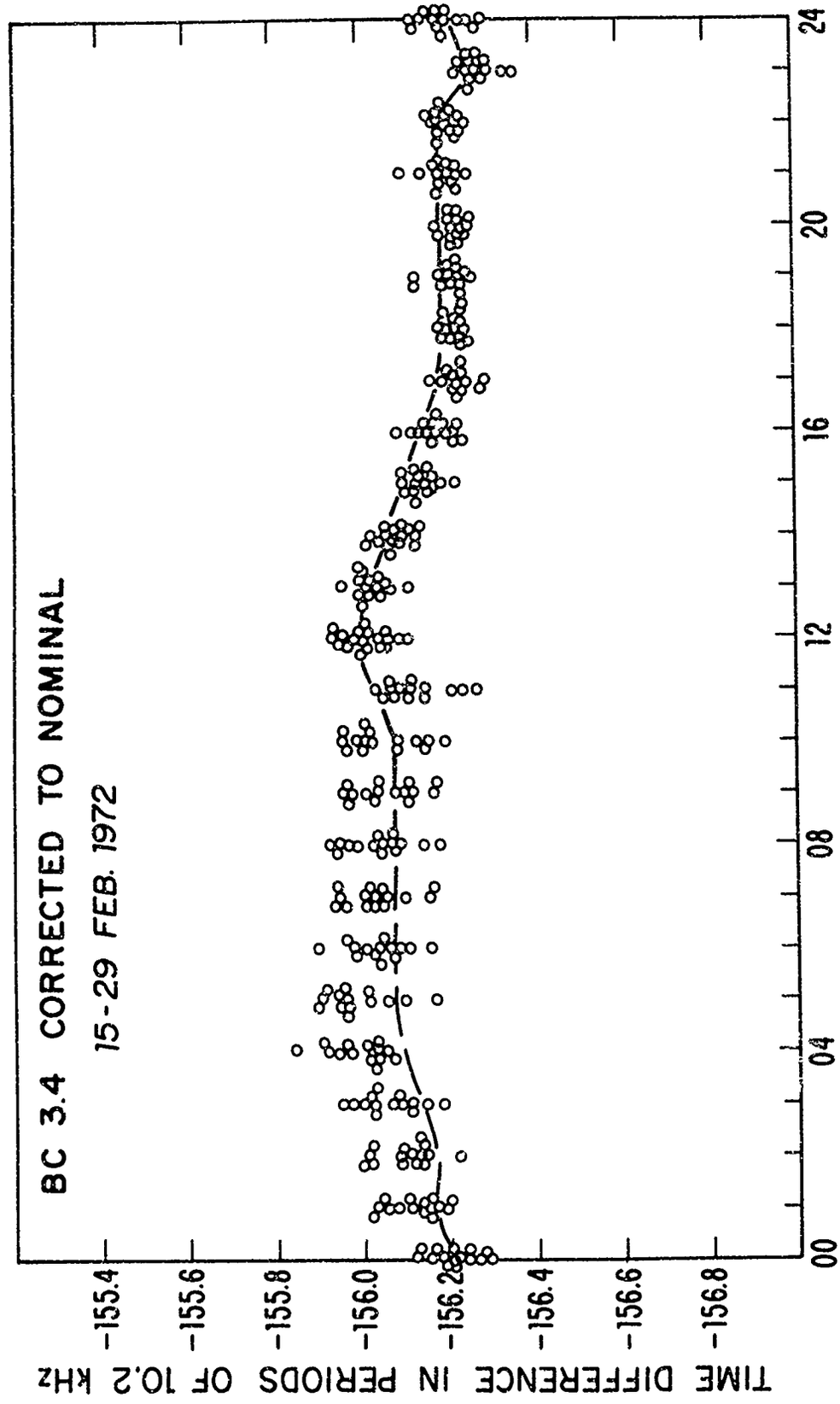

Figure 32: Corrected 3.4 Kilohertz Observations and Nominal Prediction

A technical difficulty in this plan arises from the fact that a properly-loaded Omega transmitting antenna is a relatively sharply-tuned single resonant circuit having a bandwidth of the order of 10-20 Hz; an uncertain value varying inversely with the antenna efficiency.[8] Transmission of the phase modulation signals through such a bandwidth would be very ineffective, especially at the higher modulation frequencies.

At least at 226 2/3 Hz, and perhaps at 45 1/3 Hz, this plan would require triple-tuning the transmitting antenna. This is perfectly feasible in an engineering sense, as the relative frequency separations are large in comparison with the selectivity attainable in the several required resonant circuits. Unfortunately, however, these circuits would need to operate with typical antenna currents of 500 amperes at about 200,000 volts, and would consequently be large and expensive. A number of experiments with low frequencies phase-modulated at a very low modulation index were successfully carried out, aided by the suppression of noise by the strong carrier and the use of relatively-long time constants in receiving the low frequencies. This proposal, however, never became popular.

An alternative suggestion of transmitting additional carriers at more closely spaced frequencies was also proposed. This suggestion, however, would lead to the requirement for extremely selective and consequently expensive receivers for the Omega signals.

As a result of these difficulties, real or exaggerated, the Navy decided not to implement any Omega frequencies except the original three carriers, which would, in theory, expand the ambiguous lanes to 72 nautical miles or more. Under the very reasonable assumption that a

navigator with a continuously-running navigation aid should never allow himself to be uncertain of his position by as much as 36 nautical miles, this level of ambiguity resolution was defined as adequate.

Unfortunately, this Navy decision to save money and limit the range of ambiguity resolution failed to provide the signals necessary for many potential peripheral services not involving a human operator and not requiring continuous operation, such as automatic tracking of balloons, drifting buoys, or icebergs. Of these, by far the most important is for the automatic location of the position of vessels or personnel in distress.

The obvious requirement for this kind of service has been explored in recent years, particularly under the name of "Global Rescue Alarm Net" by a team made up of people from the Navy, NASA, Air Force, and Coast Guard.[16] Relaying of Omega signals by geostationary satellite has been successfully tested and experiments in extending the range of ambiguity resolution have been begun.

In an effort to avoid the difficulties mentioned above, the exploration of increased capability is based upon a slight variant of the older ideas--the beat between beats. This concept is most easily explained by describing the use of a fourth Omega frequency which has already been subjected to preliminary tests. This fourth frequency is at 10880 Hz and is used as shown in Table VI.

By this trick a coherent signal at 226 2/3 Hz is produced without requiring a carrier whose separation from any of the first three carriers is less than 453 1/3 Hz. The beat-between-beats is demonstrably less precise than a first-order beat, but the difference between orders is not serious because, at these low frequencies, ordinary instrumental errors

TABLE VI

Frequency Beats to Identify 1133 1/3 Hz

All values in Hertz

13600 - 10200	= 3400	which identifies 10200
11333 1/3 - 10200	= 1133 1/3	which identifies 3400
10880 - 10200	= 680	
11333 1/3 - 10880	= 453 1/3	
680 - 453 1/3	= 226 2/3	which identifies 1133 1/3

tend to be dominant and the propagational contributions to error become relatively unimportant.

A lowest frequency of 226 2/3 Hz is by no means adequate. To extend this range of identification (from $72 \times 5 = 360$ nautical miles) to greater distances, there are several techniques that might be used. These are:

1. Measurement of the relative times of arrival of the bursts of Omega signals.[17]

These can be measured only at the beginning or end of each individual signal. Under poor signal-to-noise conditions, each single measurement has a standard deviation of the order of the rise time, or 15-20 milliseconds. To identify a 360-mile lane the uncertainty of the measurement must be well below one millisecond. This technique would therefore require integration over some hundreds of bursts of signal. By using all four frequencies suggested above, the total integration time

required might be kept within reasonable limits, but the writer is somewhat pessimistic about the prospect.

2. Use of one or more low modulation frequencies.

This is an attrative technique because it fits the phase-measurement pattern of the Omega system, provided that a satisfactory modulation index can be achieved without requiring multiple tuning of the transmitting antennas. The writer suggests a single modulated component, probably at 22 2/3 Hz, which should be radiated without suffering too great sideband attenuation by the transmitting antenna, and which should reliably identify a period of 226 2/3 Hz, yielding 3600 mile lanes.

3. Measurement of beats between beats using a fifth carrier frequency, to produce an effective frequency, probably of 32 8/21 Hz.

This method has the advantage of repeating the technique used for the 360-mile lanes. Since the only convenient frequencies would divide the 226 2/3 Hz frequency by seven, this method would yield 2520-mile lanes.

4. Measurement of relative amplitude or, more probably, relative signal-to-noise ratios between stations of a pair.

Typical attenuation rates are 2-3 decibels/megameter. It is probable that relative signal strengths can be predicted and measured to within 6-10 decibels. This would give a standard deviation of the order of a thousand miles, without further ambiguity.

5. Measurement of the dispersion of signals, almost certainly between 10.2 and 13.6 kHz.

Dispersion is a questionable technique. The writer's observations indicate a single-station long-term standard deviation of about 3 Cecs of 10.2 kHz per unit of m, but there are ambiguities at intervals of 25 Cecs. These values correspond to a standard deviation of a single-station distance of about 200 nautical miles but with ambiguities at about 1600 mile intervals. The chief operational difficulty with dispersion is its large diurnal variation. Because position must be known, at least roughly, before the dispersion slope can be predicted, this method would require an iterative solution.

The writer's preference among these choices is either technique number 2 or 3 to identify in lanes of 2500 miles or more, with number 4 used to reduce the operational ambiguity to zero.

A 22 2/3 Hz modulation would presumably be the easiest method to implement, because it basically requires only the addition of a low-level phase modulator at each transmitter, while the modulation can be stripped off from existing phase detectors in the receivers. A little more expensive, but most attractive, is the addition of one of two possible fifth carrier frequencies, in accordance with one of the patterns in Table VII.

Thus the addition of either 816000/63 = 12952+ Hz or 816000/84 = 9714+ Hz to the previously-recommended four frequencies would provide ambiguities separated by $7 \times 360 = 2520$ nautical miles. After this step, a relatively easy observation of signal-to-noise ratios should remove all ambiguities.

TABLE VII

Frequency Beats to Identify via 226 2/3 Hz

All values in Hertz

CHOICE A

13600	-	10200	=	3400	which identifies	10200
11333 1/3	-	10200	=	1133 1/3	which identifies	3400
10880	-	10200	=	680		
11333 1/3	-	10880	=	453 1/3		
680	-	453 1/3	=	226 2/3	which identifies	1133 1/3
10200	-	9714 2/7	=	485 5/7		
485 5/7	-	453 1/3	=	32 8/21	which identifies	226 2/3

CHOICE B

13600	-	10200	=	3400	which identifies	10200
11333 1/3	-	10200	=	1133 1/3	which identifies	3400
10880	-	10200	=	680		
11333 1/3	-	10880	=	453 1/3		
680	-	453 1/3	=	226 2/3	which identifies	1133 1/3
13600	-	12952 8/21	=	647 13/21		
680	-	647 13/21	=	32 8/21	which identifies	226 2/3

The degree of frequency division in each step attainable in the Omega pattern, where all transmitted frequencies are equal to 816 kHz divided by a whole number, is determined by the largest prime factor in the divisor. The possibilities have been listed in Table V for all frequencies where the largest prime factor is less than 11. The frequency 10074 2/27 Hz must be discarded as too close to the existing frequency 10200 Hz. Table V indicates that there is one other set of additional frequencies that might be as satisfactory as the schemes outlined above. This set is identified in Table VIII.

TABLE VIII

Frequency Beats to Identify via 283 1/3 Hz

All values in Hertz

13600	- 10200	= 3400		which identifies 10200
11333 1/3	- 10200	= 1133 1/3		which identifies 3400
13600	- 12750	= 850		which also identifies 3400
1133 1/3	- 850	= 283 1/3		which identifies 850 or 1133 1/3
11657 1/7	- 11333 1/3	= 323 17/21		
323 17/21	- 283 1/3	= 40 10/21		which identifies 283 1/3

This pattern divides 1133 1/3 Hz by 4 by 7, rather than by 5 by 7 as in the preceding table, giving lanes of 2016 nautical miles rather than 2520.

Of these three choices (A and B in Table VII, and Table VIII), the writer prefers VII A, because the beats providing the lower frequencies are all derived in the low-frequency part of the Omega spectrum. A possible administrative disadvantage is that the fifth carrier frequency lies below the 10-14 kHz navigation band, but this frequency would, of course, suffer the least from the effects of higher-order modes in the waveguide. In VII B, 680 Hz is the beat between the two lowest carrier frequencies, while 647 13/21 is the beat between the two highest frequencies. Under this condition the non-linearity of the dispersion and the tendency for 2nd mode interference to be greater at the higher frequencies are matters of some concern. In Table VIII, 1133 1/3 Hz is the beat between the two lowest frequencies while 850 Hz is the beat between the two highest frequencies. The same principles apply, although perhaps not to a serious extent because at this point the division ratio is only 4, rather than 7. This pattern is also less desirable because the smallest separation between carrier frequencies is 323 17/21 Hz, as compared with 453 1/3 Hz in the patterns of Table VII. This reduced separation would have a more serious impact upon the problems of receiver design.

Details of the way in which these frequencies may be intercompared in the lane identification process will be discussed in Section 18.

The chief problem before us here is to add a minimum amount of information to the Omega signal format to permit reliable world-wide lane identification. Clearly, in the writer's opinion, the first trials of the fourth frequency (under GRAN auspices) have been entirely satisfactory. At the accuracy level required, the signal-to-noise measurement should give no trouble, but it is easy to test this as a byproduct of other trials.

The time-of-arrival technique[17] might replace either the modulation or the fifth carrier, in spite of the writer's pessimism. It can be tested independently at any time. It would certainly supersede the signal-to-noise measurement if it were used, but it is probably not worth instrumenting unless it also forms a reliable replacement of everything beyond the fourth frequency.

15. LANE IDENTIFICATION

Since a relayed distress signal may not be accompanied by any prior knowledge about position, there is obviously a requirement for an essentially world-wide resolution of ambiguities. As a first step in this program, we have recommended the addition of a fourth carrier frequency at 10.88 kHz as outlined in Section 14. This frequency is chosen as one possible way to transmit a frequency difference five times less than the present 1133 1/3 Hz difference. This new difference does not appear directly. It is a second-order beat between beats of 680 and 453 1/3 Hz. The reason for this choice is to keep the carrier frequencies as widely separated as possible to avoid complicating the frequency-selectivity problem in Omega receivers. It is realized that the beat-between-beats degrades accuracy to some extent, but we believe that the increasing correlation between fluctuations at more closely spaced frequencies will compensate this difficulty. The proposed scheme is roughly that a phase measurement at 227 Hz will be accurate enough to identify a period at some higher frequency, say 1133 Hz, while the observation at 1133 Hz will identify a period of 3400 Hz, and so on. In practice it appears worthwhile to keep account of all beat-frequency phases and carry forward, at each step, a weighted mean of what has been established earlier, as will be explained below.

The ultimate system will require information at one frequency below 227 Hz, at least. Pending trial, our present suggestion is that a single modulation at 22 2/3 Hz (probably on the 10.88 kHz carrier) would be adequate for this purpose. Any further ambiguity resolution required would be available from consideration of relative signal-to-noise ratios as this quantity is a rough inverse measure of distance from a transmitter.

We have experience at two frequencies (10.2 and 13.6 kHz) that permits us to identify the relative phase velocities and relative attenuation rates of second-mode components of the signals at these two frequencies, under circumstances of large second-mode difficulty. These data are from flights, made a number of years ago, conducted by the (British) Royal Aircraft Establishment and the (U.S.) Naval Research Laboratory. The fact that our simulation of the propagational factors is about right is indicated in Fig. 33, where the dots represent NRL data, privately communicated, and the line is our computed variation with distance.

By interpolation we have derived corresponding propagational constants for the frequencies 10.88 and 11.33 kHz, and have calculated the phases and amplitudes of the beats (taken with respect to the first-order mode, which is the basis of the Omega distance calculations) at the four frequencies of immediate interest. These variations are shown as functions of distance in Fig. 34. The point of most obvious interest is that the departures of the four resultant phases from the first-mode reference become relatively random beyond a distance of 1 or 2 megameters. This point, unfortunately, is of no importance to our immediate problem of lane identification, which proceeds as follows using, as an example, the conditions at 3.9 megameters distance from the hypothetical transmitter.

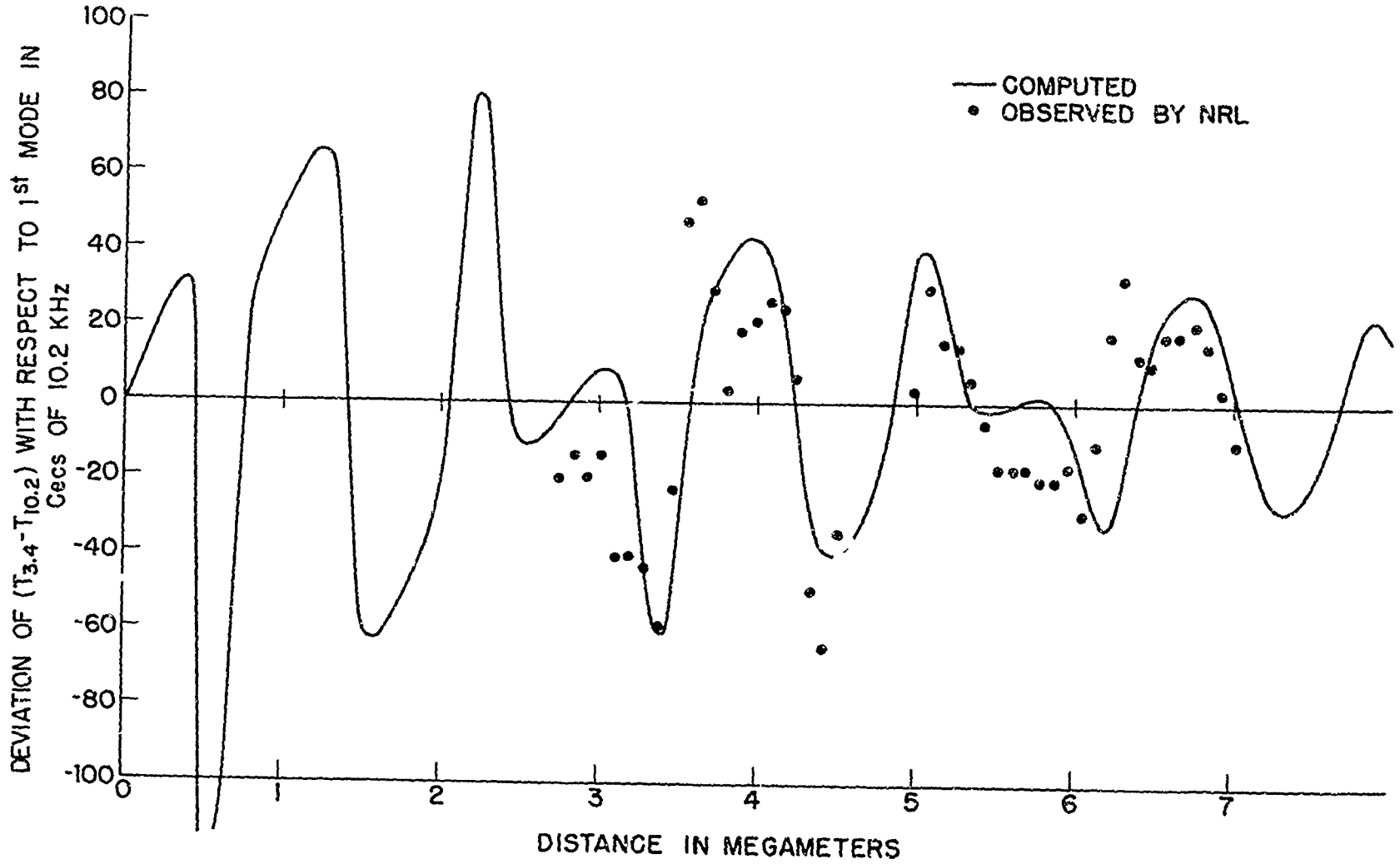

Figure 33. Observed and Computed Differences between 3.4 and 10.2 Kiloherts Transmission Times.

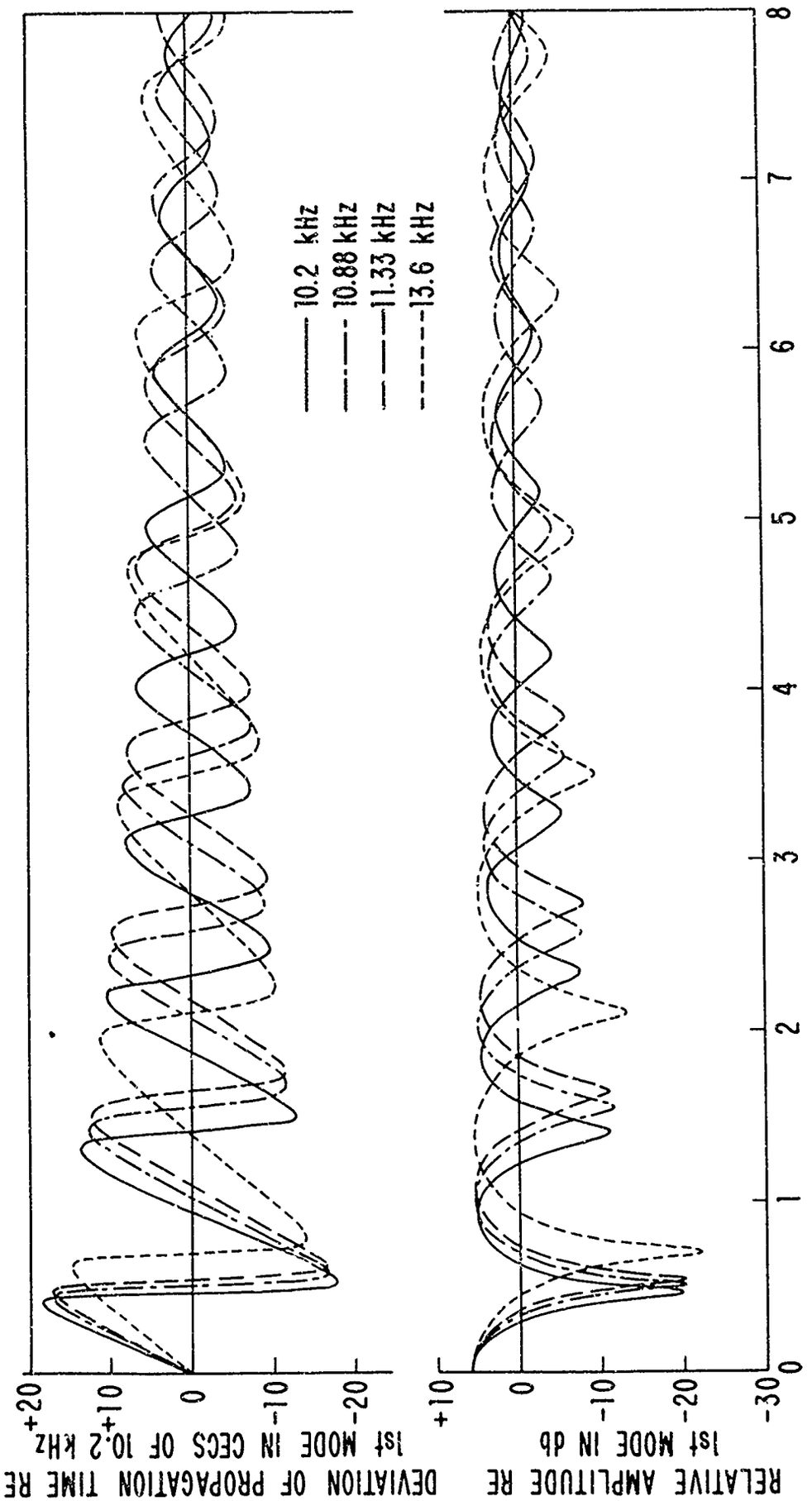

Figure 34. Synthetic Variation of Phase and Amplitude of the Resultant of Two Modes with Respect to the First Mode, at Four Frequencies.

We start by obtaining simulated data for the phases of the four carrier-frequency signals. Because the values of Fig. 34 are given in time units the procedure is as shown in Table IX.

TABLE IX

Phases in Carrier Periods at Various Frequencies

Freq.	1st mode Time	Resultant re 1st mode	Resultant Time	Phase in periods
10.2	13274.5	+4.4	13278.9	132.79
10.88	13282.4	-6.1	13276.3	141.61
11.33	13286.4	-4.2	13282.2	147.58
13.6	13302.3	-6.2	13296.1	177.28

In this table, the times are given in centicycles (or centiperiods) of 10.2 kHz. The phases are therefore determined by dividing the resultant times by 100 times the ratio 10.2 kHz/frequency. Because the Omega system measures only relative phase, we can know only the decimal fraction of these phases. The lane identification (or ambiguity resolution) problem is to reconstruct the whole phase numbers. This process is carried as far as the 3400 Hz difference frequency in Table X.

TABLE X

Resolution of Difference-Frequency Phases

1	2	3	4	5	6	7	8	9	10
Freq.	Wt.	Obs. Phase	Esti-mated Phase	Dev. of deduced phase	Deduced Phase	Sum of Phases	Divi-sor	Period in Cecs	Group Time in Cecs
227	1	0.85			2.85	2.85	0.5	4500	12825
453	2	0.97	5.70	+0.27	5.97	8.82	1.0	2250	13432
680	3	0.82	8.82	0.00	8.82	17.64	1.2	1500	13230
1133	5	0.79	14.70	+0.09	14.79	32.43	1.1	900	13311
2267	10	0.70	29.48	+0.22	29.70	62.13	1.75	450	13365
2720	12	0.67	35.50	+0.17	35.67	97.80	2.2	375	13376
3400	15	0.49	44.45	+0.04	44.49			300	13347

Weights (column 2) are taken as proportional to frequency. The difference-frequency phases are determined by subtracting the "observed" decimal part of the phase for the lower frequency in each pair in Table IX from the corresponding value for the higher frequency, with, if necessary, unity added so that the difference remains in the positive sense. For exampe, the phase at 3400 Hz is 1.28 - 0.79 = 0.49 . An exception is the phase of 227 Hz, for which the "observed" values are found in column 3 on the second and third lines of Table X; in this instance, 1.82 - 0.97 = 0.85.

The identification proceeds as follows. Having determined (from prior knowledge or from measurements at a lower frequency not yet available) that the whole observed phase at 227 Hz is 2.85 periods, the only

available estimate for 453 Hz is twice this value or 5.70 periods. In the table this value for column 4 is found by dividing the summation in column 7 by the divisor in column 8. The deduced phase must have the decimal part of the observed phase, and must lie within plus or minus 1/2 period of the estimated phase. The value in this case is 5.97.

Two estimates are possible for 680 Hz: 3 times the phase of 227, or 1 1/2 times the phase of 453. Because 227 Hz is the difference between these two frequencies, the two estimates give the same result. In the table the deduced value at 680 Hz is the sum of 2.85 and 5.97, or 8.82 periods. The deviation from the estimated value must be zero. As we proceed line by line down the table, the multiplier for each line, to reduce the summation to yield the next estimate is equal to the weight (column 2) for the wanted frequency divided by the sum of the weights above that line. For 2267 Hz, for example, the weight is 10 and the sum of the previous weights is 11. This is given in column 8 as a divisor, simply because all needed values are thus expressed in short form rather than as repeating decimals or fractions. As Table X shows, the deduced phase for 3400 Hz is 44.49 periods. Since this is equal to the difference between the phases of 13.6 and 10.2 kHz in Table IX, the identification, in this case, has been successful.

For purposes of intercomparison, column 10 of Table X gives the time of propagation for each frequency. This is, of course, the period multiplied by the deduced phase.

It is obvious that a difference between an actual phase and a predicted phase that is greater than 1/2 period will result in a mis-identification. This difference is not necessarily quite the same as the deviation in

column 5 of Table X. The tabulated deviation remains, however, an excellent measure of confidence in the ambiguity resolution, to the extent that all values are smaller than 0.50.

Actually, in this tabulation, there are only two deviations that are important criteria. This can be determined by expressing the methods of Table X in terms of the original carrier phases. This procedure yields the results in Table XI.

TABLE XI

Deviations from Expectation at Various Frequencies

Frequency	Deviation = deduced phase - estimated phase
453	$+2\phi_{10.2} - 5\phi_{10.88} + 3\phi_{11.33}$
680	Zero
1133	$1/3\,(+2\phi_{10.2} - 5\phi_{10.88} + 3\phi_{11.33})$
2267	$1/11\,(+30\phi_{10.2} - 20\phi_{10.88} - 21\phi_{11.33} + 11\phi_{13.6})$
2720	$1/7\,(+12\phi_{10.2} - 15\phi_{10.88} + 3\phi_{13.6})$
3400	$1/11\,(+4\phi_{10.2} - 5\phi_{10.88} + \phi_{13.6})$

Intercomparison of these rules shows that:

(1) Dev. 680 = 0, as mentioned above.

(2) Dev. 1133 = 1/3 Dev. 453.

(3) Dev. 3400 = 7/33 Dev. 2720.

(4) Dev. 2720 $\approx$ 4/7 Dev. 2267, without exact proof.

The success of the identification can therefore be judged from the deviations at 453 and 2267 Hz.

The relatively severe conditions of second-mode interference postulated in this study lead to a number of failures of identification at one distance or another. These occur when there happens to be such a difference between the resultant carrier phases that the observed phases lead to a "wrong" conclusion. For example, a deviation of +10 centicycles (of 10.2 kHz) from the predicted value at 13.6 kHz at the same time as a deviation of -8 centicycles at 10.2 kHz will lead to a deviation at 3400 Hz of

$$4\ (+10) - 3\ (-8) = +64 \text{ Cecs of } 10.2 \text{ kHz.}$$

Even worse, the deviation from prediction of 10.2 kHz with respect to 3400 Hz, which is the difference upon which this identification really depends, is $-8 - (+64) = -72$ centicycles. Since the half-period of 10.2 kHz is only 50 Cecs, a mis-identification will result in this case or in any case where the multiplied sum of the deviations exceeds 50 Cecs of 10.2 kHz.

Examination of the data for Fig. 34 shows that there are occasional distances at which the time variations at the four frequencies fall into reasonably straight lines when plotted against frequency or, preferably, wavelength. At these distances, lane identification at 10.2 kHz may be totally impossible because the entire family of difference frequencies agrees in pointing to a wrong cycle at 10.2 kHz. There is no evidence available to indicate that this is happening and no cure for the effect, except perhaps to transmit a sufficiently large set of frequencies so that this kind of coincidence is reduced to a negligible probability. In an

engineering sense, this solution is not satisfactory.

It is a fortunate feature, due largely to the fact that all difference frequencies are propagated at much the same group velocity, that identification as far as 3400 Hz, as in the example above, may be much more reliable than identification at 10.2 kHz can possibly be. This is very satisfying because, as we have shown in earlier sections, both the standard deviation and the time predictability at 3400 Hz are not inferior to those at 10.2 kHz, unless an unusual amount of uncorrelated variation (noise, for example) is present. We may therefore look forward to determining position at 3.4 kHz without bothering with the 10.2 kHz position unless all deviations are very small, or unless other evidence (such as station redundancy) indicates that that identification is correct.

Fixing our attention, therefore, on the 3400 Hz beat, we may examine its time variations from prediction in the light of the deviations from expectation of the 453 and 2267 Hz frequencies identified above. These interesting quantities (for the synthetic signals under examination) are shown in Fig. 35. At the top, the deviation from prediction is seen to have (besides minor variations) cyclic errors of +300 Cecs at distances of 0.5, 1.5, 1.6, 2.4, and 2.5 megameters, while errors of -1800 Cecs occur at 1.6, 3.8 and 4.8 megameters.* The three larger errors are caused by cyclic errors at 453 Hz itself when a large positive deviation (as indicated by dotted lines) had to be interpreted as a large negative one because our arithmetic will not permit a deviation larger than 0.5 period. These points are indicated by solid dots on the lower two curves of Fig. 35.

*It should be noted that both kinds of errors occur at 1.6 Mm, resulting in a net error of -1500 Cecs.

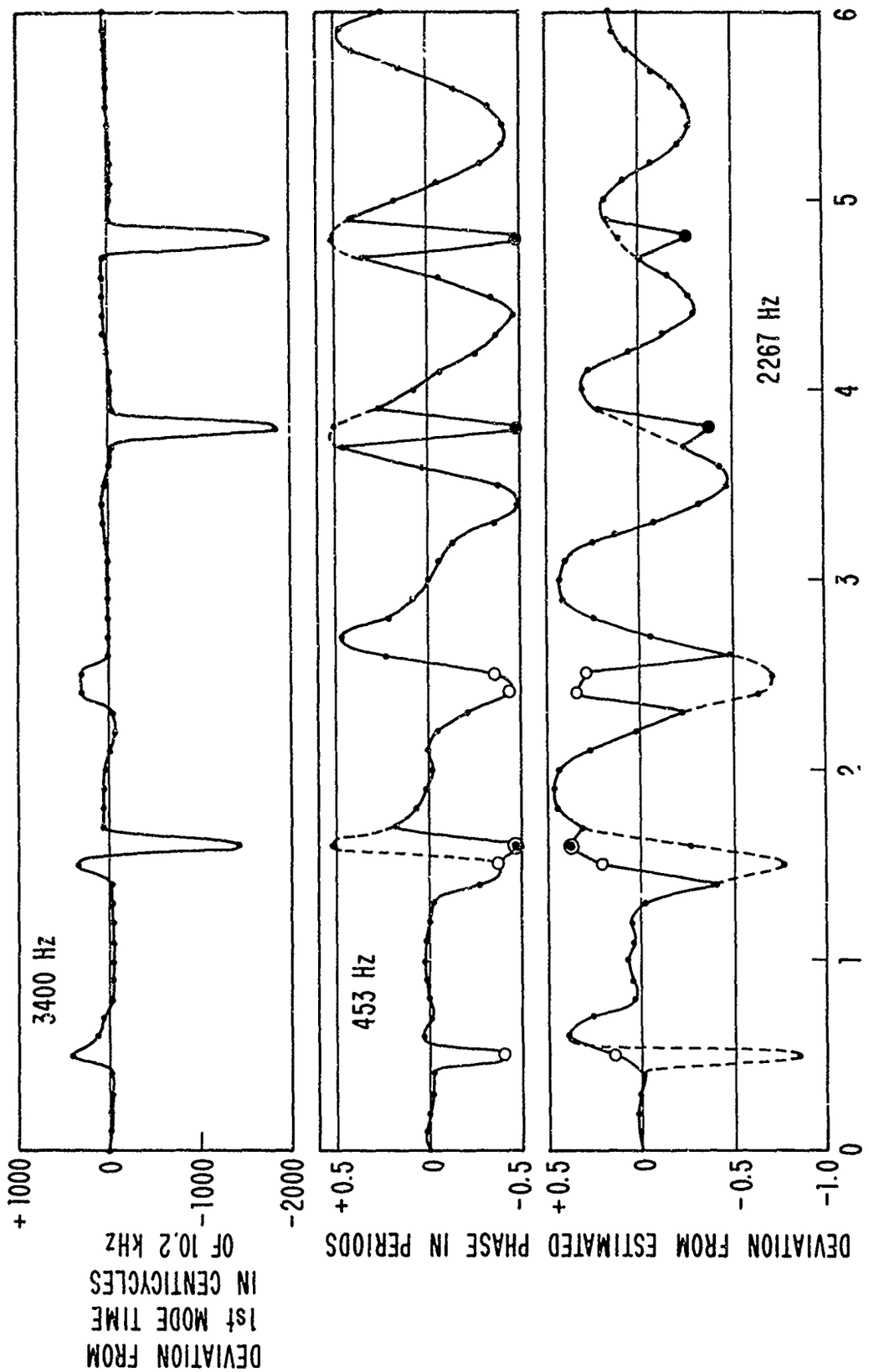

Figure 35: Deviations from Expectations in the Lane-Identification Process

As shown by the open circles in Fig. 35, the distances at which 1 period errors at 3400 Hz occur are those distances at which a large negative deviation at 453 Hz coincides with a large positive deviation at 2267 Hz.

It is, of course, conceivable that a deviation at 453 Hz might be as large as one whole period and therefore undetectable. This appears to be very unlikely as the second-mode magnitude we have assumed is the largest yet reported, while the "ordinary" more or less gaussian deviations produced by noise and uncorrelated instrumental errors do not seem likely to exceed 0.04 or 0.05 period at 453 Hz. In the practical case, such a large error as that caused by mis-identification at 453 Hz should be easily resolved by intercomparison with the data from other redundant pairs of stations.

It thus appears that, by study of the deviations at 453 and 2267 Hz, in a lane-ambiguity calculation like that of Table X, it will be possible not only to measure the confidence to be felt in the lane identification but even to repair the data for 3400 Hz in cases where second-mode interference or random errors cause trouble at 2267 and therefore 3400 Hz.

16. INTERCEPTS OR AVERAGES?

If all lane identifications have been correctly made, it is possible to reduce readings at a number of frequencies to a single value having a smaller standard deviation than have the individual readings. This is conveniently done by using the linearizing process of Section 11.

In the past, the writer has occasionally recommended that the intercept of the best m-line at $m = 0$ be used for this purpose. Trials of a

limited number of calculations had indicated that this process gave a surprisingly small error and, of course, there were obvious advantages in referring the readings to the frequency for which the Navy charts and tables are calculated.

Using the values of effective m derived in Table V, for the "first" four frequencies equally weighted, the mean value of T is, of course,

$$T_{avg} = 1/4 \, (T_{10.2} + T_{10.88} + T_{11.33} + T_{13.6}) \quad . \tag{49}$$

The least-square solution for the best straight line has the slope

$$\Delta = -0.80 \, T_{10.2} - 0.28 \, T_{10.88} + 0.01 \, T_{11.33} + 1.07 \, T_{13.6} \tag{50}$$

and the intercept at $m = 0$

$$T = 0.59 \, T_{10.2} + 0.37 \, T_{10.88} + 0.25 \, T_{11.33} - 0.21 \, T_{13.6} \quad . \tag{51}$$

It is interesting that the mean value of m_{eff} (for equal weights) is 0.4275, or almost exactly the effective m for the frequency 11.33 kHz. It is hard to assign unequal weights to the various frequencies because the ordinary standard deviation decreases with increasing frequency while the unfortunate effects of higher-order modes increase with frequency.

Two examples of the intercept solution are shown in Fig. 36, which is drawn from the calculations discussed in connection with Fig. 34 in Section 14. Because this is an hypothetical construction, it is possible to show, by dashed lines in Fig. 36, the positions of the straight lines representing the first mode alone. The calculated times for the resultant of first and second modes are shown by dots for a distance of 6 Mm and by

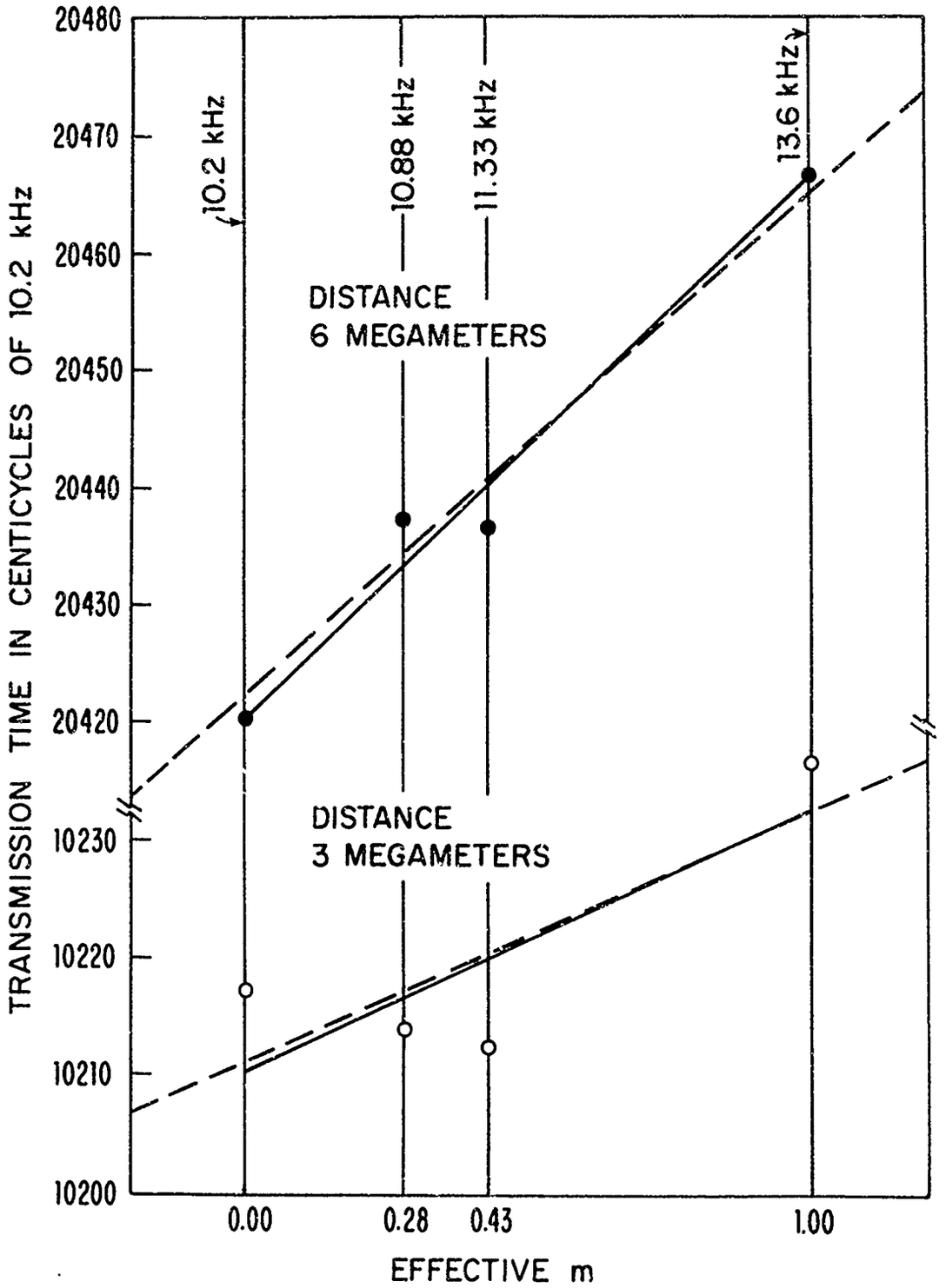

Figure 36: Calculated Transmission Times for the First Mode and for the Resultant of Two Modes.

circles for a distance of 3 Mm. The solid lines, in both cases, are the best straight lines through the resultant points, in accordance with Eqs. (50) and (51). It is conspicuous that the intercepts are close to the values of the first-mode lines at $m = 0$.

Further examination of these effects at various distances reveals that there are cases in which this agreement of the intercept is not so satisfactory. In fact, it is hard to deny the presumed fact that the mean of the four times should be the most stable quantity we can measure. That this mean works very well is shown by Fig. 37. All that one could expect of the mean of four random times is that it should have half of the deviations of the individual times. As Fig. 37 shows, beyond about 1.5 megameters the mean of the four frequencies seems to have deviations about half of the magnitude of those at 10.2 kHz. At these longer distances the second-mode phases have achieved a high degree of randomness, even though our calculations have, no doubt, made them more coherent than is to be expected in nature.

The combination of observations at several frequencies into a single best value has one important operational advantage, in addition to an improvement in accuracy, as pointed out by Mactaggart.[12] If, as Fig. 34 indicates is probable under conditions of severe mode contamination, a frequency falls into an interference null, this fact can be detected from signal-to-noise examination and the offending frequency can have its weight reduced or be eliminated from the mean. Of course the calculation of the mean (or the intercept) must, in this case, be adjusted to compensate for the dispersion. The simplest procedure for this is probably to reduce all readings separately to the chart value, or to some other convenient

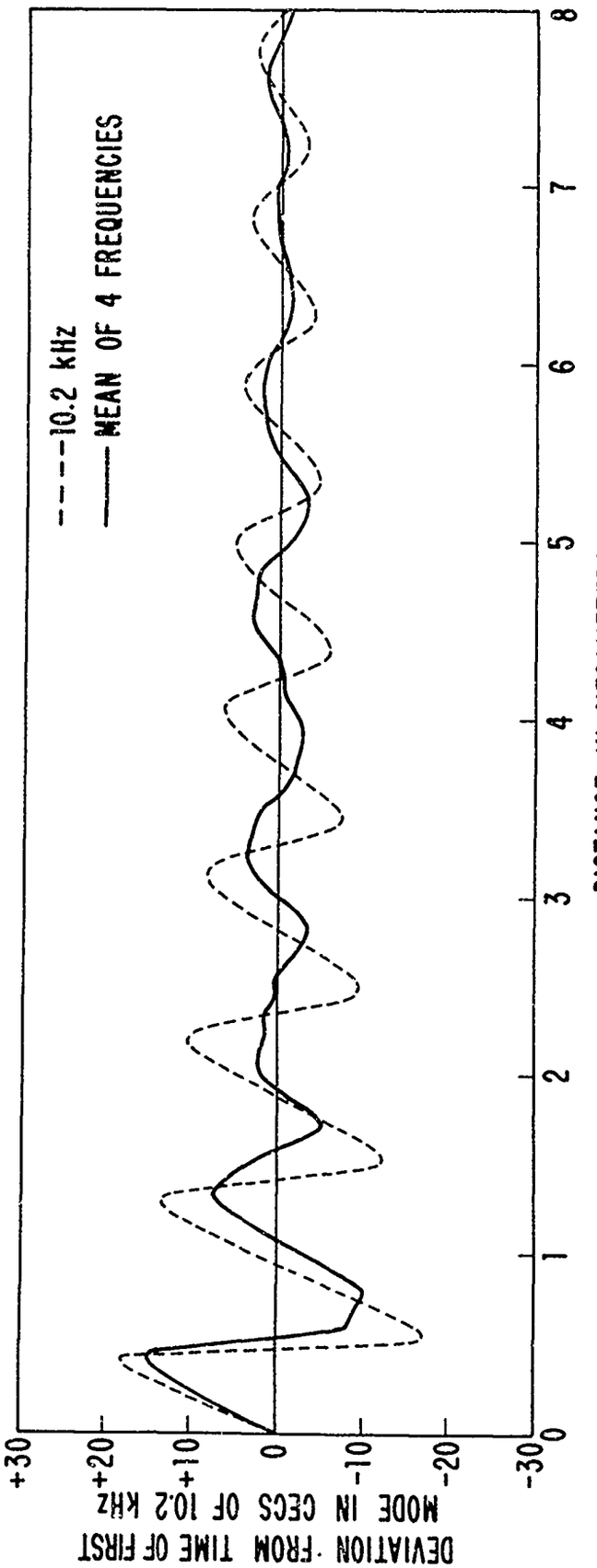

Figure 37: Comparison of Synthetic 10.2 Kilohertz 2nd-Mode Deviations and the Same for the Mean of Four Frequencies.

base, before determining the mean or the intercept. The mean has then the advantage of simplicity (if the weights are taken as equal) over the intercept, as well as a theoretical advantage.

Although Eqs. 49 to 51 have been cited for only the four-frequency case, it is obvious that similar relations can be derived for five, or for any other number of frequencies. Here, as in station redundancy, there is greater strength in a larger union.

17. 3.4 KILOHERTZ NAVIGATION

We have seen in Sections 8 and 9 that the long-term root-mean-square errors at the beat frequency of 3.4 kHz are not seriously larger than at 10.2 kHz. It has also been shown in Section 14 and elsewhere that there are both theoretical and experimental grounds for the belief that lane identification up to the 24-mile lanes of 3.4 kHz is much more reliable than is identification at the carrier frequencies. These considerations lead to the idea that navigation might well be performed at 3.4 kHz, without direct use of the carrier frequencies, in cases where the reliability of lane identification is of critical importance; for example, in the search and rescue problem; or in civil aviation where the degree of absolute accuracy is of secondary importance as compared with a guarantee that an aircraft has not strayed outside of its proper lane. This is not a new idea. It has been suggested from time to time[18] ever since the relatively small diurnal variation at 3.4 kHz was first observed.

It has been said above, in Section 9, that the effect of uncorrelated fluctuations (primarily noise) is to cause relatively large moment-to-moment variations in the phase of a beat frequency as compared with a

carrier frequency. This makes a beat frequency, such as 3.4 kHz, less attractive for many navigational uses, because one of the delights of carrier-phase navigation is its prompt response to motion through relatively small distances. In many other cases, however, especially when the short-term dead reckoning is carried forward by a inertial system[19] or other mechanism, the somewhat blurry response at 3.4 kHz does not constitute an important problem.

A defect of the ambiguity-resolution process in Omega is that a four-mile error (that demonstrably can happen at times) at 3.4 kHz can force an eight-mile error at 10.2 kHz. There is a moderate probability that four-mile (1/2 lane at 10.2 kHz) errors will occur at 3.4 kHz under the influence of large second mode interference, but apparently very little chance of errors at 3.4 kHz as large as eight miles. Under these severe conditions, it is possible that the root-mean-square distance errors at 10.2 kHz may exceed those at 3.4 kHz.

An example of this, at the shorter distances, can be drawn from the synthetic data described in Section 15. It is shown in Fig. 38. This diagram exhibits resultant timing errors as functions of distance, at 3.4* and at 10.2 kHz. In the upper part of the figure, dashed lines show the levels corresponding to $\pm$ 1/2 period at 10.2 kHz. At the distances where an error exceeds these approximate limits, the lane identification process forces an error of approximately one period at 10.2 kHz.

In Fig. 38, at 0.5 and 0.6 Mm, the deviations at 3.4 kHz are as great as those at 10.2 kHz. In the range between 1 and 3.5 Mm, there are several instances of the forced magnification of errors. As a result in the distances less than 3.5 Mm the rms deviations at 10.2 kHz are about

*"Gross" errors, indicated by dotted lines and numbers, have been corrected in this diagram. See Fig. 35.

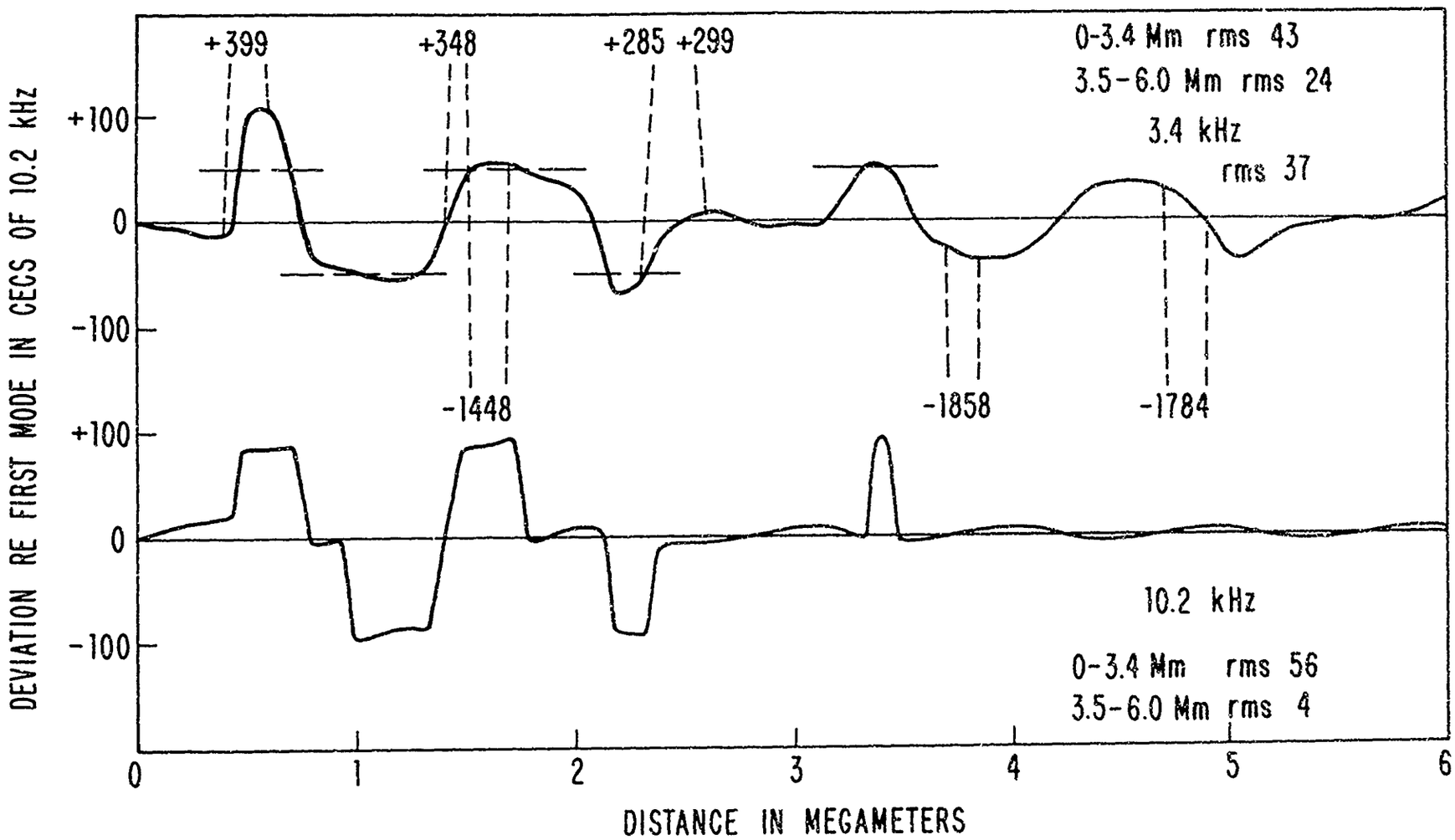

Figure 38: Forced Errors at 10.2 Kilohertz Compared with the 3.4-Kilohertz Errors that Force them.

1.3 times as great as those at 3.4 kHz. At the longer distances, where the second mode problems are not extreme, the lane identification works as it should and the 10.2 kHz deviations are far smaller than those at 3.4 kHz.

While it is interesting that there are extreme circumstances under which the errors of 3.4 kHz navigation may be less than those at 10.2 kHz, any plan for the actual use of the difference frequency should be based upon the long-term statistics. These must, of course, include the errors of prediction. Data showing, to some degree, typical deviations of both propagation and prediction, as seen at Cambridge, have shown in Section 9. Studies of similar data for a number of other places, and examinations of other methods of prediction at 3.4 kHz, ought to be carried out to define the true merits of that difference frequency for direct navigation.

As a final warning that 3.4 kHz should not be used without extreme care in the receiver design (as said at the end of Section 6), the relationships of Eq. (22) have been shown in another form in Fig. 39. This diagram plots the ratio of the standard deviation at 3.4 kHz to that at 10.2 kHz as a function of the coefficient of correlation, for the important range of $\sigma_{13.6}/\sigma_{10.2}$. As was shown in Fig. 9, the ordinary value of $\sigma_{3.4}/\sigma_{10.2}$, for the case of noise when $r = 0$, is about 4, and it is about $2^{1/2}$ times larger when $r = -1$. The important point in Fig. 39 is that $\sigma_{3.4}$ cannot be less than $\sigma_{10.2}$ unless r is greater than 0.943. In fact, for the usual range of variation of $\sigma_{13.6}/\sigma_{10.2}$, the realized correlation coefficient must be at least 0.97 or 0.98 if the deviations of 3.4 kHz are to be kept less than those at 10.2 kHz. It is to guarantee the observational realization of such a high coefficient of correlation that extreme care must be taken in the design of receiver channels.

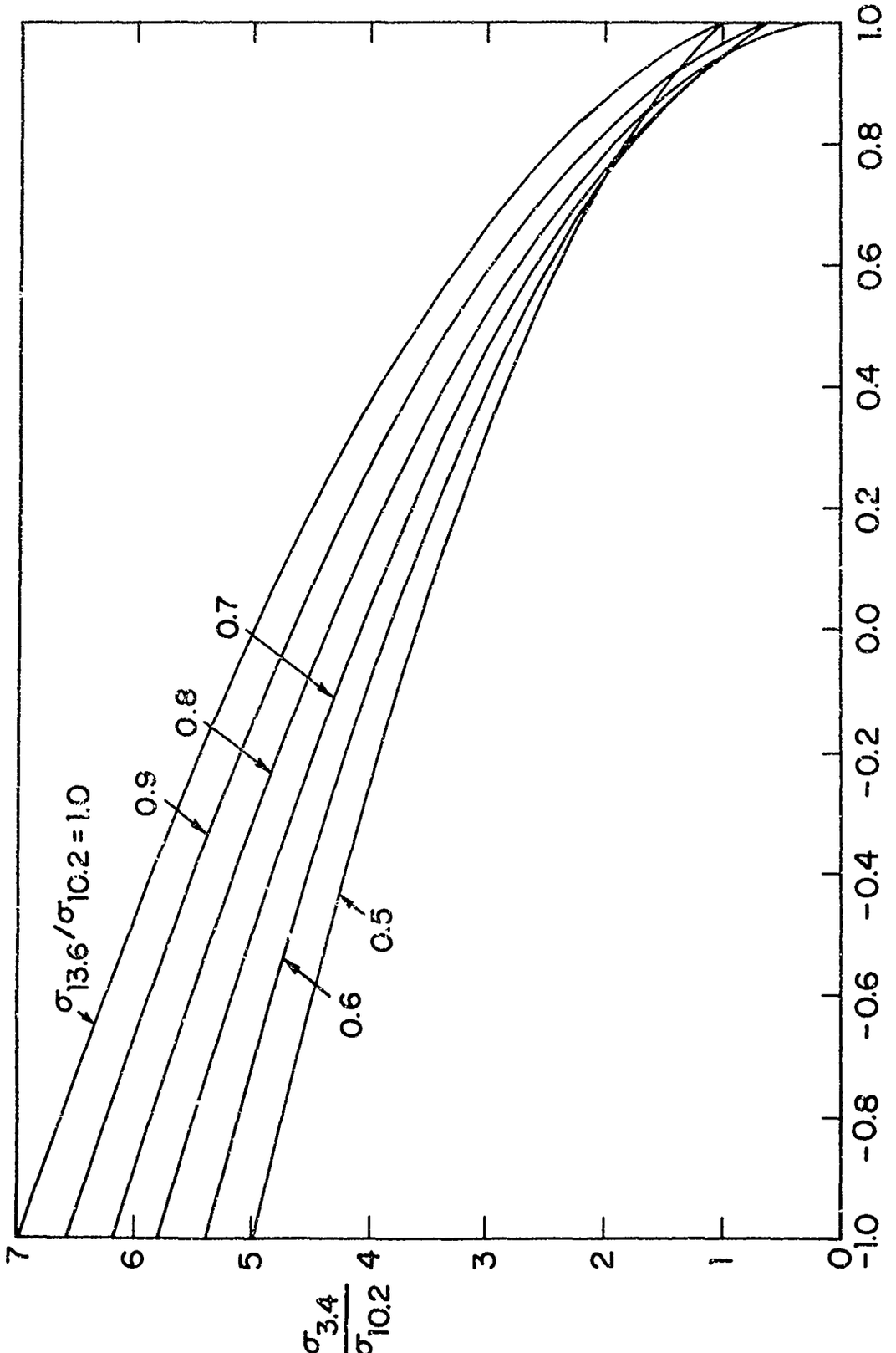

Figure 39: Ratio of Standard Deviations at 3.4 and 10.2 Kilohertz as a Function of the Coefficient of Correlation between 13.6 and 10.2 Kilohertz

18. COMPUTATION OF POSITION

When we have secured Omega time-difference readings for two or more pairs of stations, with confidence in their freedom from possible phase ambiguities, we may proceed to the determination of position. It will be assumed herein that this position is to be expressed in latitude and longitude in degrees of arc.

The fundamental difficulties in this procedure lie in the inconvenience of the hyperbolic lines of position and especially in the intractability of the mathematics for the hyperbolae on the surface of an oblate earth. It is necessary, in practice, to calculate the readings to be expected at a known position. The charts and tables of the Oceanographic Office, for example, are made by inverse interpolation between readings calculated for a grid of uniformly spaced points.

It is equally possible to calculate by successive approximations the coordinates of the point at which the observed time differences apply.[20] To do this reasonably economically, it is necessary to find a mechanism that, for any assumed position, will give an estimate of how far and in what direction to go to find a closer approximation to the true position.

In Omega, where any position is reasonably well surrounded by transmitting stations, this process is easy. To take a case of maximum simplicity, assume that a navigator is at a point where n useful signals are received from n stations at such locations that the azimuths of the transmitters are all separated by $360^{\circ}/n$, or its multiples. At such a position (say one with 4 stations north, south, east, and west of the navigator) the mean distance from the stations does not vary with the

position of the navigator until he moves far enough to invalidate the assumed condition.

In more general terms, for any group of useful Omega stations there is a point where the mean distance is a minimum. Departure from this point will lead, at first, to only a small increase in the mean distance. If the navigator should move so far that he is entirely outside of the group of stations, he will approach a situation where the mean distance may increase as rapidly as he moves. This is, however, a contrary-to-fact condition in Omega, as he should then be operating in a different group of stations. The mean distance, therefore, represents a relatively stable and predictable base of comparison for the individual station distances. It is this excess stability of the mean distance that makes detection of the error of an assumed position easy and practical.

Observed time differences for Omega pairs can easily be converted into differences between the individual station distances and the mean distance. This is done in general by saying

$$n(A\text{-mean}) = (A-A) + (A-B) + (A-C) + \ldots . \tag{52}$$

where A, B, C, --- are distances from stations and n is the number of stations.

If AB, AC, BC, and so on are taken as the usual Omega shorthand for (A-B) and the other time differences, then, for three stations

$$A - \text{mean} = 1/3\,(AB + AC) \tag{53}$$

or, since $AC = AB + BC$,

$$A - \text{mean} = 1/3\,(2AB + BC) \tag{54}$$

Similarly

$$B \text{ - mean } = 1/3 \, (-AB + BC) \tag{55}$$

and

$$C \text{ - mean } = 1/3 \, (-AB - 2BC) \tag{56}$$

This process can be extended to any number of stations to give the deviations from the mean expressed in any chosen (n-1) time differences.

Because we require position in degrees of arc, it is necessary to convert the observed time differences (or alternatively the station-minus-mean time differences) to angular measure. This is done by dividing the observed values in wavelengths by the factor

$$\frac{\pi a f}{180 v}$$

where

a = equatorial radius of the earth

f = frequency

and

v = velocity of propagation.

To refer this process to the ordinary Omega charts and tables where frequency is taken as 10.2 kHz, this factor may be taken as

$$\frac{10200 \, \pi a}{180 \, c} \quad \frac{c}{v} = 3.8222 \pm 0.0013 \quad \text{Wavelengths/degree} \tag{57}$$

where c is the velocity of light

and c/v is the relative time of transit of a signal, referred to an hypothetical signal traversing the geodesic at the velocity of light. The

writer's nominal values of c/v for the 3.4 kHz difference frequency, which is preferred for reasons of reduced ambiguity, are 1.0088 at night and 1.0095 in the daytime, or a mean (used above) of 1.00915. *

With these conversions, the iterative process proceeds as follows. The number of stations is immaterial (so far as the mathematics is concerned) but it will often be taken as three (A, B, C) because of interesting limitations when using a triplet. These will be discussed below.

(1) Compute the observed quantities (A - mean), etc., for each station of a group that is supposed (from prior knowledge or from signal-to-noise ratios, for example) to surround the unknown position. These quantities are hereafter called T_{obs} although they are now in angular measure.

(2) Assume a starting point near the center of the group of stations. An obvious choice is that point from which the stations uniformly divide the azimuth range (that is, are 120^{o} apart for a triplet) where the mean distance is a minimum. For reasons somewhat hard to explain, the

*The discussion hereafter will neglect an important point. If the required accuracy demands the correction of diurnal variation at 3.4 kHz, the relative amount of day and night along each transmission path (from which the relative velocity can be interpolated) cannot be known until the receiving position is known at least approximately. It is therefore necessary to carry the iterative process far enough to give the position with an error of only tens of miles, and then to readjust the "constant" of Eq. (57) separately for each transmission path before completing the final iterations. Alternatively, the iteration may be carried to its normal conclusion and the determined position can then be corrected for the velocities of propagation appropriate to the time of day. This is not difficult, as the distances and azimuths of the stations are available after the final iteration. If this adjustment is to be made in terms of the Oceanographic Office's "Sky Wave Corrections," it will simplify the work if the standard Omega relative chart velocity of 0.9974 is used in Eq. (57).

writer tends to prefer the point at which (for the triplet) all stations are equidistant. The distinction is not a matter of much importance. Any group of stations has, presumably, a best starting point (when there is no prior knowledge) and it should be determined and used as standard procedure. Of course if there is prior knowledge that can reduce the distance between the starting point and the true position, this knowledge should be used, as the required number of iterations depends upon the magnitude of this distance.

(3) Calculate the distances of the various stations from the starting point. The writer prefers to use the Andoyer-Lambert[21, 22] correction for the oblateness of the earth in geographic coordinates, as this seems to be sufficiently accurate for Omega purposes and avoids the conversion into and out of geocentric or parametric latitude. A convenient notation is

$$T = a\sigma + \delta s \tag{58}$$

where

T = distance

a = equatorial radius of the earth

σ = angular distance in radians

δs = a small correction for oblateness

This is solved in parts by saying

$$\cos \sigma = S + C \cos (\lambda_T - \lambda_P) \tag{59}$$

where

$$S = \sin \phi_T \sin \phi_P$$

$$C = \cos \phi_T \cos \phi_P$$

and

ϕ_T = latitude of transmitter

ϕ_P = latitude of assumed point

λ_T = longitude of transmitter

λ_P = longitude of assumed point

and

$$\delta s = \frac{a-b}{4} \left[\frac{3 \sin \sigma - \sigma}{1 + \cos \sigma} \left[(1+S)^2 - C^2\right] - \frac{3 \sin \sigma + \sigma}{1 - \cos \sigma} \left[(1-S)^2 - C^2\right] \right] \quad (60)$$

where

b = polar radius of the earth.

(4) Calculate the azimuths of the various stations from the assumed point. Since the azimuth is used only to factor the deduced angular corrections into latitude and longitude components, it is not necessary to use the Andoyer-Lambert correction to the directions. The azimuth on a sphere is accurate enough (unless the latitude is low and the difference in longitude happens to be very nearly 180°, which is not in the useful domain for Omega). The quadrantal ambiguities in the azimuth are most easily resolved by using the cosine formula

$$\text{Azimuth} = A = \cos^{-1} \frac{\sin \phi_T - \sin \phi_P \cos \sigma}{\cos \phi_P \sin \sigma} \quad (61)$$

and giving the resulting angle the algebraic sign of $(\lambda_T - \lambda_P)$.* With East longitude and angular distance from the station taken as positive, this gives azimuth in the ordinary sense.

(5) Average the distances from the various transmitters and form the deviation ΔT for each transmitter as

$$\Delta T = T - \text{mean } T - T_{obs} \tag{62}$$

where ΔT, T (step 3), and T_{obs} (step 1) are computed separately for each station. T_{obs} is used here in the negative sense because we are calculating a correction toward a station rather than distance from it.

(6) Components of ΔT for each station are formed by taking

$$\Delta\phi = \Delta T \cos\theta \tag{63}$$

and

$$\Delta\lambda = \Delta T \sin\theta / \cos\phi_P \tag{64}$$

where $\Delta\phi$ and $\Delta\lambda$ are corrections to the starting-point latitude and longitude, respectively.

It is obvious that, on a nearly spherical earth, this projection will have a large error if ΔT is large unless either θ or ϕ_P is zero. A more accurate spherical projection can be made, but it nearly doubles the whole computational complexity of each iteration and is unimportant when ΔT diminishes as the true position is approached. It therefore seems

* $(\lambda_T - \lambda_P)$ must, of course, be taken as less than 180°.

better to use an easy and approximate projection and to allow the iterative process to carry the load. At high latitudes, of course, these errors of projection are especially severe and generally require a reduction of the "gain" of the calculation, which will be discussed below.

(7) The n latitude and n longitude corrections for n stations are then averaged, multiplied by a gain factor G, and added to the coordinates of the starting point to give the coordinates of the point from which the next iteration proceeds. That is

$$\phi_{j+1} = \phi_j + G\ \overline{\Delta\phi}_j \tag{65}$$

and

$$\lambda_{j+1} = \lambda_j + G\ \overline{\Delta\lambda}_j \tag{66}$$

where j is the iteration number.

(8) The newly-derived approximate position resulting from Eq. (65) and Eq. (66) is now used as a new starting point and the iteration process goes back to repeat steps 3 through 8. Step 1 is unchanged because it contains the observed time differences at the true position, and step 2 no longer applies.

(9) The iteration is terminated when all values of ΔT have fallen below a level representing propagational uncertainty, or when their root-mean-square value stops changing, as discussed below.

The number of iterations required depends upon a number of factors: the divergence and crossing angles of hyperbolae, of course, the distance

from the starting point to the true position, the latitude, the final precision required and the "gain" used in the computation. This is a subject we have explored only by trying a number of examples that appeared interesting. As a grand average, it seems that the distance from each assumed position to the true one is approximately halved at each iteration.

Each set of iterations should proceed until each value of $\Delta\phi$ and $\Delta\lambda$, or perhaps more conveniently the rms value of ΔT, is smaller than the expected propagational error. This level might be established near $0^{\circ}.004$, or about 1/4 nautical mile.

We have once or twice mentioned the "gain" of the computation and must admit that we can define the best value only approximately. We have used the gain G as a multiplier for the mean correction for both latitude and longitude. Since $\overline{\Delta\phi}$ and $\overline{\Delta\lambda}$ are the means of n values for n stations, it would presumably cause oscillatory behavior to use a G as large as n, which must be at least 3. This is usually but not always the case. On the other hand, because we are splitting the deviation ΔT (for each station) into orthogonal components, it seems reasonable that G might be as large as the square root of two.

Figure 40 gives an example (shown for latitude only) of the variations in behavior resulting from changes in the gain of the computation. In this instance, gain 2 gives nearly critical damping, but in other cases gain 2 is found to be oscillatory. An example of this is shown in Fig. 41 which exhibits the loci of iteration from several starting points toward Cambridge. Two or three features of this diagram are important: the greater tendency to overshoot at the higher latitudes, the indications of more nearly critical damping as the true position is approached (or as the number of iterations

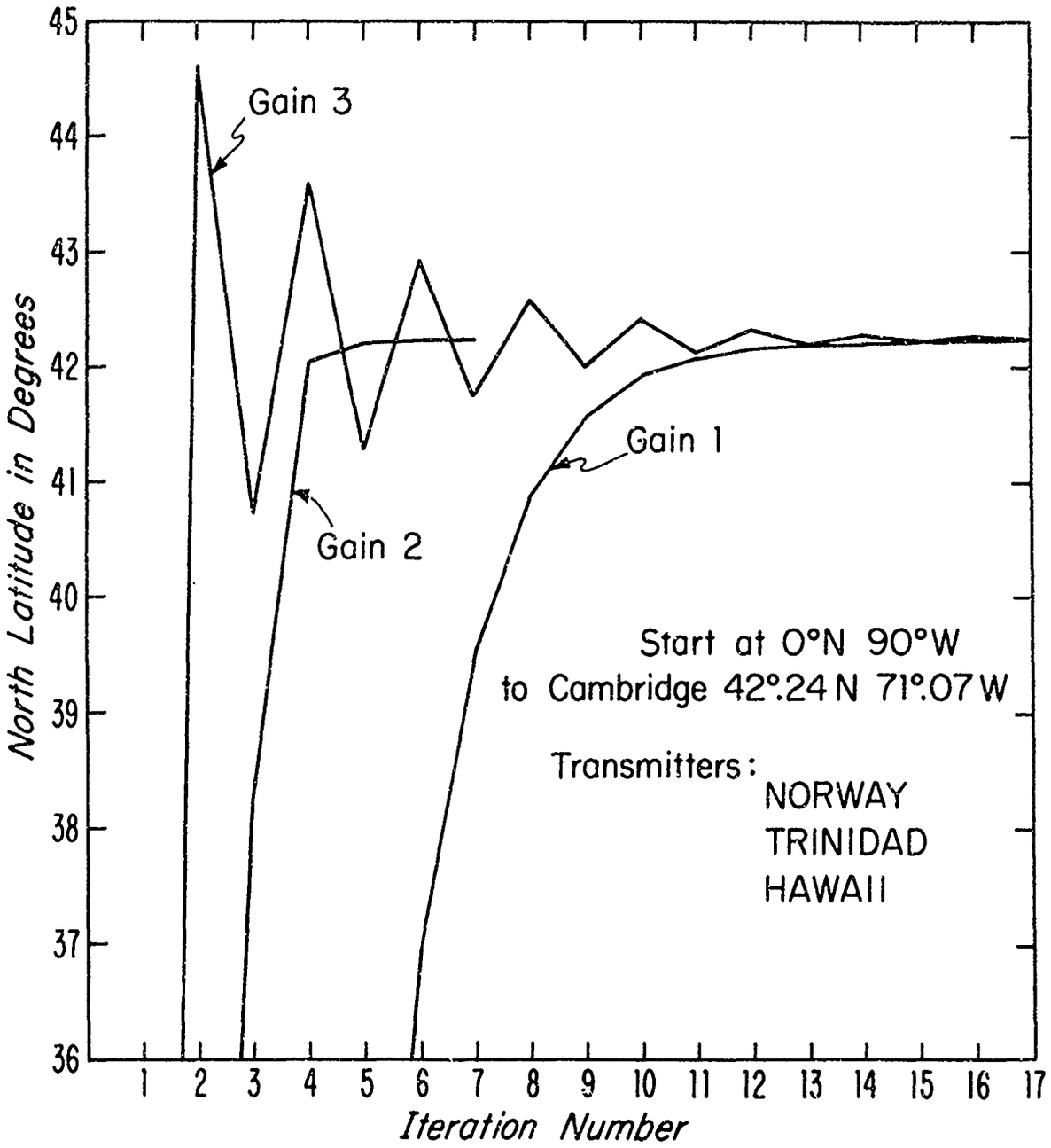

Figure 40: Closure of Iterations for Position for Various Gain Factors.

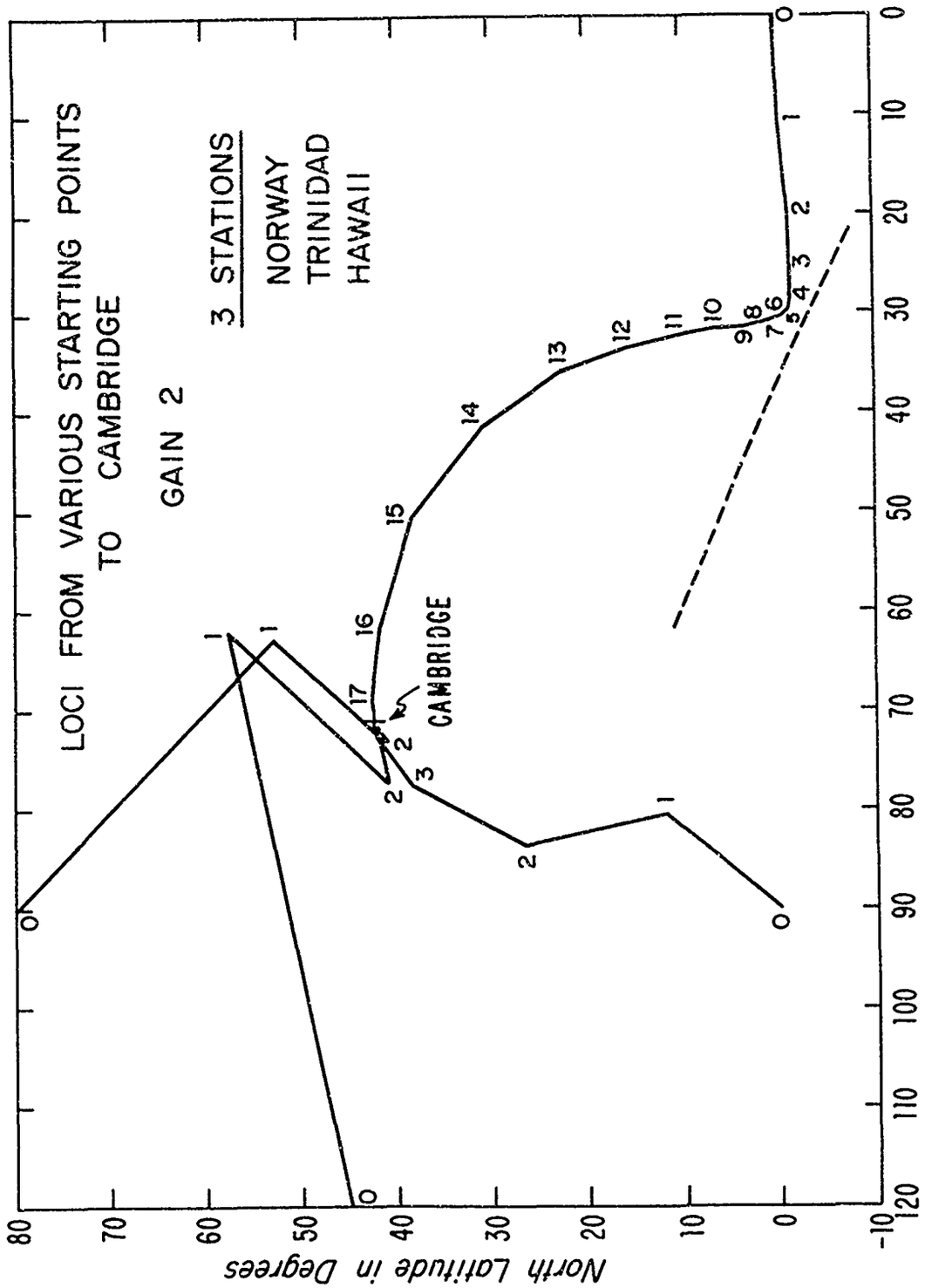

Figure 41: Loci of Iteration from Various Starting Points toward Cambridge.

increases), and the very slow approach for part of the path from the point at 0°N, 0°W. This last feature must be reserved for later discussion.

It is evident that at high latitudes a lower gain is advisable because we must take $\Delta\lambda$ as proportional to the secant of latitude. Thus errors in the projection of longitude are magnified. In fact, the whole process of solving for latitude and longitude degenerates into a zero-divided-by-zero situation at the pole itself. The self-stabilizing feature seems to be because after a number of iterations the deviations of the various station components come into a kind of coherence that makes a higher gain more tolerable for the later iterations.

A limited number of trials seems to indicate that if one must have a single optimum value for G it may be near 1.7. A variable model that has behaved well in a number of circumstances is

$$G = (1.2 + \log_{10} j) \cos^{1/4} \phi_P \tag{67}$$

where j is the iteration number. The functions in this definition have no justification except that they give a suitable increase in G as the iteration proceeds and a modest decrease in the polar regions. This choice of G seems to reach a solution in as small a number of iterations as any other choice, while allowing the locus of iteration to be reasonably smooth and direct.

The writer has come to prefer a sort of "automatic gain control" that appears to have similar properties. This function may be rationalized by noting that the root-mean-square value of ΔT in Eq. (62) is a rough measure of the distance from the assumed position to the true position. For the first iteration, when the initial assumption is taken as the point

equidistant from the transmitters, the ratio between distance and rms ΔT averages about 1.5. The sum of the squares of $\overline{\Delta\phi}$ and $\overline{\Delta\lambda}\cos\phi_p$ is, of course, the "distance made good" in each iteration and this distance is generally toward the true position. If we then take G as RMS ΔT/RSS $\overline{\Delta\phi}$, $\overline{\Delta\lambda}$ (leaving out the function $\cos\phi_p$ mentioned above) we have a gain factor which seems to have the general properties of Eq. (67), although the reduction in gain in the polar regions is more extreme for the automatic gain.

The reasons why the automatic gain is advantageous can be explained in terms of Fig. 42. This diagram shows the baselines and baseline extensions of a triplet of stations, A, B, C.[20] The region between each pair of contiguous baseline extensions is shaded. It is a feature of the iterative calculation that it cannot proceed from a starting point in an unshaded area to a true fix that is in a shaded area. It will instead converge on a false position that must be in an unshaded area. There are two facts that explain this behavior. A pair of hyperbolae on a sphere (when not confocal) have two intersections. Each hyperbola does not extend to infinity, as on a plane, but forms a continuous closed figure. In the case of hyperbolae that intersect well away from the foci, as do those marked AB-0.20 and BC+0.30 in Fig. 42, the other intersection will clearly be around on the other side of the sphere. As shown by the two intersections of the hyperbolae marked AB+0.95 and BC-0.97, however, a true fix near a vertex may have a false fix not too far away.

Any network of stations on a sphere has a geometrical image on the opposite side of the sphere, where the locations are obtained by projecting the position of each station through the center of the sphere. The angular

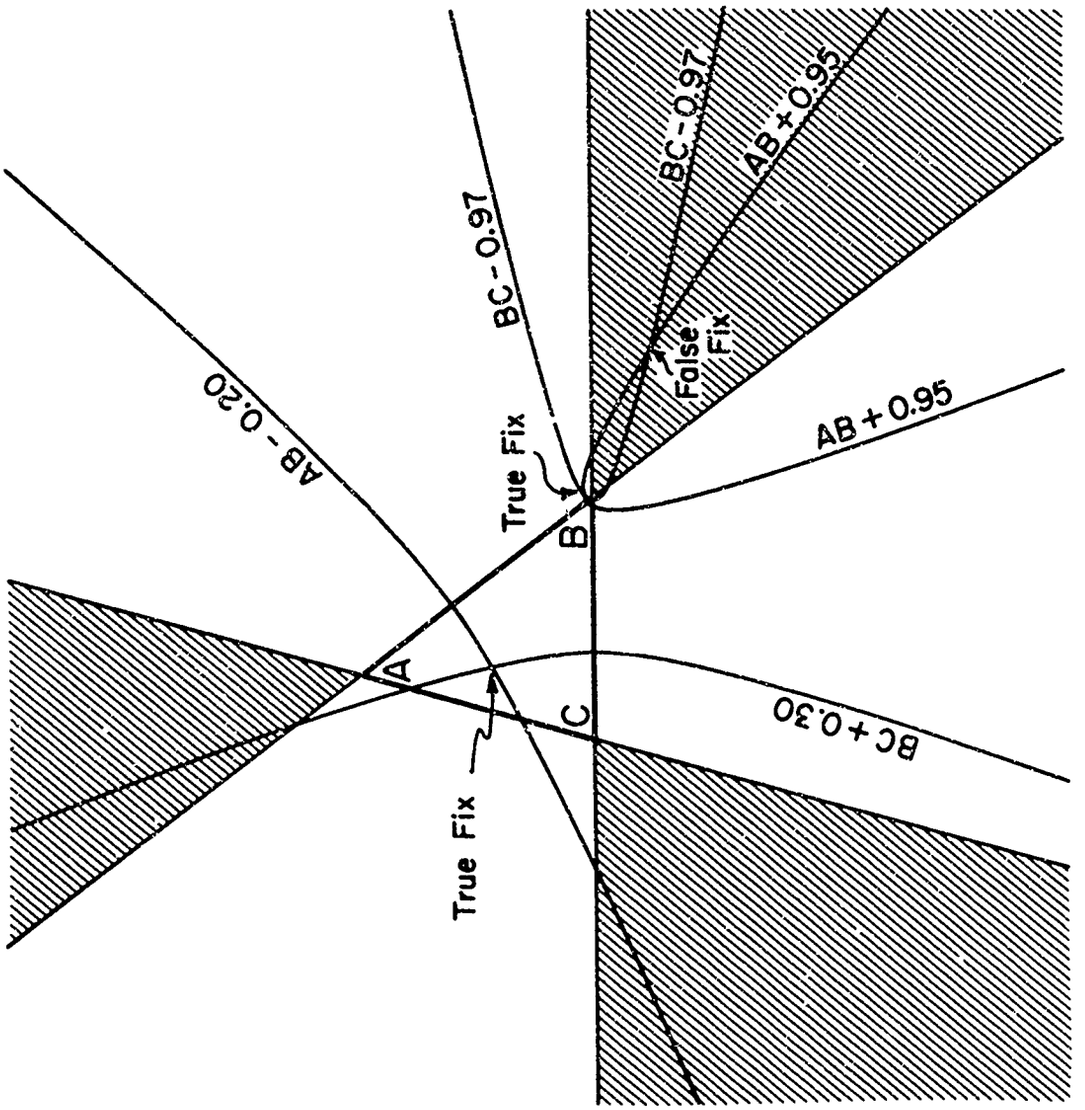

Figure 42. Double Intersections of Hyperbolae for a Triplet of Stations

distance from any point to the image of a station is 180° minus the distance from the point to the station. It follows that if the iteration in a triplet of stations proceeds to a false fix a second calculation can be performed, with the algebraic signs of all values of T_{obs} reversed. This second calculation will proceed to the antipode of the true fix. It is therefore possible, when there are four or more useful stations, to complete the iterations twice for each of two or more different triplets of stations, one direct and one reversed in each case. Half of the final positions found will agree or be antipodal, while the other half will scatter widely.

The second important point mentioned above is the inability of the three-station iteration to cross a baseline extension. This is because the positional information resides in the angle subtended by the transmitters as seen from the "navigator's" position. At any point on, say, the AB baseline extension either A or B can be used with station C to determine a line of position, but there can be no two-dimensional fix.

The behavior of the locus of iteration from 0°N, 0°W in Fig. 41 is explained by this feature. It happens that both the starting point and the terminus at Cambridge lie in the "unshaded" area for the triplet of stations used, while the original direction of the locus brings it close to the baseline extension of the Trinidad-Hawaii pair, which is roughly indicated by the dotted line. In this region near a baseline extension the distance made good in each iteration is greatly reduced. The locus does, however, sheer away from this obstacle and ultimately find its way to Cambridge.

This effective loss of gain near a baseline extension is a primary reason for preferring the "automatic gain control" described above. If the yield of an iteration (the magnitude of $\overline{\Delta\phi}$ and $\overline{\Delta\lambda}$) is relatively small

the gain increases so that the distance actually covered by the iteration is kept more nearly proportional to RMS ΔT. In the case of Fig. 41, it would have been too confusing to have included a second locus of iteration from $0^{\circ}N$, $0^{\circ}W$. This second iteration with the "AGC" can be described, however. It is more erratic in the early iterations, but closer to Cambridge after 8 iterations than is the locus shown after 16.

The terms "true" and "false" in Fig. 42 are not determined by the arithmetic. There are simply two alternative intersections of a given pair of hyperbolae. In an Omega sense, however, the identifications may stand as shown, because a series of iterations in the ABC triplet should begin near the center of the ABC spherical triangle unless prior knowledge is available so that one can begin nearer to the true position.

Examples of the loci of three-station iterations in northern North America are shown in Fig. 43. The computations were made with the automatic gain and the loci are seen to be generally smoother than those of Fig. 41. The iterations all proceed from the point from which the three stations are equally distant. The points reached at each of the first few iterations are marked. The number adjacent to each target point is the number of iterations required to reduce the error of the calculation to less than 1/4 nautical mile.

The line in Fig. 43 starting toward Copenhagen indicates a rather unnecessary experiment in iterating over a long distance toward a point that is just barely on the "true" side of the Hawaii-Norway baseline. The calculation is successful but only after a very large number of iterations, partly because the progress across the arctic is slow but chiefly because at the far end each step traverses only a very small fraction of the remaining

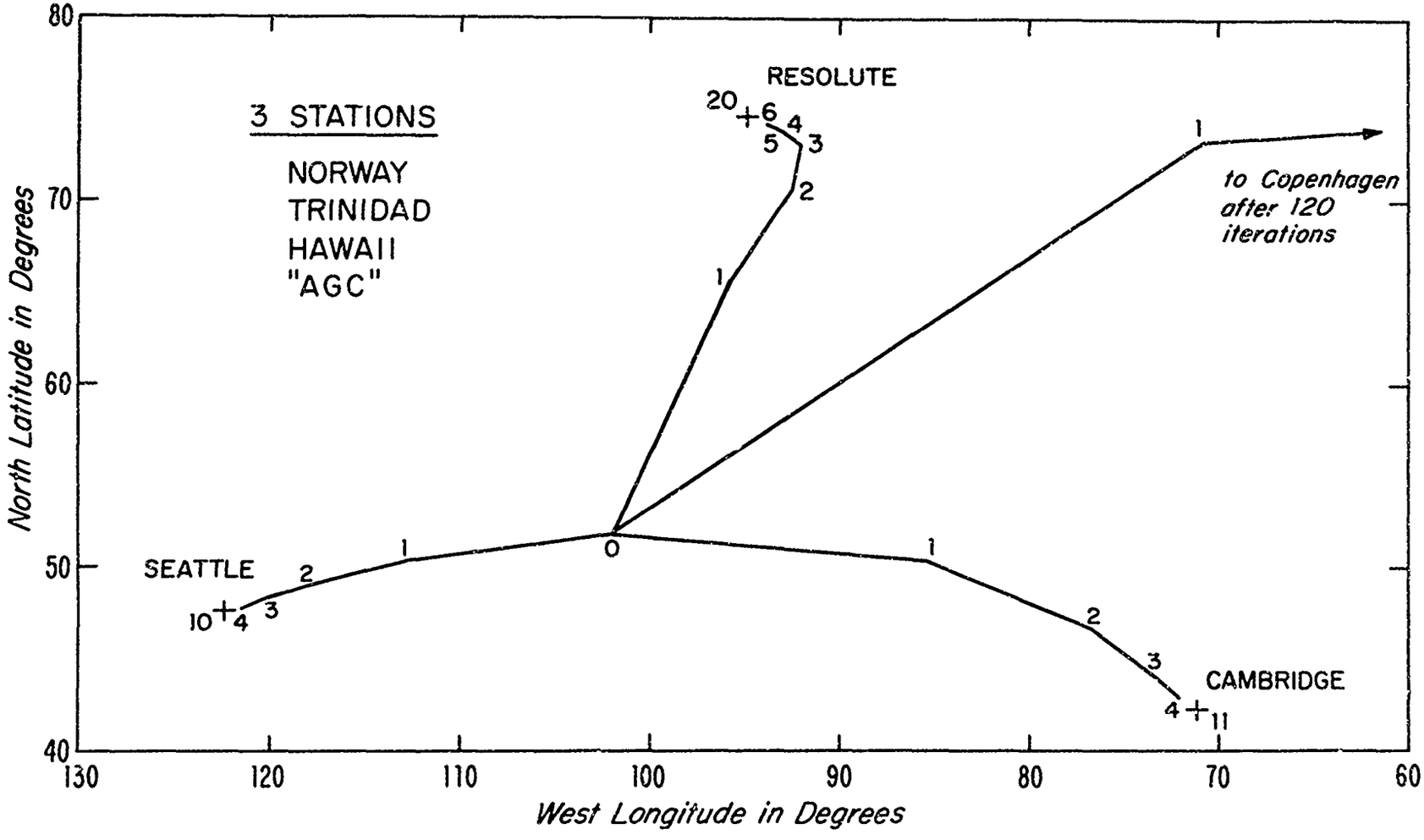

Figure 43. Loci of Iteration from the Three-Station Equidistant Point Toward Various Termini

distance. The locus passes just west of Bergen, Norway, between the tenth and eleventh iterations but then requires a hundred more iterations to cover the last 380 miles.

This difficulty in the baseline extension regions (with the associated true and false fixes) characterizes only the three-station solution. When four or more stations provide useful signals it is (given the Omega station geometry) impossible to be at a position where two-dimensional information is not available. Conveniently, the computational rules are exactly the same no matter how many stations are used. * Several examples of loci in the Atlantic area using the four named stations are shown in Fig. 44. Here, as in Fig. 43, the number of iterations to reduce the computational error to 1/4 nautical mile is given near each final point. Of especial interest in this figure is the calculation toward the point near St. Helena (about $14^{o}.7$ S., 15^{o} W.) which was carefully located to be exactly on the baseline extension of the Norway-Liberia pair. The requirement for 28 iterations shows that there was a decrease in the "power" of the later iterations, but the calculation came to a successful solution.

One other subject requires discussion. If there is some lingering doubt of the absolute accuracy of the total cycle count, we are in an unfortunate position with the 3-station iteration process. If, say, the distance from one station only is erroneously taken to be one 3.4 kHz wavelength (300 Cecs of 10.2 kHz or approximately 48 nautical miles) too large, the iteration process will lead to a position at least 24 miles from the true

*It should be noted that, with weights for the various stations assigned in terms of signal-to-noise ratio and related in a non-linear way to distance and direction, this multiple-station iteration forms one approach to the interesting problem of attaining the best possible solution for position, using all data from all Omega stations.

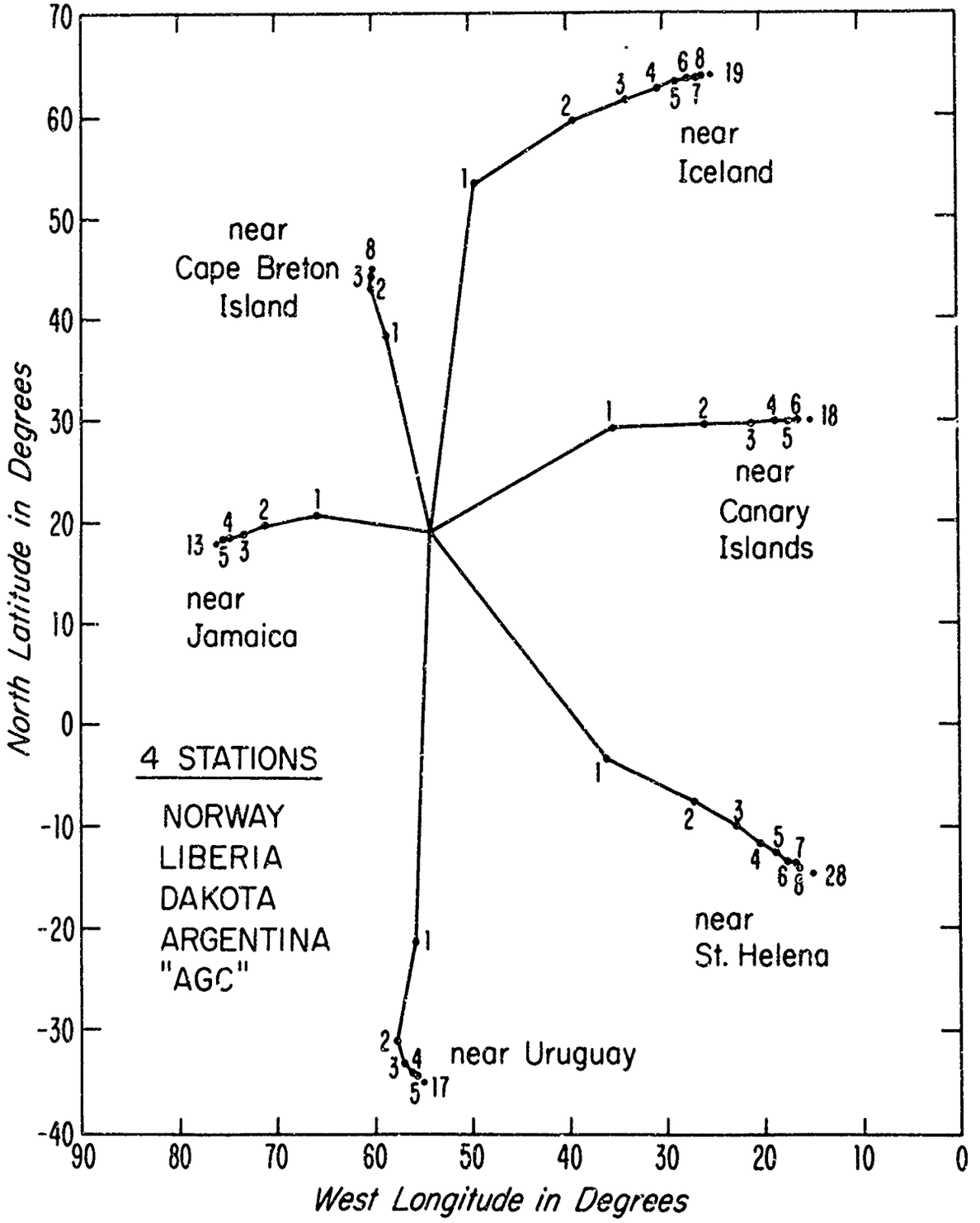

Figure 44: Loci of Iteration in a Four-Station Network

position in a direction generally further from the offending station. This is because there is in fact a position at which the three distances have the erroneously-observed differences.

If four stations are available, they can be examined in groups of three in four different ways. Unfortunately this process, with a single error in distance, will lead to four well-separated positions, only one of which is correct.

The direct four-station solution as in Fig. 44, offers one distinct advantage besides its relative simplicity and the absence of false fixes. Because there is no real point at which the 4-station differences can be what they appear to be (on the assumption of an error in a single distance) the root-mean-square value of ΔT will, with increasing iterations, reach a reasonably constant value corresponding roughly to a quarter-period. This is equivalent to about $0^{\circ}.2$ of arc, or about 12 nautical miles in distance. As this magnitude is about ten times* the normal propagationally-determined uncertainty of the measurements, it should be reliably conspicuous. The effect is that seen in Fig. 45, where the errorless computation continues until the rms value of ΔT decreases to the propagational "noise" level of $0^{\circ}.01$ or $0^{\circ}.02$ (not shown in the figure) while the computations with one error saturate at a higher level of ΔT, in this case after five iterations.

As shown in the upper part of Fig. 45, the automatic gain rises to a high and fluctuating level when this plateau in rms ΔT is reached. This

*This assumes that the calculation is carried out at 3.4 kHz. At 10.2 to 13.6 kHz, the margin in magnitude is reduced by a factor of three or four.

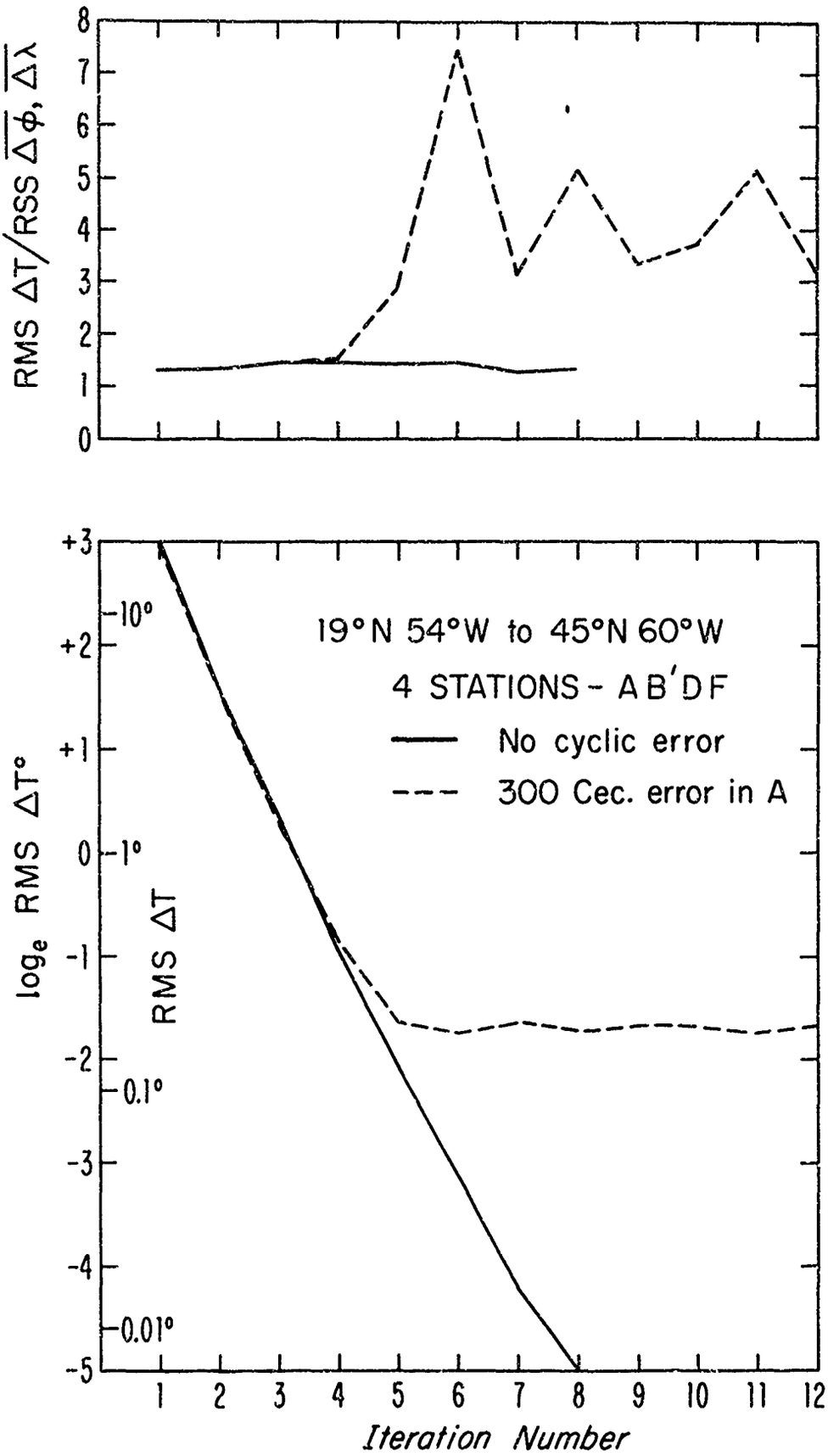

Figure 45: "Automatic Gain" Factor and RMS Position Adjustment as Functions of Iteration Number, with and without a Cyclic Error.

feature may be found useful, but it does not appear to the writer to be as good an indicator of error as is the value of rms ΔT itself. It is, however, a reminder that the solution will be found to be oscillatory in this high-gain region.

With a rather large amount of computation it is conceivable that an error in a single station distance could be identified and corrected. The argument is as follows. If four separate three-station solutions* show an rms scatter of about one 3.4 kHz wavelength/$2\sqrt{2}$ (say 15 miles, more or less) in either latitude or longitude, or both, it may be taken as an indication of a one-wavelength error in a single distance. Then, if no less than twelve four-station computations should be performed (with each station distance taken individually as observed (1), or as one wavelength greater (2), or as one wavelength less (3) than the observed value) one of these twelve resulting positions should coincide with one of the four three-station positions. Whether this method should be attempted must depend upon the experimental reliability of ambiguity resolution. This is because, at least under some circumstances (such as at the center of a perfect quadrilateral, with one distance measured as too large and the diagonally-opposite distance as too small), there can be two cooperating errors that cannot be detected. Much depends, then, upon the results of experiment. If it can be dmonstrated that single errors occur occasionally while errors in more than one path at a time are extremely rare, these suggestions may become useful.

*It probably ought to be pointed out that a later secondary computation should start at the terminus of an earlier computation. It will then either agree immediately or reach its own terminus after only a few iterations.

We must summarize these confusing statements by saying that it is possible to feel reasonable confidence in a determination of position if (a) the deviations of the observed phases from expectations in the cycle-identifying process are satisfactorily small, and if (b) the four-station solution for position proceeds to a level of rms ΔT that is commensurate with propagational experience. Equal or greater confidence may be felt if a four-station solution and a three-station solution (using any three of the four stations) are both carried out, with final positions that agree except for propagational uncertainty.

It should be obvious that, whatever lane-identification errors or propagational deviations are involved, the magnitude at which (for four or more stations) RMS ΔT limits is a measure of the error of a deduced position. This may be one of the happiest results of the iteration technique because, in general, Omega readings do not automatically yield a measure of current accuracy.

With five available stations, which should generally be the case in Omega, these same principles should lead to correction of even double lane-identification errors, although the number of computations required would be very large. A study of this kind should certainly go forward, and it seems reasonable that further study of the three- and four-station solutions should be carried out in the hope that there may be better techniques than those the writer has used, or that there may be neglected clues in the results of the iteration process that would allow better assurance of the absence of errors.

The importance of this suggested work will, of course, depend upon the results of lane-identification experiments that have not yet been made.

If these should be as successful as the writer hopes, it will follow that adequate confidence can be felt in a solution for position that uses no more than the results already available in this study.

19. SUMMARY

Suggestions have been made in this report for improving the utility of Omega by:

1. Reduction of errors of observation,
2. Reduction of errors of prediction,
3. Improvement of the reliability of lane identification,
4. Extension of the range of lane identification to cover the world, and
5. Determination of latitude and longitude from Omega observations, without the requirement of any prior knowledge of position.

REFERENCES

1. Omega - A World-Wide Navigational System, System Specification and Implementation, Pickard and Burns Electronics Publication 886B, 1 May, 1966.

2. The Omega Navigation System, E.R. Swansom and M.L. Tibbals J. Inst. Nav., Vol. 12, pp. 24-35, Spring, 1965.

3. The Development of Long-Range Hyperbolic Navigation in the United States, J.A. Pierce and R.H. Woodward, J. Inst. Nav., Vol. 18, pp. 51-62, Spring, 1971.

4. Proceedings of the First Omega Symposium, Institute of Navigation, 9-11 November, 1971.

5. The Use of Composite Signals at Very Low Radio Frequencies, J.A. Pierce, DEAP Technical Report No. 552, Harvard Univ., February, 1968.

6. A Modified Composite Wave Technique for Omega, W. Papousek and F.H. Reder, J. Inst. Nav., Vol. 20, pp. 171-177, Summer, 1973.

7. Combination of Phase Velocity and Group Velocity into a Composite Velocity, A.D. Watt and R.D. Croghan, private communication, October 10, 1968.

8. VLF Radio Engineering, A.D. Watt, Pergamon Press, 1967.

9. Theoretical and Experimental Treatment of Multifrequency Radio Wave Reception (10-14 kHz) for Investigations of the Lower Ionosphere, Gisle Bjøntegaard, The Norwegian Institute of Cosmic Physics, Univ. of Oslo, 1970.

10. Theoretical VLF Multimode Propagation Predictions, C.B. Brookes, Jr., J.H. McCabe, and F.J. Rhoads, Naval Research Laboratory Report 6663, December 1, 1967.

11. Omega Skywave Correction Tables, U.S. Naval Oceanographic Office H.O. Publication 224, various dates.

12. Navigation Performance of a Computerized 3-Frequency Omega Receiver in an Airborne Environment, D. Mactaggart, J. Inst. Nav., Vol. 19, pp. 159-174, Summer, 1972.

13. Omega Propagation Primer, E.R. Swanson and R.P. Brown, Naval Electronics Laboratory Center Technical Note 2101, 4 August, 1972.

14. Characteristics of the Earth-Ionosphere Waveguide for VLF Radio Waves, J.R. Wait and K.P. Spies, Nat. Bur. Std. Technical Note 300, 1964. Also Supplement to this Note, 1965.

15. Lane Identification in Omega, J.A. Pierce, DEAP Technical Report No. 627, Harvard Univ., July, 1972.

16. Locating Downed Aircraft by GRAN (Global Rescue Alarm Net), W.R. Crawford and W.E. Rupp, Jr., J. Inst. Nav., Vol. 19, pp. 311-316, Winter, 1972-73.

17. Omega Envelope Capability for Lane Resolution and Timing, E.R. Swanson and D.J. Adrian, Naval Electronics Laboratory Center Technical Report 1901, 20 November, 1973.

18. The Use of the 3.4 kHz Omega Difference Frequency for Aircraft Navigation, J.W. Brogden and J.P. Hauser, Naval Research Laboratory Memorandum Report 2640, September, 1973.

19. Omega-Inertial Hybrid Receiver, Winslow Palmer, J. Inst. Nav., Vol. 15, pp. 376-390, Winter, 1968-69.

20. New Algorithms for Converting LORAN Time Differences to Position, B. Friedland and M.F. Hutton, J. Inst. Nav., Vol. 20, pp. 178-188, Summer, 1973.

21. Formule donnant la longeuer de la geodesique, etc. M.H. Andoyer, Bull. Geodesique, Vol. 34, p. 77, 1932.

22. The Distance between Two Widely Separated Points on the Surface of the Earth, W.D. Lambert, J. Washington Acad. Sci., Vol. 32, p. 125, 1942.

APPENDIX

REVISION OF NOMINAL VALUES OF c/v

This paper has treated the nominal predictions, introduced in Sections 4 and 9, as though they were more absolute then one can expect them to be. This uncertainty is particularly critical at the intersection of the day and night nominal reciprocal velocities at $m_1 = 3.263$ and $c/v = 1.00725$, because this point is used to stabilize the predictions at 3.4 kHz, and for similar purposes.

This nominal point at which the mean diurnal variation is presumed to be zero must, of course, vary in both m_1 and c/v with at least some of the variables listed in Section 9. Of these, latitude may be the most important, although the writer has too few data at hand to permit the quotation of any suggested coefficient. The general subject of the migration of this "fixed" point must be left to others to investigate.

It will probably be advisable for other workers first to examine the question of whether the writer has located this "fixed" point in the correct average place. As Figs. 5 and 6 show, the chosen point agrees quite well with data taken in Cambridge and, as seen in Table II, there is general agreement with independent estimates of phase velocity and with some data taken by others.

This agreement notwithstanding, the writer has become conscious, in the last year or two, that some samples of data taken in other parts of the world seem to imply a somewhat higher group velocity than do the Cambridge data. In response to this nagging impression, a revised set of nominal velocities has been selected that seem, in general, to fit data taken

at other places rather better than do the values cited in this paper, although the agreement at Cambridge is somewhat less satisfactory. The distinction is not of very great importance. The maximum difference between the old and the revised nominal values occurs at night at 3.4 kHz, where the difference in predicted transmission time is about 2 centicycles of 10.2 kHz per megameter of distance. Since the average distance-difference in the operational Omega system is not likely to be much more than 3 Mm, this modification amounts to less than a mile average displacement of the 3.4 kHz predictions.

The importance of this suggestion of revised nominal values should be regarded as very tentative. The revised values differ from those in the body of this paper, but are not necessarily better. The magnitude of the changes is perhaps only a measure of the uncertainty of the coordinates. On the new basis, these would be $m_1 = 3.2$, $c/v = 1.0066$.

With these doubts in mind, the writer has chosen to keep the relations cited in this paper consistently on the old basis, and to suggest modification only in this appendix. The modified nominal predictions affect values in this paper chiefly in Table II (C) and in several of the equations in Section 12. Revised values, with the same table and equation numbers, are as follows.

Equations in Section 12:

$$T_{3.4\ nom} = (1.0090 - 0.0008\ F)\ T_G \qquad (38A)$$

$$S = \frac{1.0066\ T_G - T_C - (S.W.C.)_{10.2}}{3.2} \qquad (39A)$$

TABLE IIA

REVISED ESTIMATES OF RECIPROCAL VELOCITY

	c/v_2 13.6 kHz	c/v_1 10.2 kHz	$c/v_2 - c/v_1$	m_1	c/v at m_1
(C) Revised Nominal:					
Night	1.0022	1.0002	0.0020		
Day	1.0000	0.9970	0.0030		
Night-Day	0.0022	0.0032		3.20	1.0066

$$S = 0.002875\ T_C + 0.3125\ (S.W.C.)_{10.2} \qquad (41A)$$

$$T = (1 + 0.002875\,m)\ T_C - (1 - 0.3125\,m)\ (S.W.C.)_{10.2} \qquad (43A)$$

$$T_{3.4} = 1.0115\ T_C + 0.25\ (S.W.C.)_{10.2} \qquad (44A)$$

$$\text{Modified } (S.W.C.)_{3.4} = -0.0115\ T_C - 0.25\ (S.W.C.)_{10.2} \qquad (45A)$$

It is left to others to determine the best values for the nominal predictions, and, of course, the general utility of these methods.